Photoalignment of Liquid Crystalline Polymer Films

Based on the Free Surface Controls

Kei　Fukuhara

Department of Molecular Design and Engineering

Nagoya University

2014

Contents

Chapter III

Free Surface-Induced Planar Orientation in Liquid Crystalline Block Copolymer Films: On the Design of Additive Surface Active Polymer Layer

Chapter IV

Ubiquitous Photoalignment of Liquid Crystalline Polymers by a Segregated Free Surface Layer

Chapter V

Chapter I

General Introduction

Liquid crystal (LC) molecules of rod-like or discotic shaped are anisotropic. When these molecules contact with interfaces of solid surface and air, they will adapt specific molecular orientations. Especially, vast amounts of knowledge of induced orientation of LC molecules from solid substrate surfaces were accumulated because it is essential for LC display panel fabrications. On the other hands, little study has been reported on induced orientation of LC molecules from free surface (air interface) so far. Low molecular mass nematic LCs are used for LC display device for their high fluidity. To use such LC molecules, LC materials need to be sealed into solid substrates, however, little attention has been paid in this area focusing to free surface in itself.

In contrast, it is important to take into account free surface functions; because LC polymers, regardless of main or side chain, have situations to contact with free surface at materialize process of fibers and films. It is expected that free surface control should play important vales on molecular orientation in thin films. Below the phase transition temperature, the fluidity is low and, beyond this temperature, segmented mobility becomes significantly larger to be fluid. Recently, it was came across a phenomenon that shows the significance of controlling the free surface side in the course of study on photoalignment of side chain type LC polymer thin films containing azobenzene. In this chapter backgrounds of relevant studies of block copolymers in side chain type LC polymer and photoalignment behavior.

1-1. Block copolymers

Block copolymers that connect immiscible polymer components together via a covalent bond form phase separation. This process establishes very well-regulated structure having a periodicity determined from chain length of the polymer segments. Both terminal distances of the polymer ranges usually approximately several dozen nm and recurrence periods are similar in size to this length. This phase separation structure is called microphase separation (MPS) and it is different from macro phase-separated structure of polymer blends.[1,2,3] The MPS structure of block copolymer changes depending on the composition ratio of block copolymer and form a periodic nanostructure of sphere, cylinder and lamella, etc. through self-assembly. As shown in Figure 1, the AB diblock copolymers exhibit the periodic nanostructures depending on the relative volume fractions of the two blocks.[4,5] The important parameters to describe phase separation leading to the formation of nanostructures are the total degree of polymerizations, the Flory-Huggins χ parameters and volume fractions of two blocks. Additionally, block copolymers have various properties resulting from the natures of blocks.

The diblock copolymers connecting a polymer possessing mesogenic groups at the side chain and a coiled polymer exhibit liquid crystallinity, and provide hierarchical structures consisting of microphase separated structures and LC layer structures within the block copolymer domain. The LC mesogens prefer to orient uniformly with respect to the interface between the two polymer phases, denoted as the intermaterial dividing surface (IMDS).[6,7] Ober and coworkers demonstrated that both the axes of the mesogenic groups and the lamellar interfaces orient parallel to the film surface since mesogens are anchored at the IMDS (Figure 2).[6] Hammond's group revealed the influence of the length of LC spacer on orientation direction within the layers.[8] Hexyl spacer systems provide the parallel arrangement of mesogens to a

(a)
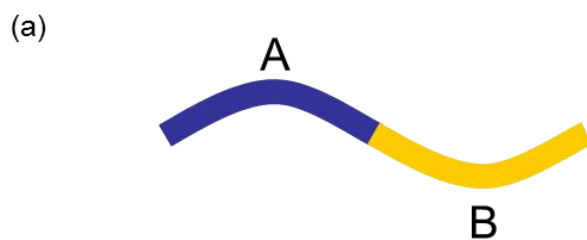
(b)
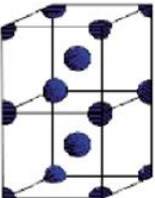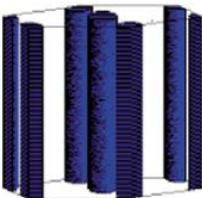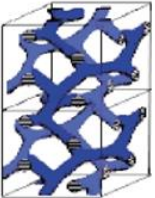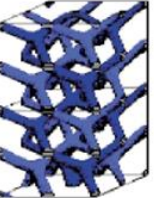
Nature of patterns	Spheres (SPH) (3D)	Cylinders (CYL) (2D)	Double gyroid (DG) (3D)	Double diamond (DD) (3D)	Lamellae (LAM) (1D)
Space group	$Im\bar{3}m$	p6mm	$Ia\bar{3}d$	$Pn\bar{3}m$	pm
Blue domains: A block					
Volume fraction of A block	0-21%	21-33%	33-37%		37-50%

Figure 1. (a) Schematic illustration of AB diblock copolymer. (b) Schematic phase diagram showing various microphase separated structures by AB diblock copolymer. (taken from Ref. 4)
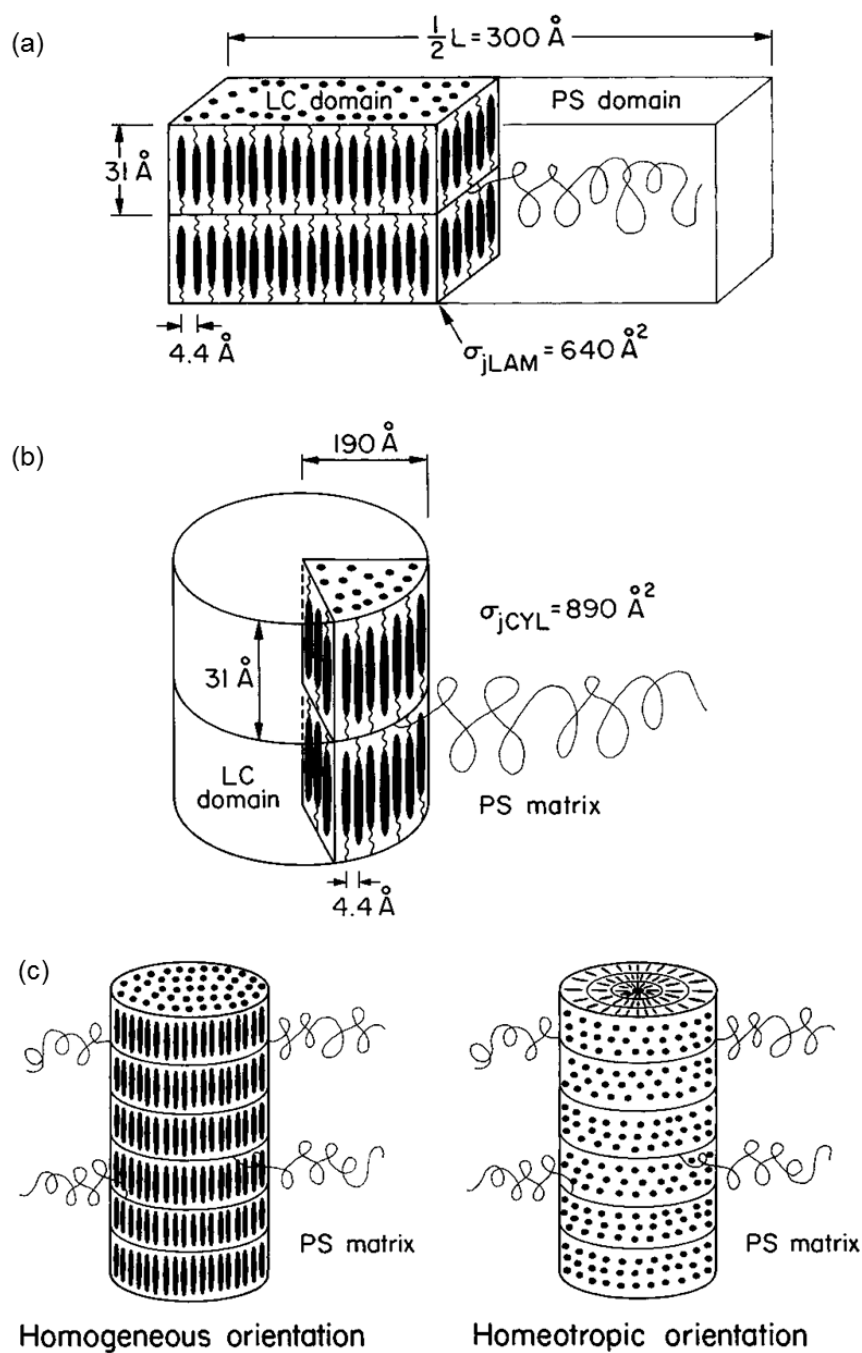
Figure 2. (a) Schematic illustration of lamellar structure of LC-segment-containing block copolymers. (b and **c**) cylinder structures (homogeneous and homeotropic orientation of mesogens to the IMDS). (taken from Ref. 6)

lamellar morphology. The longer decyl spacer systems, however, exhibit the perpendicular arrangement of mesogens to lamellae. It is assumed that these results, which have not been observed in other LC block copolymer systems, are the consequence of the decoupling of the mesogens from the polymer main chain.

1-1-1. MPS structure of thin film

In contrast to bulk structure, thin film is severely impacted and regulated by cast solvent, energy of surface and interface, period length of structure and thickness. For examples, lamella structure of thin film receives a great amount of influence from interface. In A-B diblock copolymer, when between substrate and one block component (A block) have a high degree of affinity, alternating layer type lamella structure is formed. Most of block copolymers form this structure because of the different wettability of A and B block component. When the thickness (t) of a thin film of lamella structure was controlled in terms of the period (L_0), a sea-island and a bicontinuous structures having L_0 height from free surface will be observed[9] (Figure 3a). In the case of free surface and substrate interface contacting same block component (symmetry wetting) and the case of contacting different block component (asymmetry wetting), each thickness was regulated in nL_0 and $(n+1/2)L_0$ ($n > 0$) (Figure 3b).

The MPS structure of thin film needs to be taken into account of various factors that bulk structure lacks. Conversely, if these factors are controlled, it is possible to tune the MPS structure itself. Morphology controls over large area and orientation control are essential for applications of materials.

1-1-2. Morphology of MPS structure and orientation control

Ordering thin films of MPS structure has attracted much attention. On-demand orientational controls of MPS structures are essential for nanomaterials, nanoporous membranes, photonic crystals and waveguides. Several examples in this
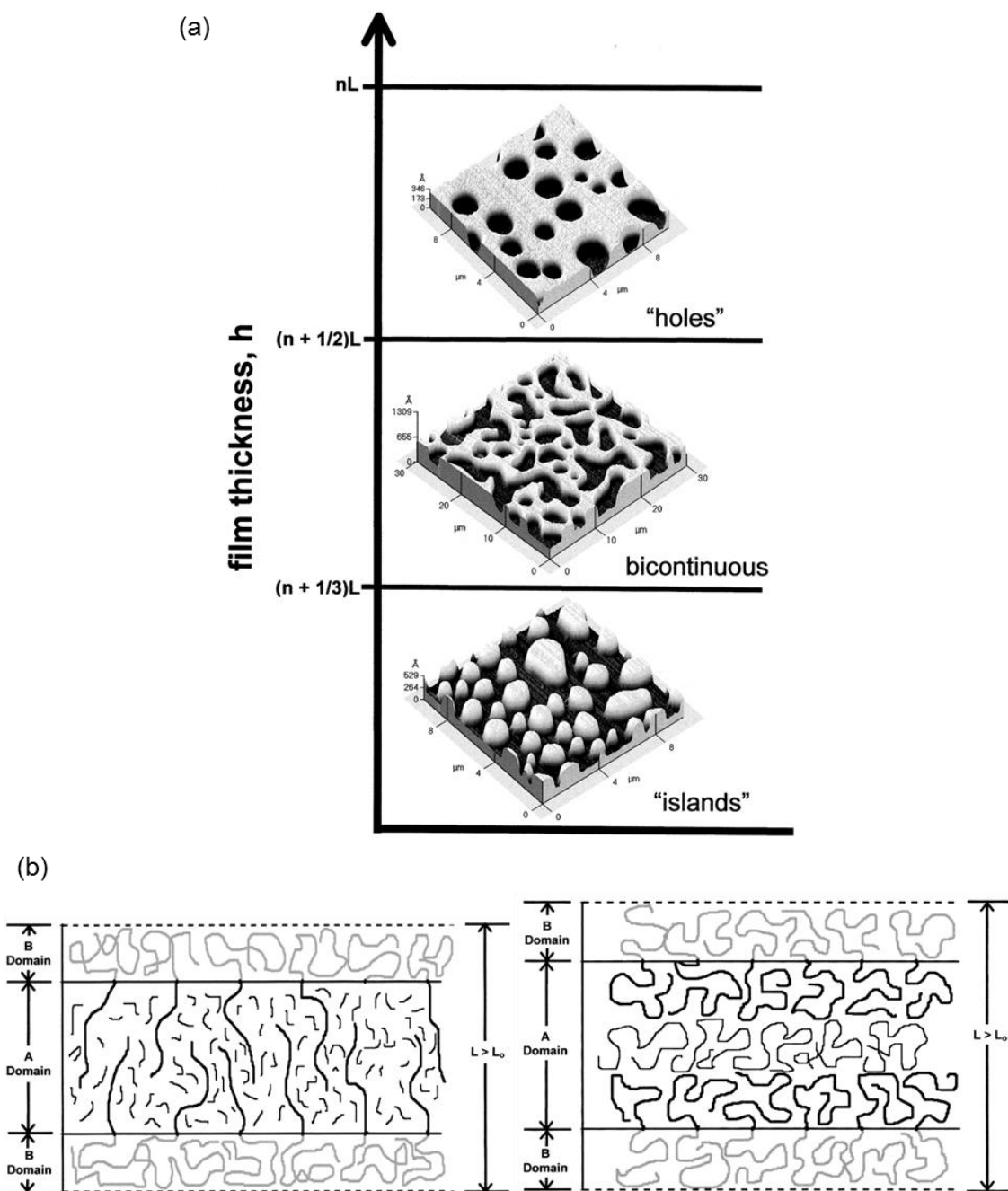
Figure 3. (a) AFM images of topographical features that appear in ordered, symmetric, PS-*b*-PMMA copolymer thin films are shown. The height of each topographical feature is equal to the interlamellar spacing, *L*. In this figure *n* is an integer. (b) Schematics of the PS-*b*-PMMA copolymer with (left) homopolymer chains distributed throughout one domain and (right) with homopolymer localized in the center of one domain. (taken from Ref. 9)

line are described below.

Russell's group reported perpendicular orientation control of well-regulated cylinder structure in large area by using polystyrene-*b*-polyethylene oxide block copolymer (PS-*b*-PEO) via combination of solvent volatilization rate control and solvent vapor annealing.[10] This is regarded as one of morphology control method. And, this group has succeeded in perpendicular orientation of lamella structure using a surface-graft film of random copolymer which adjusts the surface tension of the substrate.[11]

Nealey's group studied the effects of variations in the period of chemically modified the surface pattern with respect to on the periodic pattern of lamella forming block copolymer. The two-step process was used to prepare well-defined nano pattered surfaces (Figure 4).[12,13] Chemically patterned substrates were prepared by extreme ultraviolet interferometric lithography (EUV-IL) on self-assembled monolayer (SAM) of phenylethyltrichloro silane. Then the film of the symmetric lamella forming PS-*b*-poly(methyl methacrylate) (PMMA) was obtained by spin-coating from toluene solutions on the chemically patterned surface and then was annealed. The PMMA block preferentially wet the regions where SAMs are decomposed by EUV-IL since those areas were chemically modified to contain polar groups. The other regions exhibited neutral wetting property for the PS block. Cylinder forming PS-*b*-PMMA thin films were also directed to assemble on chemically patterned surfaces consisting of alternating stripes that are preferentially wet by the two blocks of the copolymer as well as the lamella systems.[14] The PMMA cylinders orient parallel to the film surface on the chemically modified regions for the above reason.

Sibener and co-workers reported macroscopic alignment by guiding with the trough edges in grating substrate of cylindrical domains in PS-*b*-poly(ethylene-*alt*-propylene) (Figure 5).[15] At shorter annealing time, at least two cylinders align along the trough edges, and others orient perpendicular to the edges, i.e.,
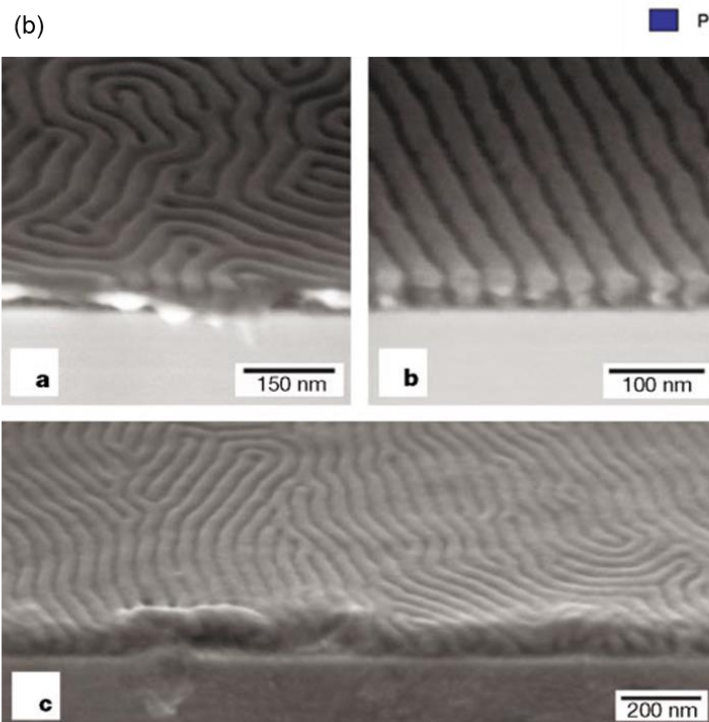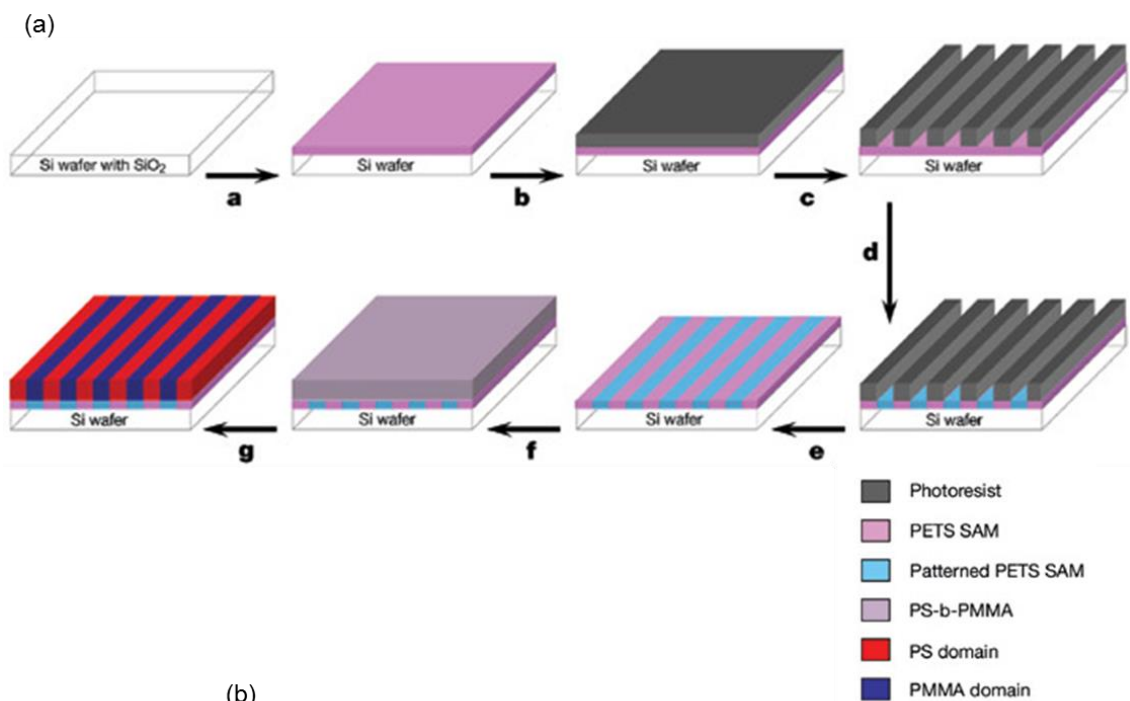
Figure 4. (a) Schematic illustration of the strategy used to creat chemically patterned surfaces and investigate the epitaxial assembly of nanodomains. (b) Cross-sectional SEM images of PS-*b*-PMMA films on unpatterned and chemically nanopatterned surfaces. (taken from Ref. 12)
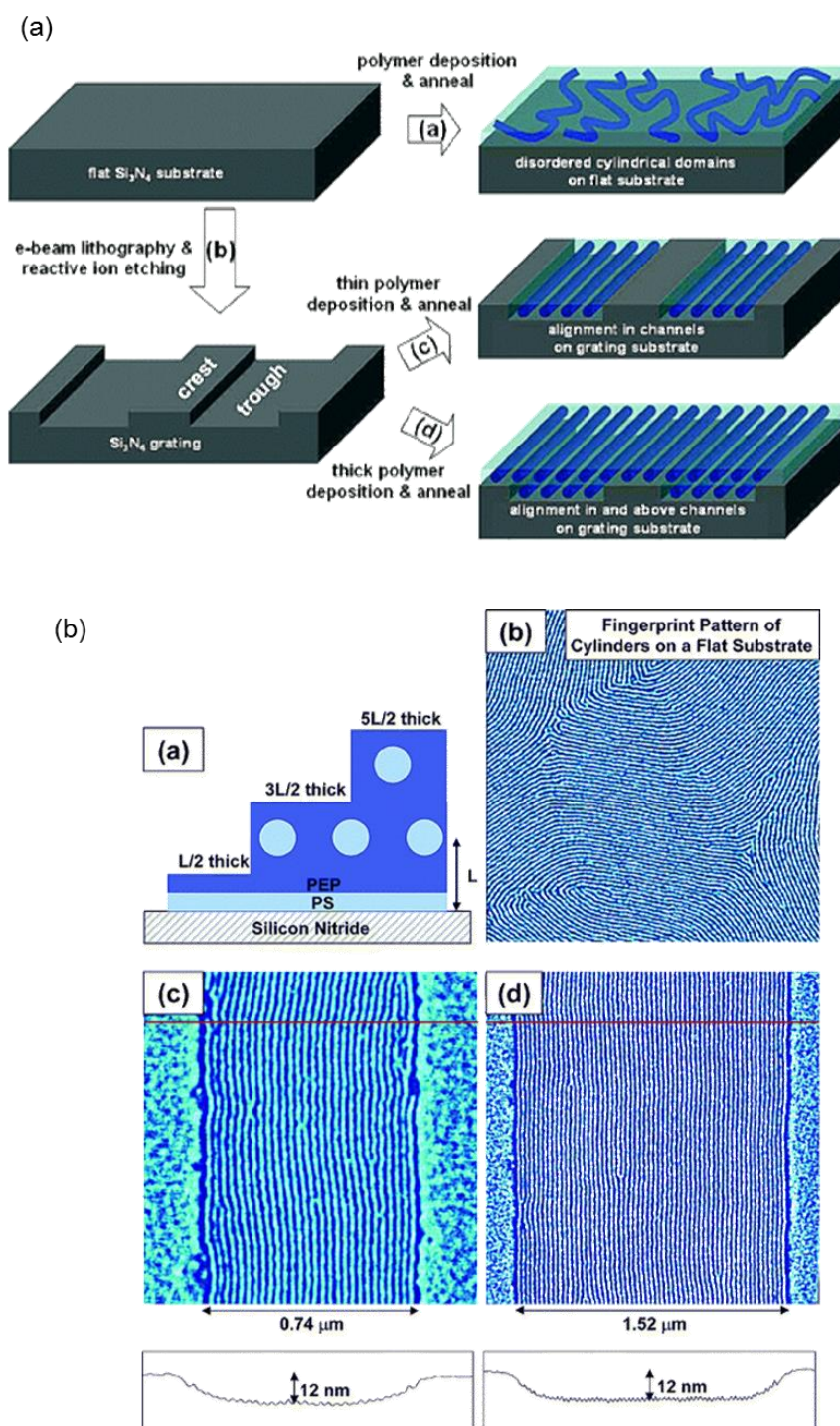
Figure 5. Schematic illustration of alignment control process of cylindrical nanodomains by utilizing topographical patterned substrate. (taken from Ref. 15)

along the direction of mass flow during an annealing process.[16] The alignment of cylinders in confined volumes is induced by the preferential wetting layer of PS on the vertical sidewalls of the trough. After enough annealing, the cylinders perfectly align parallel to the edges of the trough. This method combines the top-down and bottom-up approaches.

Moreover, there have been many investigations that induced orientation by using a magnetic field,[17] an electric field,[18] and a mechanistic shear stress.[19,20] However, they lack versatility repairing surface fabrications and modifications by the use of lithography technology or strong external fields. Nowadays, there are continuations of many studies to develop simpler methods.

1-2. Photoalignment of LC materials

LC materials with high cooperative motions can induce orientations over long distances to minimize elastic energy of the whole system in a consequence of molecular orientation at the substrate interface. The orientation control of LC in the fabrication of display devices has been made by rubbing treatment of substrate interface heretofore (Figure 6a).

Photoalignment method of surface was introduced before about 25 years ago.[21] It has been adopted in the fabrication process of LC display panels during recent years (Figure 6b). The photoalignment of LCs is ascribed to the angular selective photoreaction on a polymer film performed by linearly polarized light (LPL) irradiation within thin film surface or tilt oblige irradiation. These processes eliminate problems of roughing the surface, dusts and changing generation occurring in the rubbing method. They also enable fabrication of large area screen panels with high-resolutions by incorporating fine patterning.[22] Photoalignment of polymer materials lead to orientation of the entire thin film area and inducing optical anisotropy as the result of cooperative
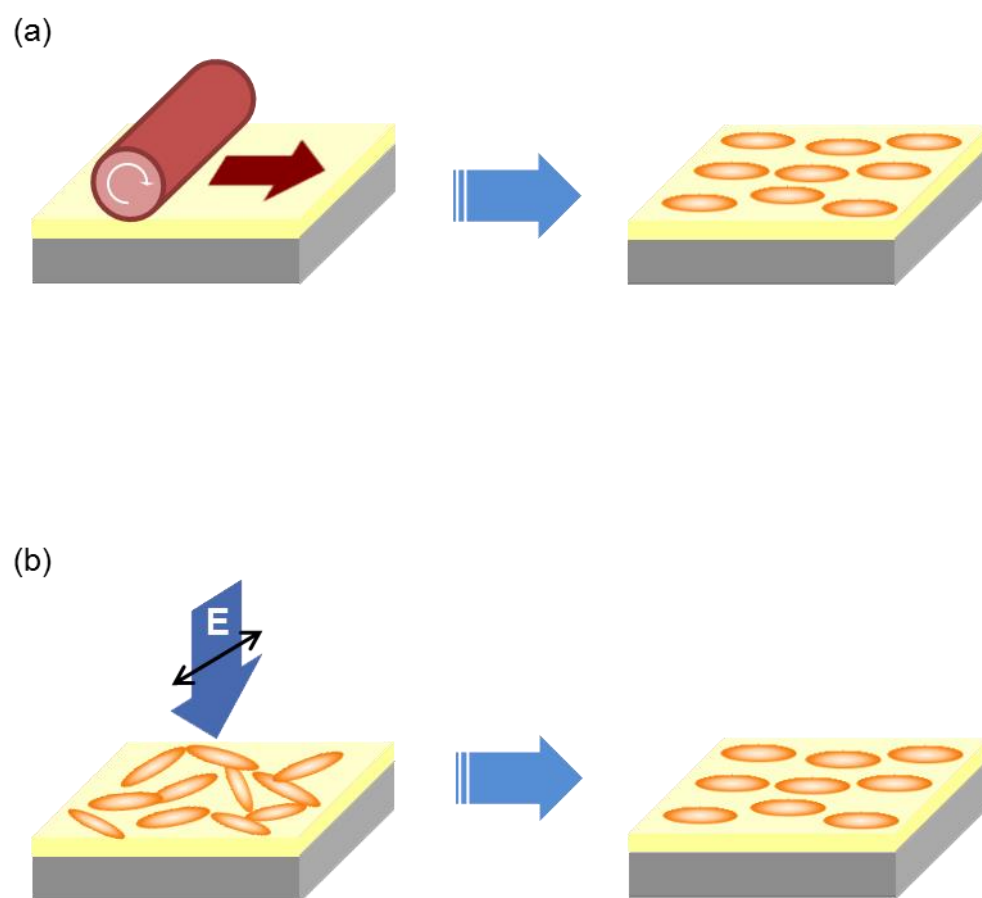
Figure 6. Schematic illustration of (a) rubbing treatment and (b) photoalignment method.

motions of LC. Thus, LC polymer thin film is expected for applications to optical recording media of hologram, etc.[23,24]

1-2-1. Azobenzene

Azobenzene (Az) compounds have been studied extensively for a long time. The earliest and widest applications are found in the use for dye-stuffs because a variety of colors could be obtained depending on their chemical structure. Also, the photoisomerization of azobenzene has long been the subject of great interest. Under irradiation with UV and visible light, the Az chromophores undergo reversible isomerization of trans-cis and cis-trans form, respectively.[25,26] The cis isomer is also reverted to the trans form through the thermal backward process. When an Az group is incorporated into various matrixes, its photoisomerization can cause a wide range of fascinating consequences. For instance, Todorov *et al.*[27] have mentioned the orientation of Az groups incorporated into a polymer film, which are aligned perpendicular to the laser beam polarization direction. Polarized light can induce significant orientation of these molecules, which lead to dichroism and birefringent characters.

In Az polymer films, the in-plane orientation is controlled by LPL irradiation.[28] The optical transition moment of Az chromophore approximately coincide to long axis of this molecule. When the polarization direction of LPL is parallel to transition moments of Az chromophores, they effectively absorbs LPL, followed by trans-to-cis isomerization. (Figure 7) When the directions of the polarization moment of LPL and the transition moment of Az chromophores are orthogonal to each other, Az chromophores hardly absorb the LPL, resulting in the inactive state. After many respecting trans-cis-trans cycles, transition moments of most Az chromophores, i.e. the long axis of Az, are orthogonally oriented to the polarization direction of LPL. For the same reason, when non-polarized light expose from the normal direction to the film plane, the Az chromophores exhibit the out-of-plane perpendicular orientation, leading
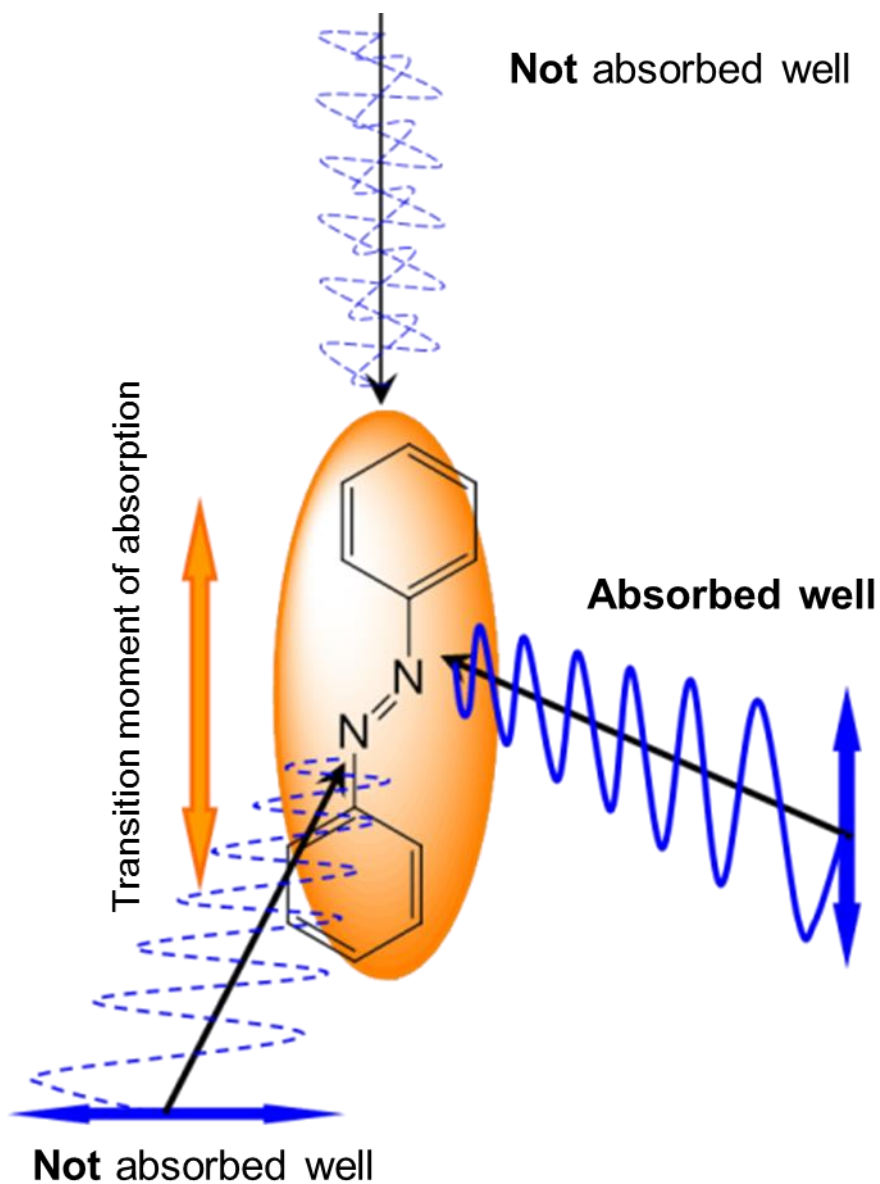
Figure 7. Schematic illustration of optical absorption property. The optical transition moment of Az chromophore approximately coincide to long axis of this molecule.

to the inactive state.

1-2-2. Command surface

When a substrate surface is chemically modified with photochromic residues of azobenzene, macroscopic orientation of low-molecular-weight nematic LC molecules can be manipulated by alternate irradiation with UV and visible light. This process is induced by the alternate isomerization between rod-like trans and bended cis forms of Az on the surface. The first observation and the extensions of research in this area were mostly performed at Ichimura's group.[21] They proposed the "*command surface*" concept, which is illustrated in Figure 8. The most interesting aspect of this process is that one can calculate that ca. 10^4 -10^5 nematic LC molecules are driven by monolayer Az groups.[21]

There are four modes of the NLC alignment controls by command surface effects; (i) out-of-plane alignment between homeotropic and planar mode,[21] (ii) out-of plane alignment between homeotropic and homogeneous mode, [29] (iii) in-plane alignment by irradiation with LPL,[30,31] and (iv) three-dimensional alignment by slantwise irradiation with non-polarized light.[32] Systematic studies on the command surface allowed the potential application to other types of liquid crystalline materials involving semctic, [33] cholestic, [34] discotic, [35] lyotropic, [36,37] and polymer liquid crystals.[34] Excellent reviews covering the surface photo-alignment phenomenon can be found the *Chemical Review* paper,[38] for earlier works and polymer for most recent activities.[39]

Ichimura *et al.*[40,41] have further demonstrated an exciting application of these kinds of phenomena, physical migrations of an olive oil droplet using light. When the azobenzene isomerizes, a gradient the surface free energy is produced, and this actually moves the oil drop at a millimeter scale.
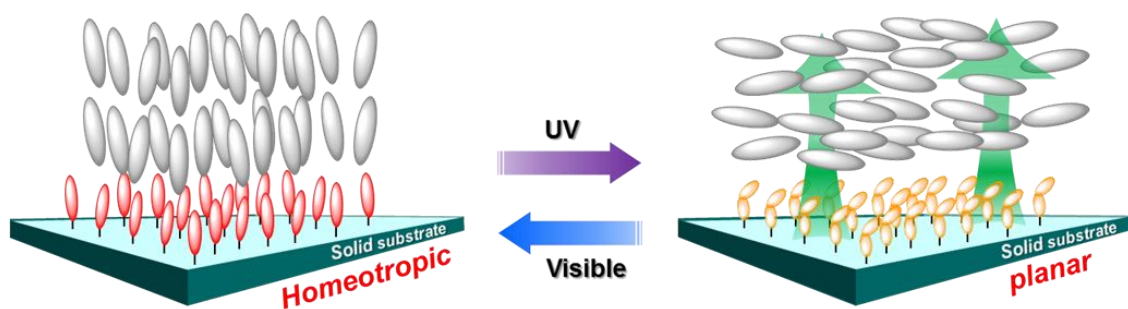
Figure 8.   Schematic representation for the reversible change of liquid crystal alignment mode induced by the photoisomerization of azobenzene unit attached to a outermost solid surface.

1-2-3. LC block copolymers

There have been extensive studies on the orientation order and long axis/distance order to MPS structure with a combination of LC polymer and block copolymer architecture. For example, Iyoda et al, have successfully developed PAz diblock copolymers (PEO-*b*-PAz) containing polyethylene oxide. PEO-*b*-PAz film exhibits the vertical orientation of PEO cylinders with high regularity over large area through the homeotropic orientation of Az unit in the smectic phase.[42]

LC block copolymers are different from ordinary block copolymers, and indicate asymmetry phase diagram in the coil-LC block copolymers. It has been reported that PEO cylinder structure form in the volume ratio ranging from 30 to 90 % for LC material of PEO-*b*-PAz[43] and also for other block copolymers.[44] Theoretical considerations have also been made.[45]

In our group, photoalignment and 3D photopatterning of MPS structure have been demonstrated by using a diblock copolymer composed of PEO-*b*-PAz.[46] This optical method is based on the angular selected photoreaction of azobenzene side chains and the collective molecular motions. The nanocylinders of PEO are aligned orthogonal to the direction of the electric field vector of irradiated polarized light. The key to the successful photoalignment control seem to be the use of stimuli-responsive soft block component of PEO exhibiting the low glass transition temperature (T_g). In terms of thermal and mechanical stability, it was shown for a diblock copolymer that consists of polystyrene (PS) and an LC Az-containing polymer is able to alter the orientation as a result of an MPS cylinder structure (distance between cylinders of ca. 32 nm, PS-*b*-PAz) of coiled PS domains in response to LPL.[47] The photoalignment procedure for PS-*b*-PAz (T_g of PS = 102°C) was achieved through LPL irradiation and annealing followed by successive slow cooling. (Figure 9)
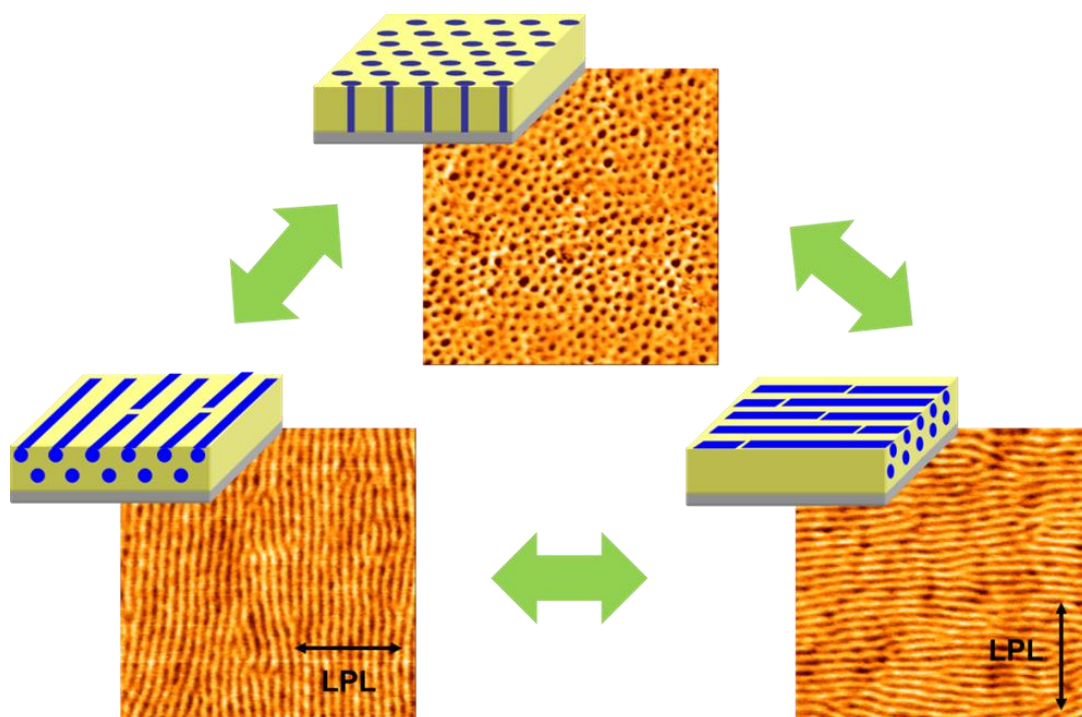
Figure 9. Schematic and experimental AFM images of three dimensional orientation control of PS cylinder in PS-*b*-PAz thin film.

1-3. Molecular orientation from the free surface

There have been enormous investigations examined on LC orientation control by solid substrate surface. Although the significance of the free surface for the LC orientation has been recognized experimentally and rhetorically, there is no report on utilization of active orientation control to indicate an importance of free surface.[48,49] In the bulk, any orientation will not be induced in the continuous space. However, the situation can be different when the interface exists. In the free surface, rod-like molecules tend to be aligned at the interface to minimize the excluded volume by sticking preferably long axis to the free space. Therefore, rod-like molecules of side chain mesogen have a tendency to orient direction perpendicular to free surface. On the other hands, mesogen have a tendency to orient direction parallel to substrate interface to avoid colliding, because the solid substrate surface is considered to exclude molecules. The orientational behavior at interface for rod-like molecules accords with knowledge of obtained from simulations.[50]

1-3-1. Orientation control of block copolymers from free surface

Ordering and structural patterning of MPS domains in block copolymer thin films have been developed as important elements for the next-generation lithography.[4] In these cases, the perpendicular orientation of MPS domains is desired. The orientation of MPS structure having a different surface tension polymer domain is selectively absorbed onto either the domain component of substrate interface or free surface properties. It is proposed that a neutral polymer layer is introduced on substrate surface and on the free surface. Russell and Hawker et al indicated the way to control the parallel and perpendicular direction of the lamella MPS domains by placing a random block copolymer through surface grafting on the substrate.[51,52,53,54,55,56] These findings show the importance of considering free surface and that only the modification of solid substrate is not enough to align domain orientations.

1-3-2. Induced planar orientation for low surface tension block copolymers

Nagano et al have reported that PAz diblock copolymers containing poly(butyl methacrylate) (PBMA-*b*-PAz) exhibited the random planar alignment of LC phase and PBMA microphase cylinders.[57] The unexpected LC orientations are probably attributed to the balance of surface tension of the LC and amorphous polymer blocks. A low surface tension and the high flexibility of PBMA block is presumed to drive the segregation to the "*free surface*" of the films. The coverage of the free surface should impede the homeotropic orientation of the mesogens.

1-4. Aim of this thesis

This work demonstrates the alignment control of LC and microphase cylinder structure in thin films by the free surface modification. Adding the small amount of PBMA-*b*-PAz unit low surface energy and high flexibility induces the orientational alternations from the homeotropic LC Az polymer to planar orientations due to the surface segregation and coverage of PBMA at the free surface. The present thesis consists of the following chapters.

In chapter 2, Alignment Control of Liquid Crystalline Polymer and Block Copolymer Domains via a Segregated Free Surface Layer.

In chapter 3, Free Surface-Induced Planar Orientation in Liquid Crystalline Block Copolymer Films: On the Design of Additive Surface Active Polymer Layer.

In chapter 4, Ubiquitous Photoalignment of Liquid Crystalline Polymers by a Segregated Free Surface Layer.

Finally the overall summary of this work and outlook for the future are provided in chapter 5.

References

1 M. W. Matsen, *Macromolcules* **1995**, *28*, 5765.

2 S. Walheim, M. Boltau, J. Mlynek, G. Krausch, U. Steiner, *Macromolecules* **1997**, *30*, 4995.

3 A. Berlinger, H. Gliemann, M. Barczewski, P. E. R. Durigon, D. F. S. Petri, Th. Schimmel, *Surf. Interface Anal.* **2001**, *32*, 144.

4 C. Park, J. Yoon, E. L. Thomas, *Polymer* **2003**, *44,* 6725.

5 *Developments in Block Copolymer Science and Technology*; Hamley, I. W., Ed., John Wiley & Sons, Ltd. West Sussex, **2004**.

6 G. Mao, J. Wang, S. R. Clingman, C. K. Ober, J. T. Chen, E. L. Thomas, *Macromolecules* **1997**, *30*, 2556.

7 C. Y. Chao, X. Li, C. K. Ober, C. Osuji, E. L. Thomas, *Adv. Funct. Mater.*, **2004**, *14*, 364.

8 M. Anthamatten, W. Y. Zheng, P. T. Hammond, *Macromolecules* **1999**, *32*, 4838.

9 P. F. Green, R. Limary, *Advances in Colloid and Interface Science* **2001**, *94*, 53.

10 S. H. Kim, M. J. Misner, T. Xu, M. Kimura, T. P. Russell, *Adv. Mater.* **2004**, *16*, 226.

11 S. Ham, C. Shin, E. Kim, D. Y. Ryu, U. Jeong, T. P. Russell, C. J. Hawker, *Macromolecules* **2008**, *41*, 6431.

12 S. O. Kim, H. H. Solak, M. P. Stoykovich, N. J. Ferrier, J. J. de Pablo, P. F. Nealey, *Nature* **2003**, *424*, 411.

13 E. W. Edwards, M. F. Montague, H. H. Solak, C. J. Hawker, P. F. Nealey, *Adv. Mater.*, **2004**, *16*, 1315.

14 E. W. Edwards, M. P. Stoykovich, H. H. Solak, P. F. Nealey, *Macromolecules* **2006**, *39*, 3598.

15 D. Sundrani, S. B. Darling, S. J. Sibener, *Nano. Lett.*, **2004**, *4*, 273.

16 D. Sundrani, S. J. Sibener, *Macromolecules* **2002**, *35*, 8531.

17 C. Osuji, P. J. Ferreira, G. Mao, C. K. Ober, J. B. V. Sande, E. L. Thomas, *Macromolecules* **2004**, *37*, 9903.

18 V. Olszowska, M. Hund, V. Kuntermann, S. Scherdel, L. Tsarkova, A. Böker, *ACS NANO* **2009**, *3*, 1091.

19 S. S. Petal, R. G. Larson, K. I. Winey, H. Watanabe, *Macromolecules* **1995**, *28*, 4313.

20 S. Pujari, M. A. Keaton, P. M. Chaikin, R. A. Register, *Soft Matter* **2012**, *8*, 5358.

21 K. Ichimura, Y. Suzuki, T. Seki, A. Hosoki, K. Aoki, *Langmuir*, **1988**, *4*, 1214.

22 K. Miyachi, K. Kobayashi, Y. Yamada, S. Mizushima, *SID Symp. Digest Tech. Papers*, **2010**, *41*, 579.

23 M. Eich, J. H. Wendorff, B. Reck, H. Ringsdorf, *Makromol. Chem. Rapid Commun.* **1987**, *8*, 59.

24 A. Shishido, *Polymer Journal* **2010**, *42*, 525.

25 P. P. Birnbaum, J. H. Linford, D. W. G. Style, *Transactions of the Faraday Society* **1953**, *49*, 735.

26 G. Zimmerman, L. Y. Chow, U. J. Paik, *J. Am. Chem. Soc.* **1958**, *80*, 3528.

27 T. Todorov, L. Nikolova, N. Tomova, *Appl. Opt.*, **1984**, *23*, 4309.

28 M. Han, S. Morino, K. Ichimura, *Macromolecules*, **2000**, *33*, 6360.

29 K. Kawanishi, T. Tamaki, M. Sakuragi, T. Seki, Y. Suzuki, K. Ichimura, *Langmuir*,

1992, *8*, 2601.

30 K. Ichimura, Y. Hayashi, N. Ishizuki, *Chem. Lett.*, **1992**, 1063.

31 K. Ichimura, Y. Hayashi, H. Akiyama, T. Ikeda, N. Ishizuki, *Appl. Phys. Lett.*, **1993**, *63*, 449.

32 K. Kawanishi, T. Tamaki, K. Ichimura, *Polym. Mater. Sci. Eng.*, **1992**, *66*, 263.

33 M. Kidowaki, T. Fujiwara, K. Ichimura, *Chem. Lett.*, **1999**, 643.

34 C. Ruslim, K. Ichimura, *Adv. Mater.*, **2001**, *13*, 641.

35 K. Ichimura, S. Furumi, S. Morino, M. Kidowaki, M. Nalagawa, M. Ogawa, Y. Nishimura, *Adv. Mater.*, **2000**, *12*, 950.

36 K. Ichimura, M. Momose, T. Fujiwara, *Chem. Lett.*, **2000**, 1022.

37 C. Ruslim, M. Hashimoto, D. Matsunaga, T. Tamaki, K. Ichimura, *Langmuir*, **2004**, *20*, 95.

38 K. Ichimura, *Chem. Rev.*, **2000**, *100*, 1847.

39 T. Seki, S. Nagano, M. Hara, *Polymer*, **2013**, *54* (22), 6053.

40 K. Ichimura, S. K. Oh, M. Nakagawa, *Science*, **2000**, *288*, 1624.

41 S. K. Oh, M. Nakagawa, K. Ichimura, *J. Mater. Chem.*, **2002**, *12*, 2262.

42 Y. Tian, K. Watanabe, X. Kong, J. Abe, T. Iyoda, *Macromolecules* **2002**, *35*, 3739.

43 H. Yu, T. Iyoda, T. Ikeda, *J. Am. Chem. Soc.* **2006**, *128*, 11010.

44 M. Anthamatten, W. Y. Zheng, P. T. Hammond, *Macromolecules* **1999**, *32*, 4838.

45 M. Anthamatten, P. T. Hammond, *Journal of Polymer Science Part B*: *Polymer Physics* **2001**, *39*, 2671.

46 Y. Morikawa, N. Nagano, K. Watanabe, K. Kamata, T. Iyoda, T. Seki, *Adv. Mater.* **2006**, *18*, 883.

47 Y. Morikawa, T. Kondo, S. Nagano, T. Seki, *Chem. Matter* **2007**, *19*, 1540.

48 B. Ocko A. Braslau, P. Pershan, J. Alsnielsen, M. Deutsch, *Phys. Rev. Lett.*, **1986**, *57*, 94.

49 N. Scaramuzza C. Berlic, E. Barna, G. Strangi, V. Barna, A. Ionescu, *J. Phys. Chem. B*, **2004**,*108*, 3207.

50 H. Kimura, *Ekisho*, **2006**, *10*, 159.

51 A. Hariharan, S. K. Kumar, T. P. Russell, *J. Chem. Phys.*, **1993**, *98*, 4163.

52 P. Mansky, Y. Liu, E. Huang, T. P. Russell, C. Hawker, *Science*, **1997**, *275*, 1458.

53 P. Mansky, T. P. Russell, C. Hawker, M. Pitsikalis, J. Mays, *Macromolecules*, **1997**, *30*, 6813.

54 E. Huang, L. Rockford, T. P. Russell, C. J. Hawker, *Nature*, **1998**, *395*, 757.

55 E. Huang, T. Russell, C. Harrison, P. Chaikin, R. Register, C. Hawker, J. Mays, *Macromolecules*, **1998**, *31*, 7641.

56 T. Xu, C. J. Hawker, T. P. Russell, *Macromolecules*, **2005***, 38*, 2805.

57 S. Nagano Y. Koizuka, T. Murase, M. Sano, Y. Shinohara, Y. Amemiya, T. Seki, *Angew. Chem., Int. Ed.*, **2012**, *51*, 5884.

Chapter II

Alignment Control of Liquid Crystalline Polymer and Block Copolymer Domains via a Segregated Free Surface Layer

2-1. Introduction

The surface effects and anchoring of liquid crystals (LCs) have long been significant concerns for material chemists and physicists.[1] The surface alignment of LCs by mechanical rubbing[2,3] is a widely recognised phenomenon and of particular significance in technological applications for display device fabrication.[4] Surface molecular orientations[5,6] and topographical grooves and undulations[7,8] of the substrate provide LC alignment effects. Furthermore, in the past two decades, the photoalignment of LCs on photoreactive polymer film surfaces by anisotropic irradiation[9,10,11,12,13,14] has become a significant tool and an alternative to mechanical rubbing processes. The aligning substrates are not limited to polymer surfaces; various types of surfaces, such as hard inorganic materials[15] and soft bio-related interfaces,[16,17] can be used for the alignment induction. In addition to low-molecular-mass LCs, polymer LC materials are also aligned by the surface effect.[18,19,20] Despite the tremendous amount of accumulated knowledge and the number of potential applications, the surface alignment processes developed to date mostly involve manipulations on the surfaces of solid or condensed phases.

Herein, it is reported on LC alignment alternation, which is attained via a modification of the free surface (air-film interface). The homeotropic surface anchoring effect and layer structuring at the free surface of calamitic LC molecules have been shown experimentally [21,22] and have been further verified by theoretical simulations.[23,24,25] To modify the free surface, the present approach adopts the surface

segregation[26,27,28] of a small amount of a free-surface-active polymer. It isdemonstrated here that the coverage of the surface with the free-surface-active polymer leads to a homeotropic-to-parallel orientation change of LC mesogens, which further leads to an efficient in-plane photoalignment of microphase separation (MPS) domains of a relevant LC block copolymer by linearly polarised light (LPL).[29,30,31] With regard to the MPS alignment control, the important role of a top coat layer has recently been demonstrated by Bates et al.[32] In this case, a polar-to-nonpolar chemical conversion of the top layer is achieved to fulfil the requirement of spin-casting from an aqueous solvent and to provide a neutral (non-preferential) layer for the hydrophobic block copolymer during the annealing. In the present approach, in contrast, no additional coating procedure is required, providing a simple, versatile method for the desired alignment control of MPS domains.

2-2. Experimental

2-2-1. Materials

Styrene (99.5%, Kishida) and butyl methacrylate (BMA) (98.0+%, Wako) were passed through a column filled with neutral alumina to remove inhibitor, dried over calcium hydride, and distilled under reduced pressure. CuBr (95.0%, Kanto Chem.) and CuCl (99.9%, Wako) were washed with acetic acid containing a drop of HCl solution and diethyl ether for several times, and dried in vacuum. The initiators of ethyl 2-bromoisobutyrate (EBB) (98.0%, Tokyo Chem. Ind.) and 1-phenylethyl bromide (1-PEBr) (95.0%, Tokyo Chem. Ind.) and the ligands of 4,4'-dinonyl-2,2'-dipyridyl (Bpy9) (97.0%, Aldrich) and 1,1,4,7,10,10-hexamethyltriethylenetetramine (HMTETA) (97.0%, Aldrich) were used as received. Tetrahydrofuran (THF) of dehydrated stabilizer free grade (Kanto Chem.) was used for polymerization. Aluminum oxide 90 active neutral (Merck, active stage 1, particle size: 63-200 μm) was used for column

chromatography.

2-2-2. Synthesis of diblock copolymers

2-2-2-1. Polymerisation of polystyrene (PS) via bulk ATRP

Synthetic route of PS is shown in Scheme 1a. CuBr (47.0 mg, 3.3 x 10^{-4} mol) and Bpy9 (270.3 mg, 6.6 x 10^{-4} mol) were added into a 15 ml pressure glass tube. Next, in a glove box, the copper complex in degassed styrene (10.0 ml, 8.7 x 10^{-2} mol) was added. The resulting mixture was stirred for 10 min, and then 1-PEBr (15.0 μl, 1.1 x 10^{-4} mol) was added. The sealed mixture solution was removed from the glove box and placed for 2 h in a ChemStation at 110 °C. The polymerization was terminated by exposing the catalyst to air. The reaction solution was dissolved in chloroform and passed through an activated neutral alumina column to remove the Cu catalyst. After being concentrated, the solution was poured to methanol to remove styrene monomer. Yield 1.32 g (10 %). GPC data: M_n = 1.3 x 10^4, M_w/M_n = 1.07 (averaged number of repeating unit : 123 (PS$_{123}$)).

2-2-2-2. Polymerisation of poly(butyl methacrylate) (PBMA) via ATRP

Synthetic route of BMA is shown in Scheme 1b. CuCl (1.3 mg, 1.3 x 10^{-5} mol) and Bpy9 (11.0 mg, 2.7 x 10^{-5} mol) were added into a 15 ml pressure glass tube. Next, in a glove box, the copper complex in degassed BMA (0.8 ml, 5.4 x 10^{-3} mol) was added. The copper complex was dissolved in THF (1.3 ml). The resulting mixture was stirred for 10 min, and then EBB (2.0 μl, 1.3 x 10^{-5} mol) was added. The sealed mixture solution was removed from the glove box and placed for 12 h in a ChemStation at 70 °C. The polymerisation was terminated by exposing the catalyst to air. The reaction solution was dissolved in chloroform and passed through an activated neutral alumina column to remove the Cu catalyst. After being concentrated, the solution was poured to methanol to remove BMA monomer. Yield 50.1 mg (70 %). GPC data: M_n = 4.3 x 10^4, M_w/M_n = 1.08 (averaged number of repeating unit: 306 (PBMA$_{306}$)).

(a)

(b)

(c)
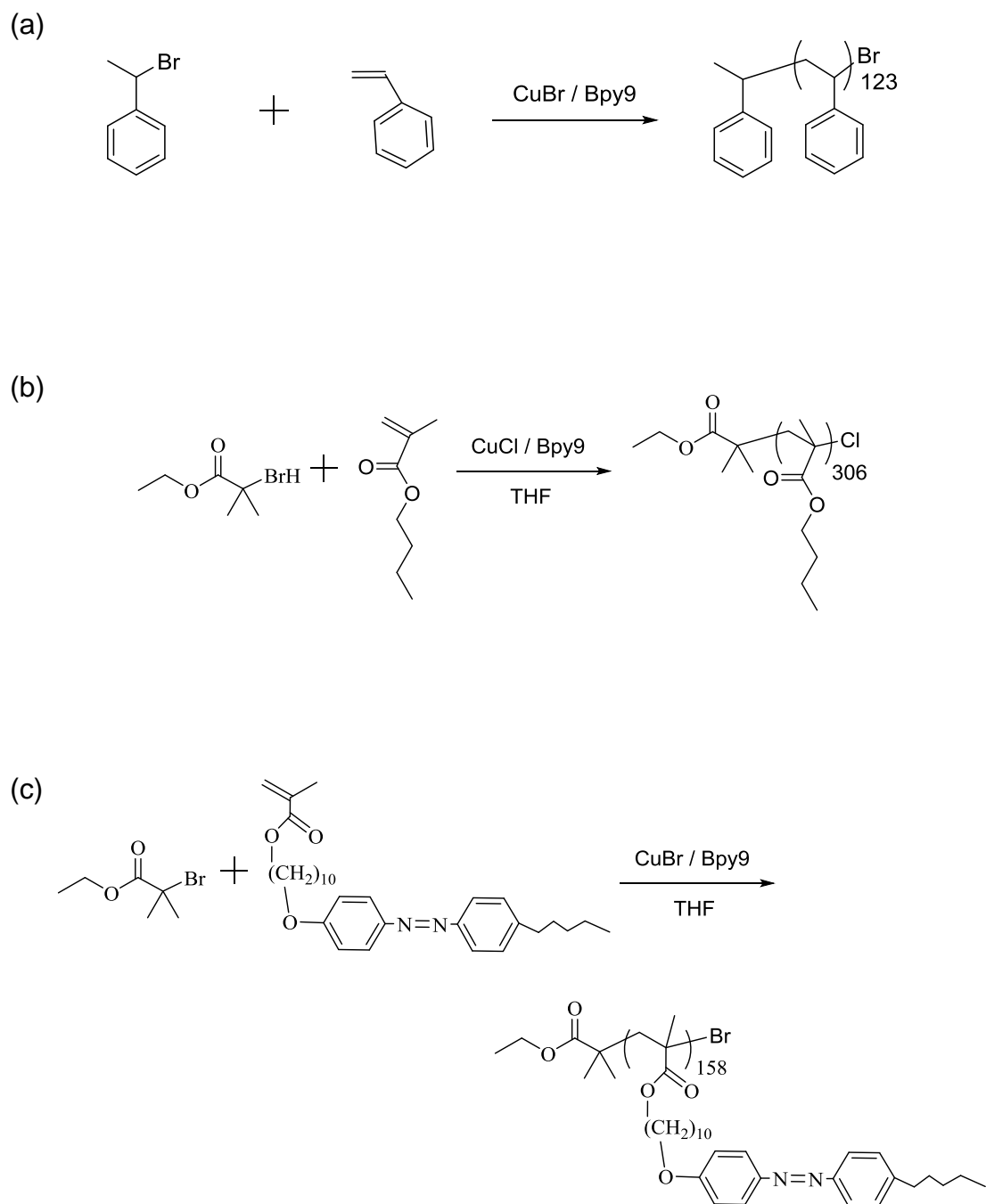
Scheme 1. The synthetic route of (a) PS-Br, (b) PBMA-Cl and (c) PAz-Br homopolymers.

2-2-2-3. Polymerization of PAz via ATRP

Synthesis of 4-(10-methacryloyloxydecyloxy)-4'-pentylazobenzene (Az) was described previously.[29] Synthetic route of PAz is shown in Scheme 1c. CuBr (19.2 mg, 1.3 x 10^{-4} mol), Bpy9 (109.6 mg, 2.7 x 10^{-4} mol) and Az monomer (1.3 g, 2.7 x 10^{-3} mol) were added into a 15 ml pressure glass tube. The mixture was dissolved in THF (2.7 ml) in glove box. The resulting mixture was stirred for 10 min, and then EBB (2.0 μl, 1.3 x 10^{-5} mol) was added. The sealed mixture solution was removed from glove box and placed for 24 h in ChemStation at 70 °C. The polymerization was terminated by exposing the catalyst to air. The reaction solution was dissolved in chloroform and passed through an activated neutral alumina column to remove the Cu catalyst. After being concentrated, the solution was poured to hexane to remove Az monomer. Yield 1.1 g (85 %). GPC data: M_n = 8.0 x 10^4, M_w/M_n = 1.13 (averaged number of repeating unit : 158 (PAz$_{158}$)). Thermophysical properties by DSC: glass43 °C-SmC-100 ^{o}C-SmA-120 ^{o}C-iso.

2-2-2-4. Synthesis of diblock copolymer PS-*b*-PAz via ATRP

Scheme 2a. shows synthetic route of PS-*b*-PAz. PS-Br (58.0 mg, 4.5 x 10^{-6} mol), CuCl (33.9 mg, 3.4 x 10^{-4} mol), Bpy9 (278.4 mg, 6.8 x 10^{-4} mol), and 5Az10MA (894.7 mg, 1.8 x 10^{-3} mol) were add into a 15 ml pressure glass tube. The mixture was dissolved in THF (0.95 ml) in glove box. The sealed mixture solution was removed from the glove box and placed for 24 h in a ChemStation at 70 °C. The polymerization was stopped by exposing the catalyst to air. The reaction solution was dissolved in chloroform and passed through an activated neutral alumina column to remove the Cu catalyst. After being concentrated, the solution was poured to methanol to remove PS-Br macroinitiator and Az monomer. The averaged number of repeating unit of styrene and Az being 123 and 218, respectively (PS$_{123}$-*b*-PAz$_{218}$); M_n = 1.2 x 10^5, M_w/M_n = 1.29. Thermophysical properties by DSC: glass-59 °C -SmC-90 °C-SmA-118 °C-iso, glass transition temperature (T_g) of PS = ca. 104 °C.
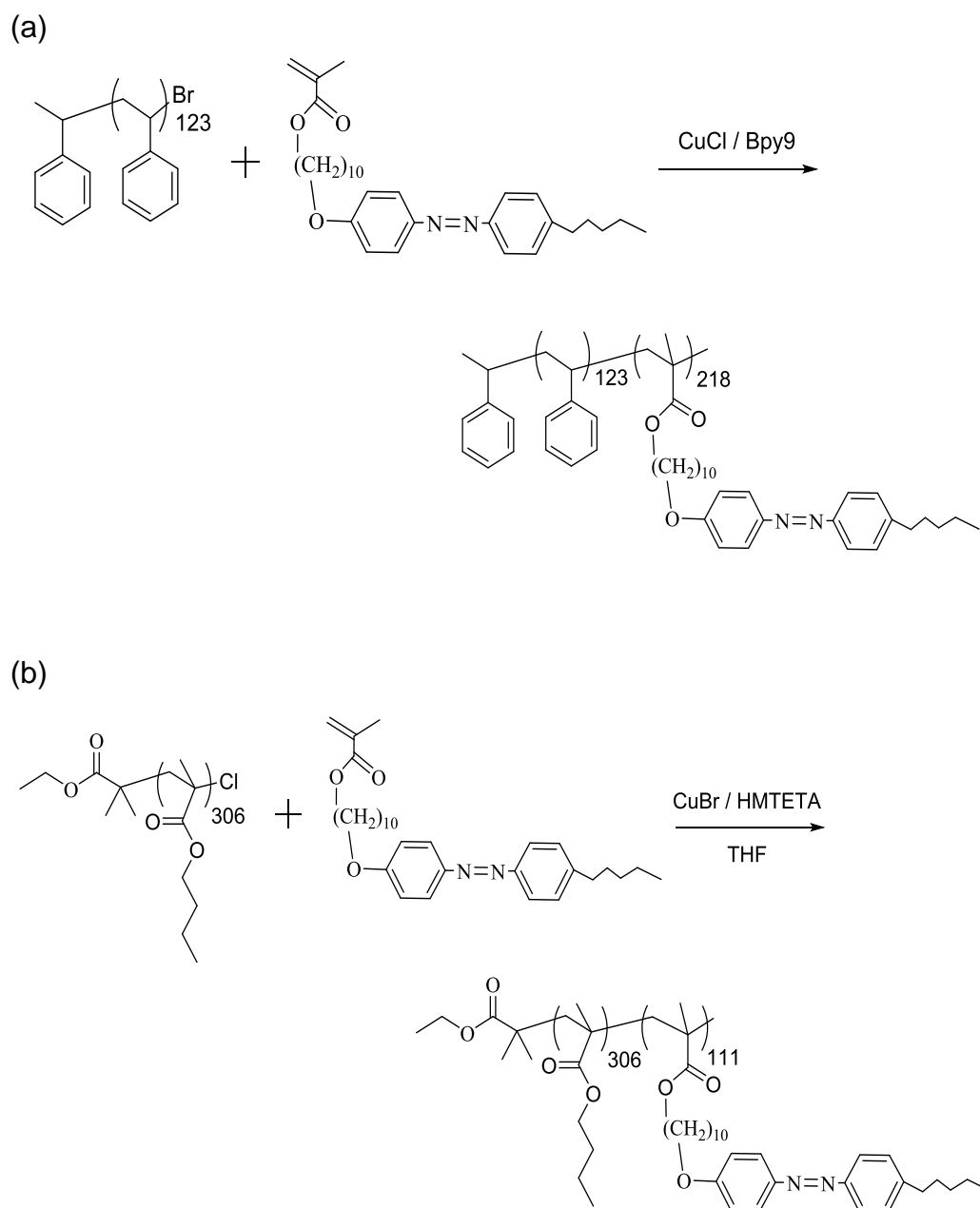
Scheme 2. The synthetic route of (a) PS-*b*-PAz, (b) PBMA-*b*-PAz block polymers.

2-2-2-5. Synthesis of diblock copolymer PBMA-*b*-PAz via ATRP

Scheme 2b. shows synthetic route of PBMA-*b*-PAz. PBMA-Cl (0.5 g, 1.1 x 10^{-5} mol), CuBr (16.5 mg, 1.1 x 10^{-4} mol), HMTETA (31.0 μl, 1.1 x 10^{-4} mol), and 5Az10MA (0.9 g, 1.7 x 10^{-3} mol) were add into a 15 ml pressure glass tube. The mixture was dissolved in THF (0.9 ml) in glove box. The sealed mixture solution was removed from the glove box and placed for 24 h in a ChemStation at 70 °C. The polymerisation was terminated by exposing the catalyst to air. The reaction solution was dissolved in chloroform and passed through an activated neutral alumina column to remove the Cu catalyst. After being concentrated, the solution was poured to methanol to remove PBMA-Cl macroinitiator and Az monomer. The averaged number of repeating unit of BMA and Az being 306 and 111, respectively (PBMA$_{306}$-*b*-PAz$_{111}$); M_n = 8.3 x 10^4, M_w/M_n = 1.22. Thermophysical properties by DSC: glass-57 °C-SmC-90 °C-SmA-118 °C-iso, T_g of PBMA = ca. 20 °C.

2-2-3. Preparation of blend thin films

Thin films were prepared by spin coating from a chloroform solution and successively annealing the films at 130 °C for 10 min. The films were irradiated with LPL of 436 nm visible light at 1000 mJ cm^{-2} through an optical polarizer. Linear polarized light at 436 nm irradiated on cooling process under immersing in the liquid. The in-plane anisotropy of the Az chromophore, smectic phase and the MPS structure alignment in the resulting films were observed by the polarized absorption spectroscopy and grazing incidence small angle X-ray scattering (GI-SAXS) measurement, respectively.

2-2-4. Characterizations

2-2-4-1. ^{1}H NMR

^{1}H NMR spectra (JNM-GSX270, JEOL) was recorded 16 th steps using tetramethylsilane as the internal reference for deuterated chloroform solution (Across).

A small amount of polymerized solution was measured and conversion of polymerization was calculated by value of integral of a monomer and a polymer. Thus, redeposit samples was checked whether to remain a monomer and a macroinitiator.

2-2-4-2. Gel-permeation chromatography

Gel-permeation chromatography (GPC) has been used a measuring of size-exclusion chromatography (SEC) (Shodex DS-4/UV-41/RI-101) and GPC two columns (Shodex KF-403 and KF-405). THF was used as an eluent at a flow rate of 1.0 mL/min. The calibration of molecular weight was calculated by using polystyrene standards (TSK standard polystyrene, TOSOH). The polymerization products of polymers were used by GPC to calculate distribution of molecular weight.

2-2-4-3. Differential scanning calorimetry

Differential scanning calorimetry (DSC) (TA DSC Q200) has been used a measuring tool of calorimeter. DSC scans were performed within the temperature range 25~200 °C at a heating rate of 2 °C min^{-1} under nitrogen. About 5.00 mg mass was used for DSC measurements for all samples. An empty aluminum pan was used as a reference. The glass transition (T_g) and between the liquid crystal phase and the isotropic phase transition temperature was determined by DSC scans.

2-2-4-4. UV-Vis absorption spectroscopy

Polarized UV-visible absorption spectra were taken on an Agilent 8453 spectrometer (Agilent Technologies) with a polarizer in front of the samples. A source of illumination used a D2-W lamp. Quartz was used as a substrate in measuring thin films. Whether to orient a homeotropic or a planar orientation was judged from absorption wavelength of around 360 nm.

2-2-4-5. Atomic force microscopy

Atomic force microscope (AFM) has been used scanning probe microscope (SPA400) and probe station (SPI3800N) (Seiko Instruments Inc.). Scanner table and silicon-based cantilever (SI-DF20) used to measuring at DFM mode of non-contact.

AFM image size of annealed thin films at 130 ^{o}C for 10 min was 2.0 x 2.0 μm of phase mode for checking cylinder structures.

2-2-4-6. X-ray measurements (WAXS and GI-SAXS)

XRD measurement was performed on voltage 40 kV, current 40 mA, irradiation time 1 h to create copper Cu Kα radiation (λ = 1.542 Å) and camera length was 300 mm (FR-E X-ray diffractometer and R-AXIS IV two-dimensional (2D) detector) (Rigaku Co.). It was read and measured an X-ray diffraction pattern exposed by an imaging plate (FUJIFILM Co.). The diffraction patterns of the in-plane and out-of-plane direction that obtained from thin film samples were informed about Liquid crystalline structures and surface separation of azobenzene. Thus, FR-E was carried on by using a ceramic heater attached on the sample holder of FR-E under controlling temperature. In addition, XRD measurement was performed on voltage 45 kV, current 60 mA and camera length was 960 mm with a detected by the imaging plate. (NANO-Viewer X-ray diffractometer) (Rigaku Co.). GI-SAXS measurements were carried on the incident angles of X-ray beam to the films were set at 0.18-0.22 ^{o} by using pulse controllers (ATS-C316-EM/ALV-300-HM) (CHUO PRECISION INDUSTRIAL CO., LTD.). The diffraction patterns of the in-plane direction were informed about microphase-separated structures of diblock copolymers by GI-SAXS. Samples were stained in RuO$_4$ vapor for ca. 20 min.

2-2-4-7. Transmission electron microscopy (TEM)

For the TEM observation, the thin film was prepared onto a 100 μm thick Kapton film. Annealed thin film was photoaligned by irradiation of linear polarized light (436 nm) under heating at 110 ^{o}C for 1000 s. The sample is previously embedded in epoxy resin (Quetol-812, Nissin EM). After curing, the sample is microtomed using an Ultracut N microtome, Reichert-Nissei. Diamond knives (ultra 35°, DIATOME) were used for both the trimming and cutting process. The sample was trimmed and cut at r. t. From the ultra-microtoming process, ca. 200 nm thick slices are obtained and placed

over carbon coated copper grids (grid 75/300 mesh Cu, Veco). The thin sections were picked up onto copper grids and stained in RuO_4 vapor for ca. 10 min. TEM (H-800, HITACHI Co.) is performed with electron beam energy of 100 keV.

2-3. Results and Discussion

2-3-1. Induced planar orientation of PBMA-*b*-PAz/PAz blend films

First, the alignment behaviour of an LC Az homopolymer (PAz in Figure 1a, M_n =8.0 x 10^4, M_w/M_n = 1.13 and g-43 °C-SmC-100 °C-SmA-120 °C-iso) was examined. A spincast film of PAz was prepared (thickness: 100-200 nm) from a chloroform solution. After annealing at 130 °C (above the isotropisation temperature) for 10 min followed by gradual cooling via a smectic LC phase to room temperature, this film spontaneously formed the out-of-plane (perpendicular) orientation of Az side mesogens, as judged by a significant reduction in $\pi-\pi^*$ light absorption around 320 nm (1b, solid line). By adding 10 weight % (%) PBMA-*b*-PAz in Figure 1a (M_n = 8.3 x 10^4, M_w/M_n = 1.22, g-57 °C-SmC-90 °C-SmA-118 °C-iso, T_g (PBMA) = ca 20 °C), the same procedure led to a drastic spectral change (dotted line), showing that the Az mesogenic group of the total PAz film tends to orient randomly or nearly parallel to the substrate.

In the grazing angle incidence X-ray diffraction (GI-XRD) measurement (Figure 2a and b), the diffraction spots ascribed to the smectic layer structure of pure PAz and PBMA-*b*-PAz (10 %)/PAz blend films of the Az mesogens (d = 3.5 nm) were observed in the out-of-plane (vertical, d = 3.3 nm) (a) and in-plane(horizontal, d = 3.5 nm) (b) directions, respectively. Thus, marked orientational alternations in the molecular and layer orientations were observed by the adding PBMA-*b*-PAz. Addition of the same amount of PBMA homopolymer did not lead to this effect, indicating that sufficient compatibility of the block copolymer of PBMA-*b*-PAz containing the PAz block is required for the alignment alternation.

(a)
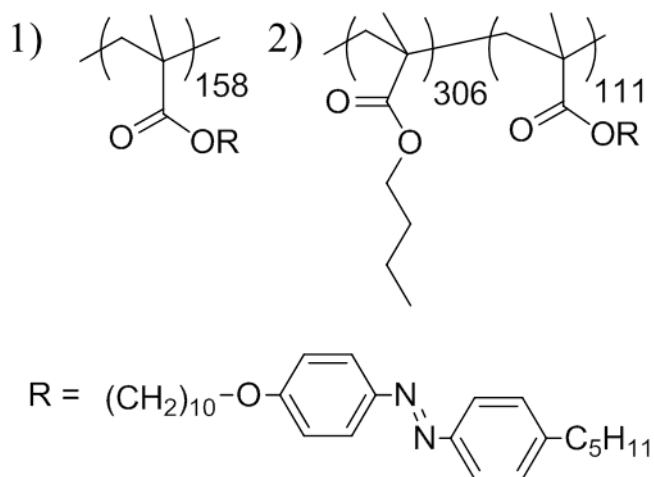
(b)
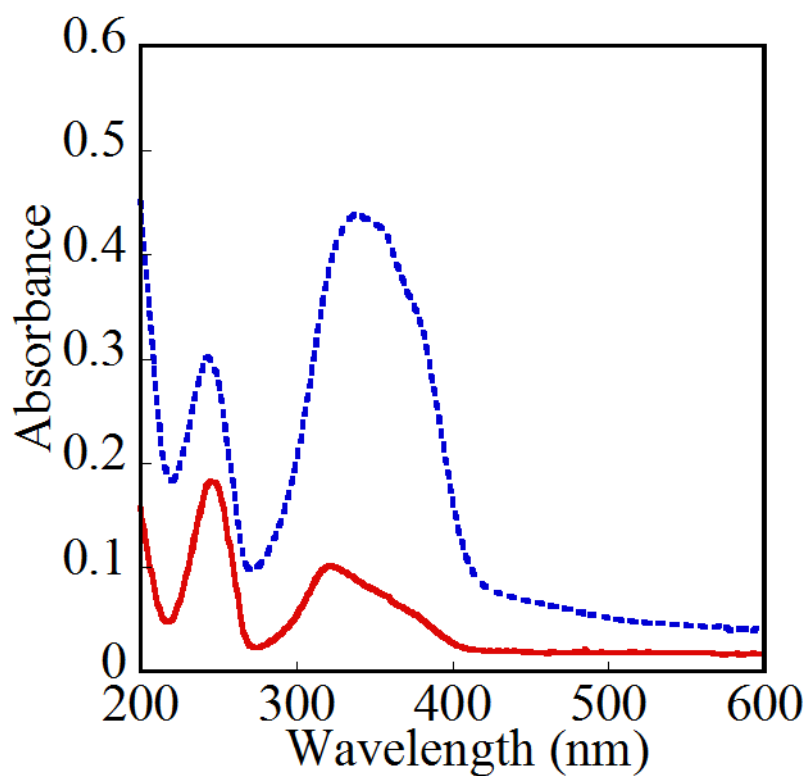
Figure 1. (a) Molecular formula of PAz and PBMA-*b*-PAz. (b) UV-Vis absorption spectra of the PAz thin film (solid line) and the PBMA-*b*-PAz (10%) /PAz blend thin film (dotted line) after annealing at 130 °C.
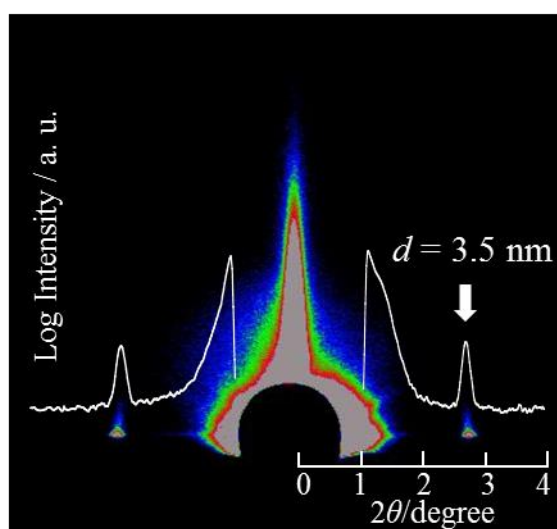
(a)
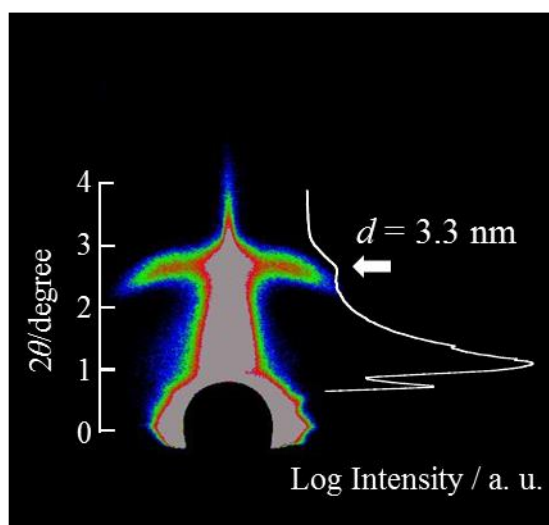
(b)

Figure 2. (a) and (b) show the 2D GI-XRD patterns of pure PAz film and PBMA-*b*-PAz (10%)/PAz blend thin films after annealing at 130 °C, respectively. In the XRD patterns, 1D intensity profiles are indicated as white lines.

2-3-2. The contact angles on the surfaces of the polymer films

The contact angles of water droplets (θ_w) on the surfaces of the polymer films under study are summarised in Table 1. For all polymer films, annealing led to slightly larger θ_w, indicating that more hydrophobic moieties, such as the hydrocarbon part and the chain ends,[33] became exposed to the air side. θ_w of the PAz homopolymer (107 ± 0.9 °) was significantly lowered by adding 10 % PBMA-*b*-PAz to 95.5 ± 0.2 °. The lowered value virtually agrees with that of a pure PBMA-*b*-PAz film (θ_w = 97.0 ± 0.6 °), indicating that the minor amount of PBMA-*b*-PAz migrated and was enriched at the free surface. This enrichment of PBMA-*b*-PAz should occur because of the lower surface free energy of PBMA[34] and also because of the entropic requirement,[35] i.e., PBMA possessing a flexible side chain (T_g = 20 °C) should migrate to the free surface. The direct visual evidence of the PBMA-*b*-PAz segregation at the surface will be discussed later for the block copolymer system. Thus, PBMA-*b*-PAz works as a free-surface-active polymer.

2-3-3. Induced planar orientation of PBMA-*b*-PAz/PS-*b*-PAz blend films

Next, the same procedures were conducted for a polystyrene (PS)-based block copolymer film (PS-*b*-PAz in Figure 3a, M_n = 1.2 x 10^5, M_w/M_n = 1.29, and g-59 °C-SmC-90 °C-SmA-118 °C-iso, T_g (PS) = ca 104 °C) that forms cylindrical MPS domains of coiled PS. UV-Vis absorption spectra of pure PS-*b*-PAz and blended PBMA-*b*-PAz (10 %)/PS-*b*-PAz films after annealing at 130 °C for 10 min followed by a gradual cooling are shown in Figure 3b. These marked changes show that, also for the block copolymer system, the homeotropic-to-parallel orientational change of Az mesogens occurs upon addition of the PBMA-*b*-PAz and subsequent annealing.

GI-XRD measurements revealed that the addition of PBMA-*b*-PAz and annealing drastically changes the orientation of the smectic layer (d = 3.6 nm), as shown in Figures 4. The MPS cylindrical pattern within the PBMA-*b*-PAz (10 %)/PS-*b*-PAz film are oriented parallel to the substrate following the Az mesogen alignment.[30,31]

Table 1 Contact angles of water droplet (θ_w) on polymer surfaces of as-cast films and after annealing at 130 °C.

Compound	Contact angle θ_w (°)	
	As-cast	After annealing
PS	95.0 ± 0.9	98.0 ± 0.7
PBMA	95.0 ± 1.0	99.7 ± 1.0
PAz	103.7 ± 0.3	107.2 ± 0.9
PS-*b*-PAz	103.4 ± 0.7	109.8 ± 0.9
PBMA-*b*-PAz	95.2 ± 0.7	97.0 ± 0.6
PAz/PBMA-*b*-PAz	94.3 ± 0.8	95.5 ± 0.2
PS-*b*-PAz/PBMA-*b*-PAz	95.3 ± 0.8	99.5 ± 0.5

(a)
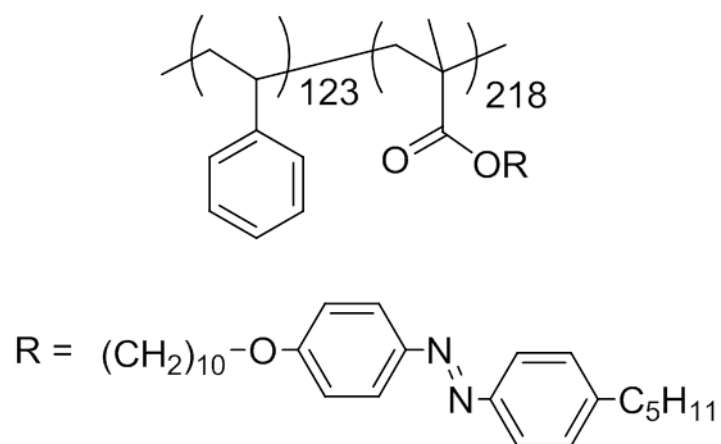
(b)
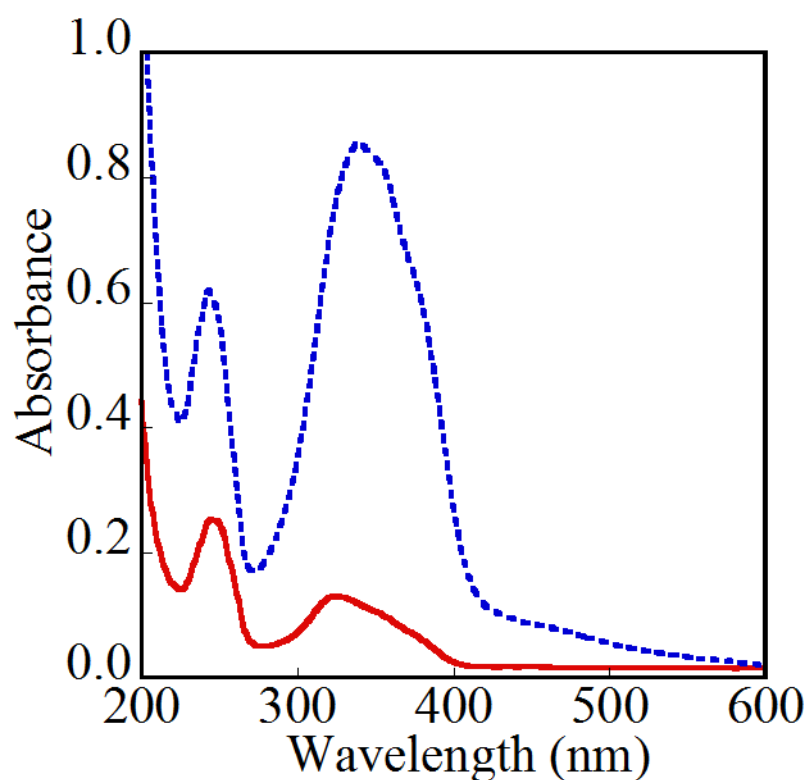
Figure 3. (a) Molecular formulus of PS-*b*-PAz, (b) UV-Vis absorption spectra of a PS-*b*-PAz thin film (solid line) and the PBMA-*b*-PAz (10%)/PS-*b*-PAz blend thin film (dotted line) after annealing at 130 ℃.

(a)
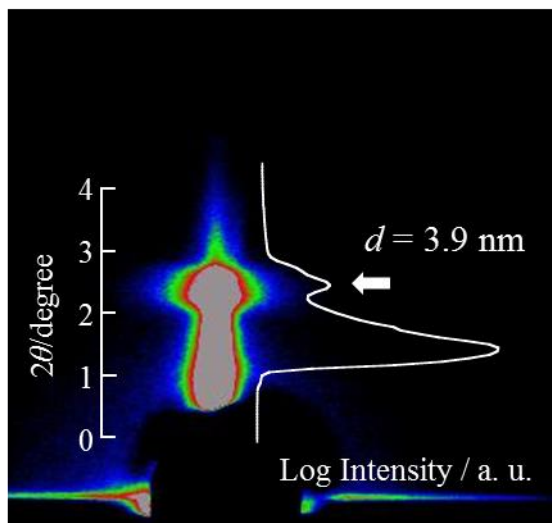
(b)
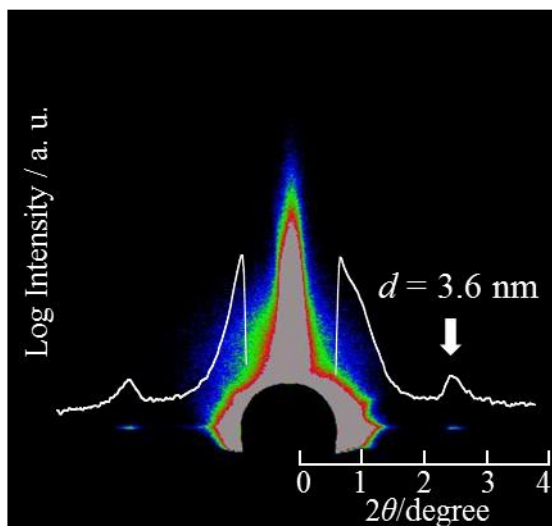
Figure 4. (a) and (d) show the 2D GI-XRD patterns of pure PS-*b*-Az film and PBMA-*b*-PAz (10%)/PS-*b*-PAz blend thin films after annealing at 130 °C, respectively. In the XRD patterns, 1D intensity profiles are indicated as white lines.

39

Similarly to the PAz homopolymer case, θ_w of the PS-*b*-PAz film surface significantly decreased from 109.8 ± 0.9 ° to 99.5 ± 0.5 ° (Table 1) by adding 10 % PBMA-*b*-PAz and annealing, which is indicative of the surface segregation and enrichment of PBMA-*b*-PAz. The surface morphology evaluated by atomic force microscopy (AFM) revealed that the vertically oriented cylindrical domains of PS are exposed to the surface in the pure PS-*b*-PAz film (Figure 5a). The AFM image in the phase mode showed a dot array structure (average dot-to-dot distance; 46 ± 0.7 nm), which coincides well with the $2/\sqrt{3}$ times the (1 0) cylindrical plane spacing of the bulk structure (40 nm) assuming hexagonal packing. In contrast, the surface of the blend film of PBMA-*b*-PAz (10 %)/PS-*b*-PAz exhibited a highly uniform surface. This fact directly shows that the MPS domains of PS-*b*-PAz are buried beneath the surface-segregated PBMA-*b*-PAz layer (Figure 5b).

2-3-4. Photoalignment of liquid crystalline polymer and block copolymer

Based on these observations, the photoalignment behaviour by irradiation with linearly polarised light (LPL) was examined for the surface-segregated films because the planar orientation of Az mesogenic groups is favourable for photoalignment in the in-plane directions.[36,37] The PAz homopolymer and PS-*b*-PAz blended with 10 % PBMA-*b*-PAz and annealing at 130 °C for 10 min first, and then irradiated with 436 nm LPL at 1 mW cm^{-2} for 1000 s at 90 °C and 110 °C was performed, for PAz and PS-*b*-PAz, respectively. The resultant polarised UV-Vis absorption spectra are shown in Figures 6a and 6b. In both cases, highly aligned Az mesogens in the in-plane direction were obtained. The order parameter S [$= (A_\perp - A_\parallel)/(A_\perp + 2A_\parallel)$], where $A_\perp$ and $A_\parallel$ denote absorbance at the λ_{max} of the $\pi-\pi*$ absorption band of the Az unit (ca. 350 nm) obtained by measurements using polarised light with *E* perpendicular and parallel to that of actinic polarised light respectively, reached 0.67 and 0.48, respectively. The GI-XRD results indicate the existence of more ordered, vertically aligned smectic layers in the film when the direction of the X-ray beam incidence was set orthogonal to the actinic

(a)
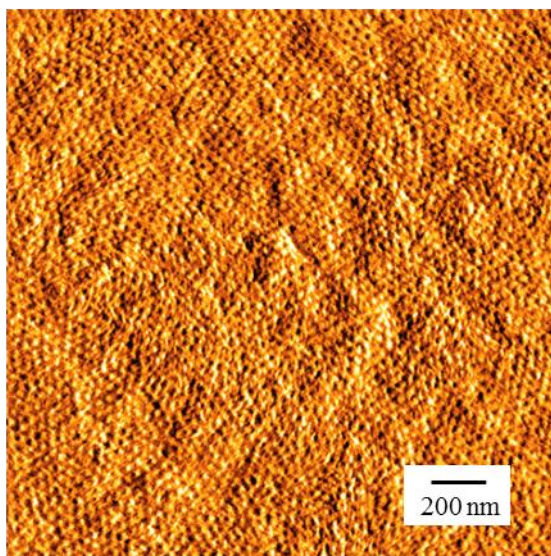
(b)
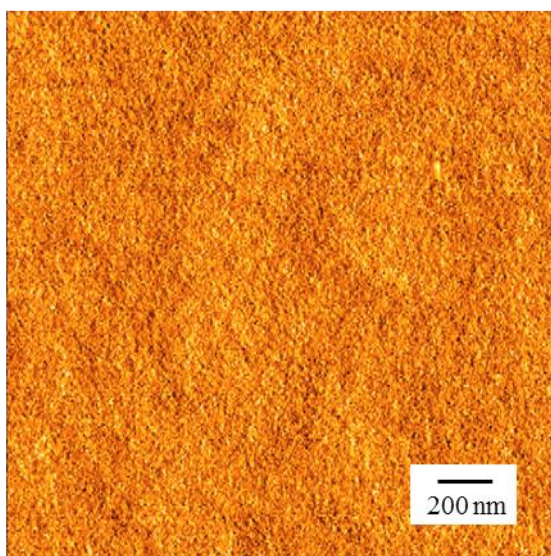
Figure 5. (a) and (b) indicate 2.0 x 2.0 µm AFM images (phase mode) of annealed PS-*b*-PAz and PBMA-*b*-PAz (10%)/PAz blend films, respectively.

(a)

(b)
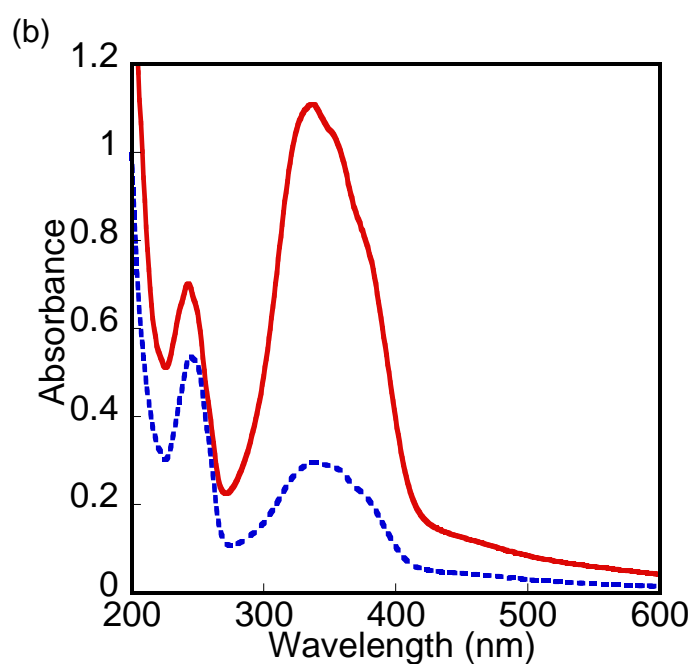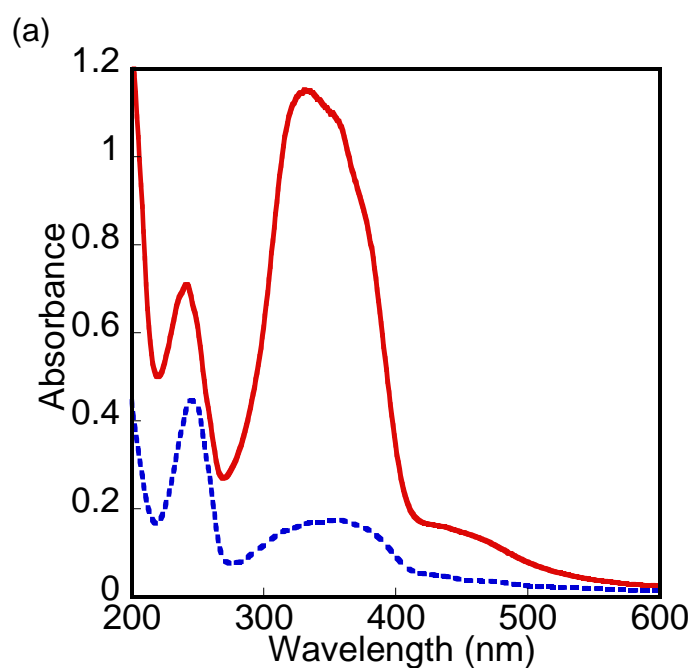
Figure 6. UV-Vis absorption spectra of PBMA-*b*-PAz (10 %)/PAz (a) and PBMA-*b*-PAz (10%)/PS-*b*-PAz blend (b) films after irradiation with 436 nm LPL at 1000 mJ cm^{-2}. The spectra were taken with the probing beam parallel (dotted line) and orthogonal (solid line) to the actuating light.

(a)
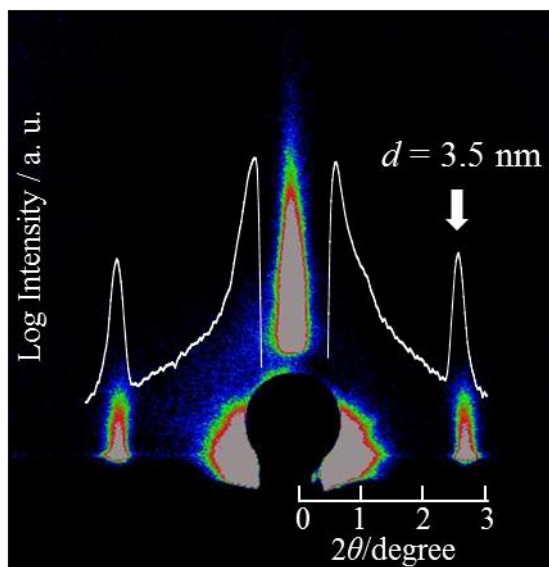
(b)
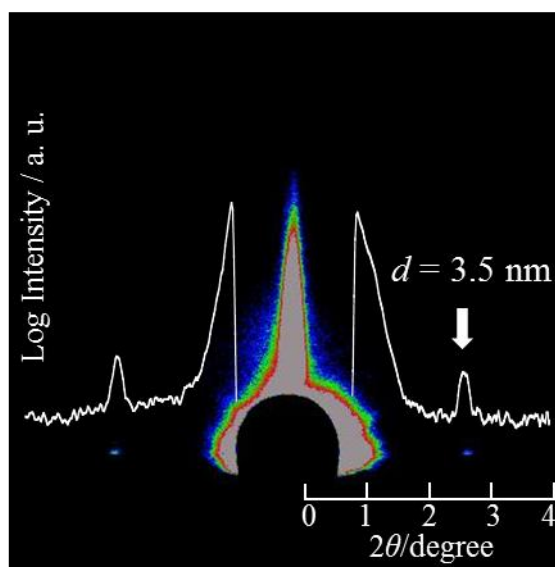
Figure 7. (a) and (b) show the 2D GI-XRD patterns of LPL-irradiated PBMA-*b*-PAz (10%)/PAz (homopolymer) and PBMA-*b*-PAz (10%)/PS-*b*-PAz (block copolymer) blend films, respectively (X-ray incidence: orthogonal to the actinic LPL).

LPL direction (Figures 7a and 7b).[30,36,37]

For the photoaligned block copolymer film of PBMA-*b*-PAz (10 %)/PS-*b*-PAz, the structure of the MPS cylinders of the PS-*b*-PAz film was evaluated by GI-small angle X-ray scattering (GI-SAXS) measurements (Figure 8) and transmission electron microscopy (TEM, Figure 9b). The scattering spots in the GI-SAXS were observed at (q = 0.22 nm^{-1} (d = 40 nm, white arrows), which corresponds to the in-plane aligned MPS cylindrical domains.

In the TEM image of a RuO$_4$-stained sample, a cross-section sliced in the parallel direction to the actinic LPL provided regularly arranged dark dot parts of the PS domains within the film with a total thickness of ca. 200 nm. The averaged centre-to-centre domain distance between the PS cylinders was 46 nm, in good agreement with the above X-ray and AFM (Figure 5a) data. It should be noted that the light dose required for MPS alignment is 1000 mW cm^{-2}, which is much less than that required for the relevant PS-*b*-PAz film without the segregated layer (6000 mJ cm^{-2}),[29] indicating that more efficient in-plane MPS domain alignment is attained due to the pre-orientation in the in-plane direction by the surface layer.

More importantly, the TEM image revealed the existence of a thin skin layer of ca. 20 nm thickness at the topmost surface, observed as a brighter region. This surface skin layer should correspond to the surface-segregated PBMA-*b*-PAz. In this case, 10 % PBMA-*b*-PAz was blended, and therefore the thickness of the top layer was almost 10 % of the total thickness. In the skin layer, no MPS was recognised, which can be understood from the fact that the skin thickness is below the level of MPS domain formation of this PBMA-*b*-PAz (lamella-forming polymer with a 49 nm period).

The orientation and alignment behaviours proposed in this work are illustrated in Scheme 3. In the pure PAz film (upper process), the homeotropic anchoring to the free surface of Az mesogens (rodlike orange units) induces the normal orientation. For the PS-*b*-PAz block copolymer film (lower process), the MPS cylindrical domains (blue

(a)
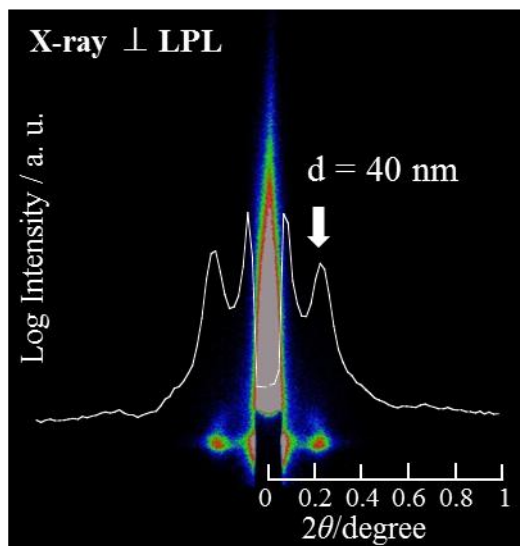
(b)
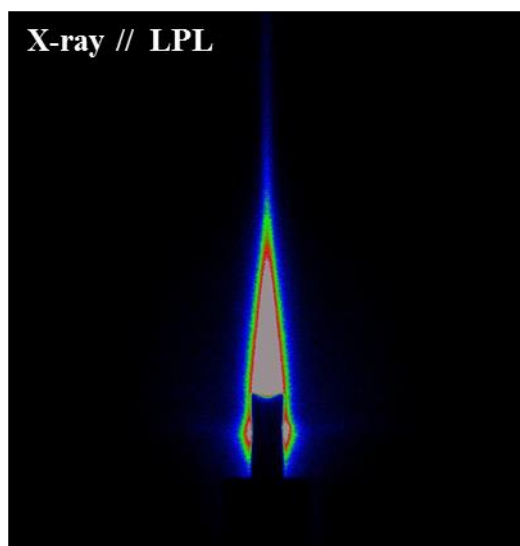
Figure 8. GI-SAXS patterns for the MPS cylinder domain detection (X-ray incidence: parallel (a) and vertical (b) to the actinic LPL). In the GI-XRD and GI-SAXS patterns, 1D intensity profiles are indicated as white lines.

45

(a)

Cut plate
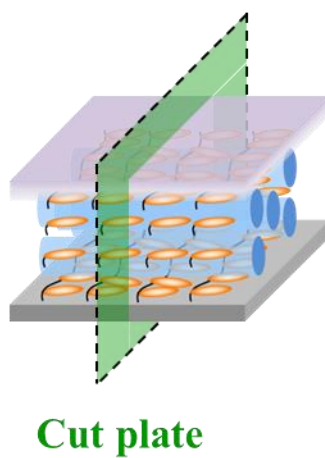
(b)
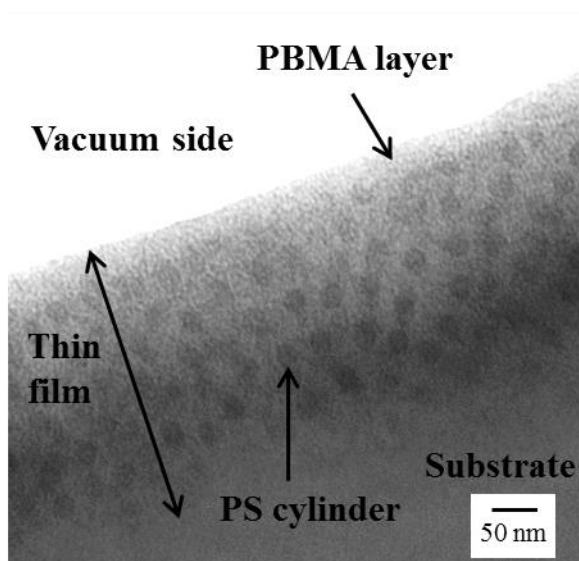
Figure 9. Schematic illustrations of cutting the PBMA-*b*-PAz (10%)/PS-*b*-PAz ultra-thin film (upper) and TEM image of a cross-section. The sample was sliced in the direction parallel to the actinic LPL.
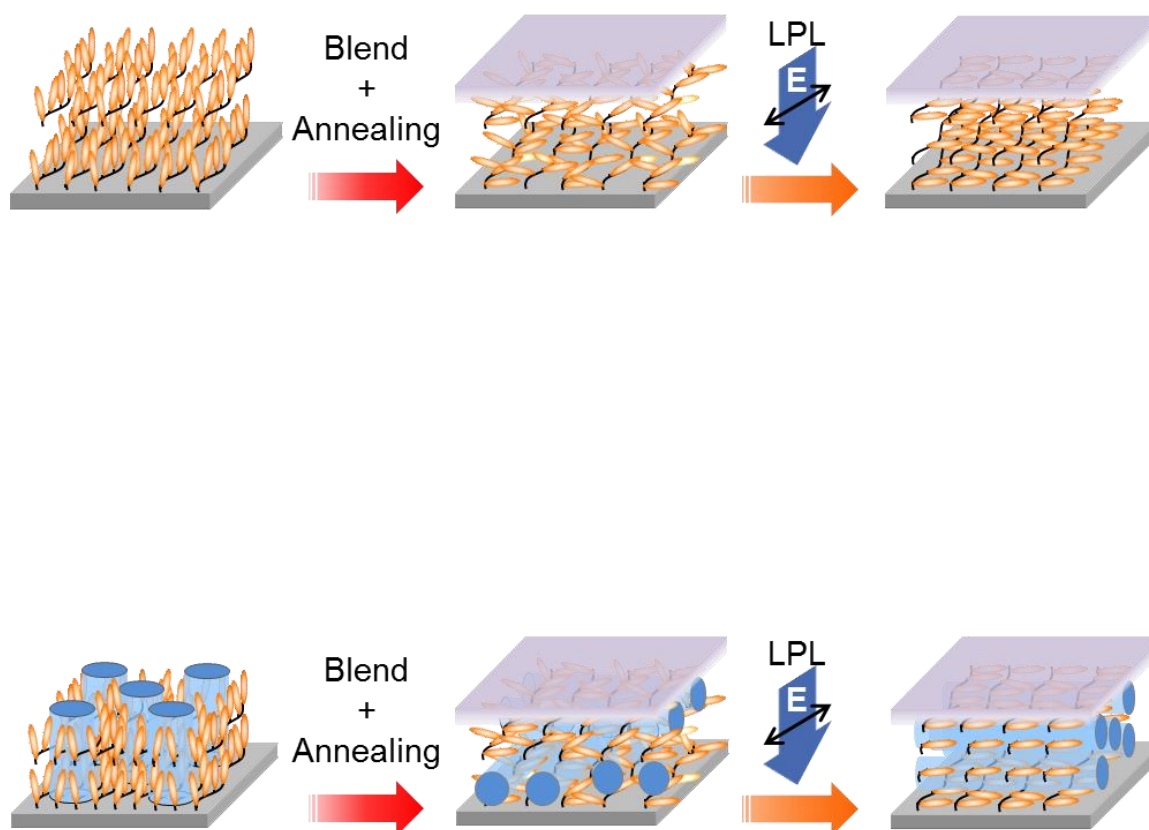
Scheme 3. Schematic illustrations of the alignment process for the PAz homopolymer (upper) and PS-*b*-PAz block copolymer (lower) in this work.

cylinders) are accordingly oriented perpendicularly to the substrate (top left). Blending the surface-active PBMA-*b*-PAz and subsequent annealing lead to a skin layer formation on the surface, which blocks the homeotropic anchoring of Az mesogens, and provides planar orientation of Az mesogens and MPS cylindrical domains with the substrate surface (schemes in the middle for both processes). Due to the preformed parallel orientation, LPL irradiation efficiently leads to homogeneous in-plane alignment orthogonal to the electric field of the LPL (top right schemes for both processes).

The homeotropic anchoring of rodlike LC molecules at the free surface has been predicted by theoretical considerations[21,22,38], and experimental observations of side chain LC polymer thin films are in agreement with this.[39,40,41] When the free surface is covered with a segregated layer, the excluded volume effect from the plane solid substrate should dominate.[42] An alternative explanation can be the tendency to adopt a planar orientation of the mesogenic groups in the segregated PBMA-*b*-PAz.[30] It is noteworthy that the LC mesogens and MPS domain orientations in pure LC polymer films were unaffected by the surface energy of the substrate surface. LC and MPS domain orientations were evaluated for both clean hydrophilic ($\theta_w < 10°$) and hydrophobised ($\theta_w = $ ca. 80°) quartz plate surfaces, and the orientation were the same, regardless of the surface energy of the solid substrate. This fact implies the predominant role of the free surface in the vertical orientation in the LC polymer film. The importance of the free surface for the Az mesogen orientation was also suggested recently by Iyoda et al.[43] Further investigation is needed to elucidate what factors significantly affect the alignment alternation. The blend ratio, molecular weight, block ratio of the added polymer, chemical structure, thermophysical property of the coil block of the added polymer, total film thickness, annealing procedures should greatly influence the orientation behaviour. For example, reduction of the mixing ratio to 5 weight % of PBMA-*b*-PAz resulted in an incomplete planar orientation. It is now

making efforts to gain a better understanding of this phenomenon.

2-4. Conclusions

In conclusion, this work first demonstrates the clear orientational alternations of LC mesogens and the MPS domains by modifying the free surface, which is accomplished by simply blending a surface-active polymer and performing the appropriate annealing step. This strategy is very simple and is therefore expected to open up new possibilities for orientation controls of various types of LC materials. Selective surface segregation of a surface-active polymer component has promising applications for imposing surface functions such as adhesive and frictional properties[44] and for improving biocompatibility.[45] In addition to such functions accessing the 'exterior' phase, the present work indicates that free surface segregation is also valuable for the control of the 'interior' structure of the polymer film.

References

1. B. Jerome, *Rep. Prog. Phys.* **1991**, 54, 391-451.

2. P. Chatelain, *Bull. Soc. Fr. Mineral.*, **1943**, 66, 105.

3. J. Cognard, *Mol. Cryst. Liq. Cryst. Supp. Series* **1982**, 1(supp1), 1-77.

4. M. Schadt, *Liq. Cryst.* **1993**, 14, 73-104.

5. M. Toney, T. Russell, J. Logan, H. Kikuchi, J. Sands, S. Kumar, *Nature* **1995**, 374, 709-711.

6. K. Weiss, C. Woll, E. Bohm, B. Fiebranz, G. Forstmann, B. Peng, V. Scheumann, D. Johannsmann, *Macromolecules* **1998**, 31, 1930-1936.

7. D. Berreman, *Phys. Rev. Lett.* **1972**, 28, 1683-1686.

8. T. Ohzono, J. Fukuda, *Nat. Commun.* **2012**, 3.

9. K. Ichimura, *Chem. Rev.* **2000**, 100, 1847-1873.

10. T. Seki, *Bull. Chem. Soc. Jpn.* **2007**, 80, 2084-2109.

11. K. Ichimura, Y. Suzuki, T. Seki, A. Hosoki, K. Aoki, *Langmuir* **1988**, 4, 1214-1216.

12. W. Gibbons, P. Shannon, S. Sun, B. Swetlin, *Nature* **1991**, 351, 49-50.

13. M. Schadt, K. Schmitt, V. Kozinkov, V. Chigrinov, *Jpn. J. Appl. Phys.* **1992**, 31, 2155-2164.

14. O. Yaroshchuk, Y. Reznikov, *J. Mater. Chem.* **2012**, 22, 286-300.

15. S. Chae, B. Hwang, W. Jang, J. Oh, J. Park, S. Lee, K. Song, H. Baik, *Soft Matter* **2012**, 8, 1437-1442.

16. J. Brake, M. Daschner, Y. Luk, N. Abbott, *Science* **2003**, 302, 2094-2097.

17. J. Brake, N. Abbott, *Langmuir* **2007**, 23, 8497-8507.

18. T. Seki, K. Fukuda, K. Ichimura, *Langmuir* **1999**, 15, 5098-5101.

19. M. Kidowaki, T. Fujiwara, K. Ichimura, *Chem. Lett.* **1999**, 641-642.

20. T. Fujiwara, J. Locklin, Z. Bao, *Appl. Phys. Lett.* **2007**, 90, 232108.

21. B. Ocko, A. Braslau, P. Pershan, J. Alsnielsen, M. Deutsch, *Phys. Rev. Lett.* **1986**, 57, 94-97.

22. P. S. Pershan, *Faraday Discuss. Chem. Soc.* **1990**, 89, 231-245.

23. N. Scaramuzza, C. Berlic, E. Barna, G. Strangi, V. Barna, A. Ionescu, *J. Phys. Chem. B* **2004**, 108, 3207-3210.

24. S.-M. Chen, T.-C. Hsieh, R.-P. Pan, *Phys. Rev. A* **1991**, 43, 2848-2857.

25. A. A. Canabarro, I. N. de Oliveira, M. L. Lyra, *Phys. Rev. E* **2008**, 77, 011704.

26. Q. Bhatia, D. Pan, J. Koberstein, *Macromolecules* **1988**, 21, 2166-2175.

27. K. Tanaka, A. Takahara, T. Kajiyama, *Macromolecules* **1998**, 31, 863-869.

28. E. Huang, T. Russell, C. Harrison, P. Chaikin, R. Register, C. Hawker, J. Mays, *Macromolecules* **1998**, 31, 7641-765.

29. Y. Morikawa, T. Kondo, S. Nagano, T. Seki, *Chem. Mater.* **2007**, 19, 1540-1542.

30. S. Nagano, Y. Koizuka, T. Murase, M. Sano, Y. Shinohara, Y. Amemiya, T. Seki, *Angew. Chem., Int. Ed.* **2012**, 51, 5884-5888.

31. H. Yu, T. Iyoda, T. Ikeda, *J. Am. Chem. Soc.* **2006**, 128, 11010-11011.

32. C. Bates, T. Seshimo, M. Maher, W. Durand, J. Cushen, L. Dean, G. Blachut, C. Ellison, C. Willson, *Science* **2012**, 338, 775-779.

33. D. Kawaguchi, K. Tanaka, T. Kajiyama, A. Takahara, S. Tasaki, *Macromolecules* **2003**, 36, 6824-6830.

34. M. Khayet, M. Alvarez, K. Khulbe, T. Matsuura, *Surf. Sci.* **2007**, 601, 885-895.

35. S. Wu, *J. Phys. Chem.* **1970**, 74, 632-638.

36. T. Uekusa, S. Nagano, T. Seki, *Macromolecules* **2009**, 42, 312-318.

37. H. A. Haque, S. Nagano, T. Seki, *Macromolecules* **2012**, 45, 6095-6103.

38. H. Kimura, H. Nakano, *J. Phys Soc. Jpn.* **1985**, 54, 1730-1736.

39. B. Sapich, A. Vix, J. Rabe, J. Stumpe, *Macromolecules* **2005**, 38, 10480-10486

40. N. Zettsu, T. Seki, *Macromolecules* **2004**, 37, 8692-8698.

41. S. Asaoka, T. Uekusa, H. Tokimori, M. Komura, T. Iyoda, T. Yamada, H. Yoshida, *Macromolecules* **2011**, 44, 7645-7658.

42. K. Okano, Jpn. *J. Appl. Phys.* **1983**, 22, L343-L344.

43. H. Komiyama, T. Iyoda, K. Kamata, *Chem. Lett.* **2012**, 41, 110-112.

44. T. Schaub, G. Kellogg, A. Mayes, R. Kulasekere, J. Ankner, H. Kaiser, *Macromolecules* **1996**, 29, 3982-3990.

45. T. Hirata, H. Matsuno, M. Tanaka, K. Tanaka, *Phys. Chem. Chem. Phys.* **2011**, 13, 4928-4934.

Chapter III

Free Surface-Induced Planar Orientation in Liquid Crystalline Block Copolymer Films: On the Design of Additive Surface Active Polymer Layer

3-1. Introduction

Recently, numerous studies have been carried out to control the orientation of micro phase-separation (MPS) structures of block copolymer films due to the practical interests for nanolithography, fabrication of high density media and photonic crystals.[1,2] Among many aligning techniques, photoalignment methods[3,4] has been becoming increasingly important to achieve on-demand orientation controls of MPS domains.[5,6,7,8]

The photoalignment technique leads to static uniform orientational inductions of MPS structures[5-8] and further to dynamic rewritable functions.[9] It have been demonstrated such dynamic rewritable photoalignment controls by using a block copolymer of poly(butyl methacrylate) (PBMA) connected with an azobenzene (Az)-containing liquid crystalline (LC) polymer (PBMA-*b*-P5Az10MA, see Scheme 2). In this polymer film, the Az mesogens and PBMA cylinder domains are always directed in the in-plane directions, and the out-of-plane induction is not observed. This tendency can be interpreted as a consequence of surface coverage of PBMA possessing a lower surface tension. The importance of the surface coverage in the orientation control of MPS structures have been also pointed out for other block copolymers.[10,11]

The above facts inspired us to investigate blend film systems in which a polystyrene-based Az LC block copolymer (PS-*b*-P5Az10MA, see Scheme 2) exhibiting the homeotropic orientation and the in-plane orienting PBMA-*b*-P5Az10MA are mixed. In such system, it was expected that the addition of a minor amount of
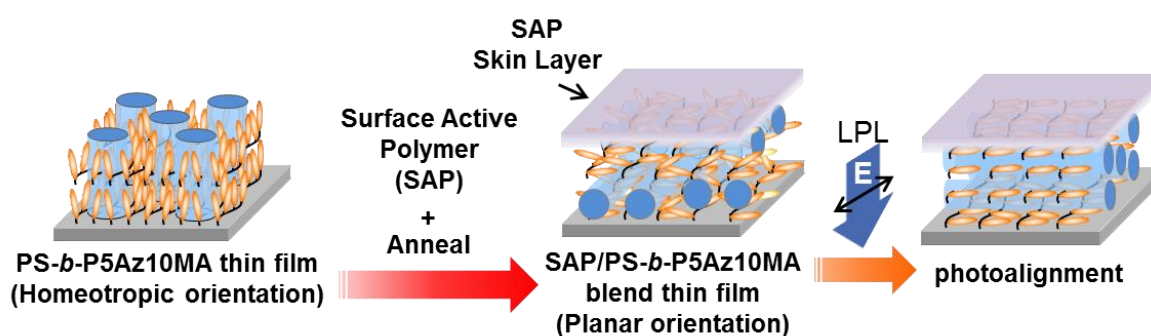
Scheme 1. Illustration of the orientation change of mesogens and MPS domains by the surface segregation layer of SAP and photoalignment process for the PS-*b*-P5Az10MA film described in this study.

PBMA-*b*-P5Az10MA in the PS-*b*-P5Az10MA film crucially changes the molecular and domain orientations from a homeotropic direction to a planar one. Upon annealing, the blended PBMA-*b*-P5Az10MA segregates to the free (air) surface in the blend film due to the lower surface tension, and acts as a surface active polymer (SAP).[12] The plainly oriented MPS cylinder domains are then readily aligned homogeneously by irradiation with linearly polarized light (LPL) (Scheme 1).[12] Surface segregation at the surface and interface is of practical importance.[13,14,15] The present work is achieved to gain further understandings on the design of the SAP (PBMA-*b*-P5Az10MA). Factors such as i) polymer architecture, namely, block copolymer or homopolymer of PBMA, ii) blending amount, and iii) molecular weight of SAP is explored in this work.

3-2. Experimental

3-2-1. Materials

Styrene (99.5 %, Kishida) and butyl methacrylate (BMA) (98.0 %, Wako) were passed through a column filled with neutral alumina to remove polymerization inhibitor, dried over calcium hydride, and distilled under reduced pressure. CuBr (95.0 %, Kanto Chem.) and CuCl (99.9 %, Wako) were washed with acetic acid containing a drop of HCl solution and diethyl ether for several times, and dried in vacuum. The initiators of ethyl 2-bromoisobutyrate (EBB) (98.0 %, Tokyo Chem. Ind.) and 1-phenylethyl bromide (1-PEBr) (95.0 %, Tokyo Chem. Ind.) and the ligands of 4,4′-dinonyl-2,2′-dipyridyl (Bpy9) (97.0%, Aldrich) and 1,1,4,7,10,10-hexamethyltriethylenetetramine (HMTETA) (97.0 %, Aldrich) were used as received. Tetrahydrofuran (THF) of dehydrated stabilizer free grade (Kanto Chem.) was used for polymerization. 90 % active neutral aluminum oxide (Merck, active stage 1, particle size: 63-200 μm) was used for column chromatography.

(a)
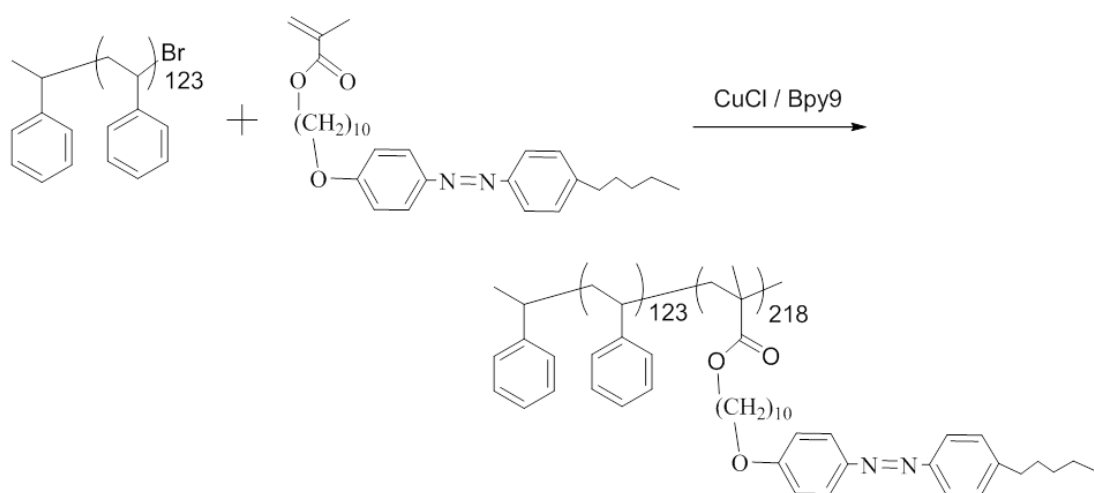
(b)
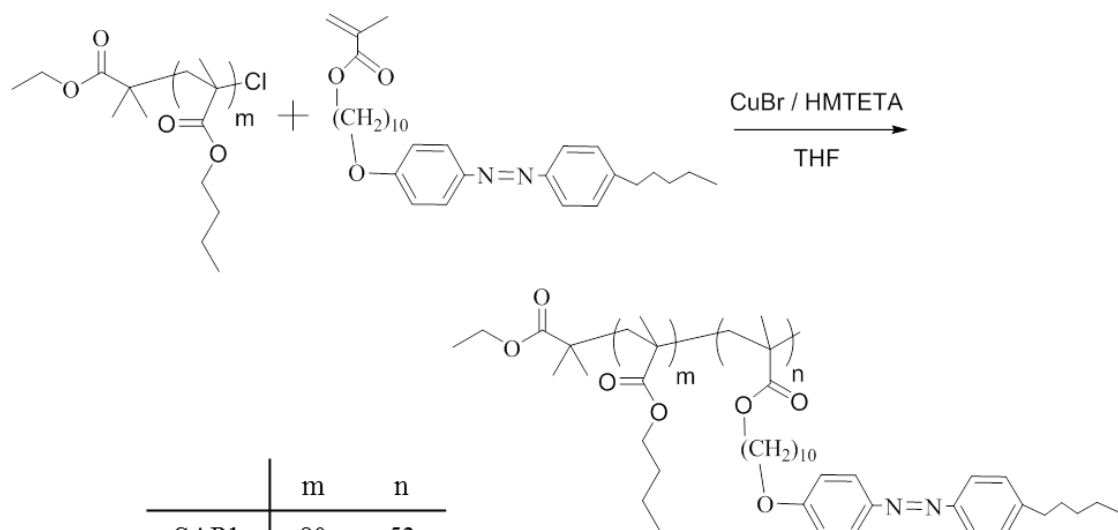
	m	n
SAP1	80	53
SAP2	306	107
SAP3	510	144

Scheme 2. Synthetic route of PS-*b*-P5Az10MA (a) and PBMA-*b*-P5Az10MA (b).

3-2-2. Synthesis of diblock copolymers

3-2-2-1. PS-*b*-P5Az10MA via ATRP

Synthesis of 4-(10-methacryloyloxydecyloxy)-4'-pentylazobenzene (5Az10MA) was described previously. [16] Polystyrene-Br macroinitiator was polymerized by ATRP. Scheme 2a. shows the synthetic route of PS-*b*-P5Az10MA. PS-Br, CuCl, Bpy9, and 5Az10MA were add into a 15 ml pressure glass tube. The mixture was dissolved in THF in glove box. The sealed mixture solution was removed from the glove box and placed for 24 h in a ChemStation at 70 °C. The polymerization was stopped by exposing the catalyst to air. The reaction solution was dissolved in chloroform and passed through an activated neutral alumina column to remove the Cu catalyst. After being concentrated, the solution was poured to methanol to remove polystyrene-Br macroinitiator and 5Az10MA monomer. The averaged numbers of repeating unit of S and 5Az10MA were 123 and 218, respectively (PS_{123}-*b*-P5Az10MA$_{218}$). M_n (^{1}H-NMR) = 1.2 x 10^5, M_w/M_n (GPC) = 1.29. In this paper, this polymer will be denoted as PS-*b*-P5Az10MA.

3-2-2-2. PBMA-*b*-P5Az10MA (SAP) via ATRP

PBMA-Cl macroinitiator was polymerized by ATRP. The polymers were synthesized in similar procedures as described for PS-*b*-P5Az10MA. Scheme 2b shows the synthetic route of PBMA-*b*-P5Az10MA. For this polymer, three block copolymers possessing different molecular weight were synthesized. The block copolymers will be denoted as SAP1, SAP2, and SAP3, the molecular weight being larger in this order, for simplicity (See Scheme 2). M_n (^{1}H-NMR) = 3.7 x 10^4, M_w/M_n (GPC) = 1.27 for SAP1, M_n (^{1}H-NMR) = 9.6 x 10^4, M_w/M_n (GPC) = 1.22 for SAP2, and M_n (^{1}H-NMR) = 1.4 x 10^5, M_w/M_n (GPC) = 1.17 for SAP3. The averaged number of repeating unit of BMA and 5Az10MA were 80 and 53, respectively, for SAP1, 306 and 111, respectively, for SAP2 and 510 and 144, respectively, for SAP3. These data on the numbers of repeating unit are also listed in Scheme 2.

3-2-3. Preparation of thin films and photoirradiation

Thin films of PS-*b*-P5Az10MA and PBMA-*b*-P5Az10MA/PS-*b*-P5Az10MA were prepared by spincoating. In the blended thin films, the PBMA-*b*-P5Az10MA of SAP1, SAP2, and SAP3 were blended at different mixing ratios. After spincoating, thin films were successively annealed at 130 °C for 10 min followed by gradual cooling to room temperature. The thin films were irradiated with LPL (436 nm visible light) at 1000 mJ cm^{-2} through an optical polarizer. Photoirradiation was performed with a REX-250 (ASAHI SPECTRA Co.). LPL at 436 nm was irradiated at 110 °C to the blended PBMA-*b*-P5Az10MA/PS-*b*-P5Az10MA thin film. The in-plane anisotropy of the Az chromophore in the resulting films was evaluated by polarized UV-Visible absorption spectroscopy.

3-2-4. Characterizations

Differential scanning calorimetry (DSC) measurements were achieved with a TA DSC Q200. DSC scans were performed in the temperature range of 30~150 °C at a heating rate of 2 °C min^{-1} under nitrogen. About 5.0 mg of a polymer sample was used for DSC measurements. An empty aluminum pan was used as a reference. The glass transition temperature (T_g) for amorphous polymer chains and phase transition temperatures of LC phase to isotropic phase for the LC block were evaluated by the DSC scans.

Polarized UV-visible absorption spectra were taken on an Agilent 8453 spectrometer (Agilent Technologies) with a polarizer in front of the samples. A D$_2$-W lamp was used as the light source. Quartz plates were used as the substrate for the spectroscopic measurements.

Atomic force microscope (AFM) has been used scanning probe microscope (SPA400) and probe station (SPI3800N) (Seiko Instruments Inc.). Scanner table and silicon-based cantilever (SI-DF20) used to measuring at DFM mode of non-contact.

AFM image size of annealed thin films at 130 ^{o}C for 10 min was 2.0 x 2.0 μm of phase mode for checking cylinder structures.

Grazing incidence small angle X-ray scattering (GI-SAXS) measurement was performed on voltage 45 kV, current 60 mA and camera length was 960 mm with a detected by the imaging plate. (NANO-Viewer X-ray diffractometer) (Rigaku Co.). GI-SAXS measurements were carried on the incident angles of X-ray beam to the films were set at 0.18-0.22^o by using pulse controllers (ATS-C316-EM/ALV-300-HM) (CHUO PRECISION INDUSTRIAL CO., LTD.). The diffraction patterns of the in-plane direction were informed about microphase-separated structures of diblock copolymers by GI-SAXS. Samples were stained in RuO_4 vapor for ca. 20 min.

3-3. Results and Discussion

Thermal properties of the block copolymers were investigated by DSC. Figure 1 shows the DSC curves of the PS_{123}-*b*-$P5Az10MA_{218}$, $PBMA_{80}$-*b*-$P5Az10MA_{53}$ (SAP1) on their second heating processes. In the case of the PS_{123}-*b*-$P5Az10MA_{218}$ on heating, well-defined sharp endothermic transitions was observed at 118 ^{o}C, and minor transition were observed at 59 and 89 °C. These transitions were repeatedly observed on the cooling process at a few degrees lower temperatures due to supercooling. These transitions can be assigned as glass-59 °C -SmC-89 ^{o}C-SmA-118 °C -iso, T_g of PS = ca. 104 ^{o}C). Similarly, SAP1, SAP2, and SAP3 gave endothermic peaks at 116, 118, and 118 ^{o}C, respectively. The three PBMA-based block copolymers differ in molecular weight, however, the minor transition temperatures around 60 and 90 °C did not change, therefore only the DSC profile of SAP1 is displayed in Figure 1b. The transition behavior are assigned as follows. SAP1: glass-60 °C-SmC-91 ^{o}C-SmA-116 ^{o}C-iso, SAP2: glass-61 °C-SmC-91 ^{o}C-SmA-118 ^{o}C-iso, and SAP3 glass-60 °C-SmC-90 ^{o}C-SmA-118 ^{o}C-iso: T_g of PBMA was ca. 20 ^{o}C.
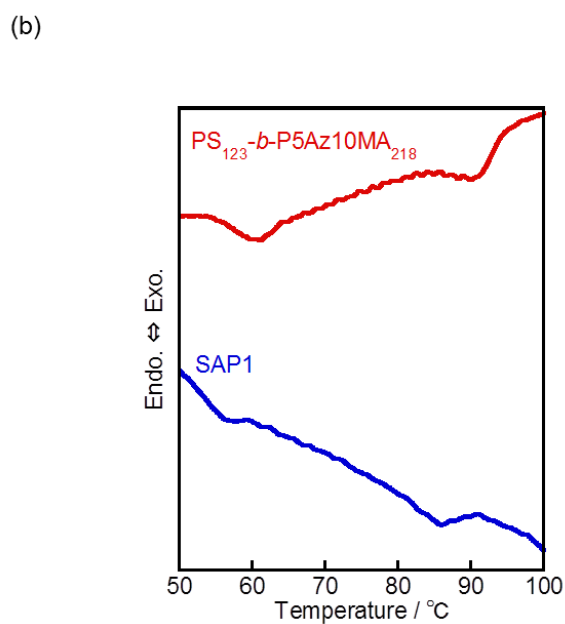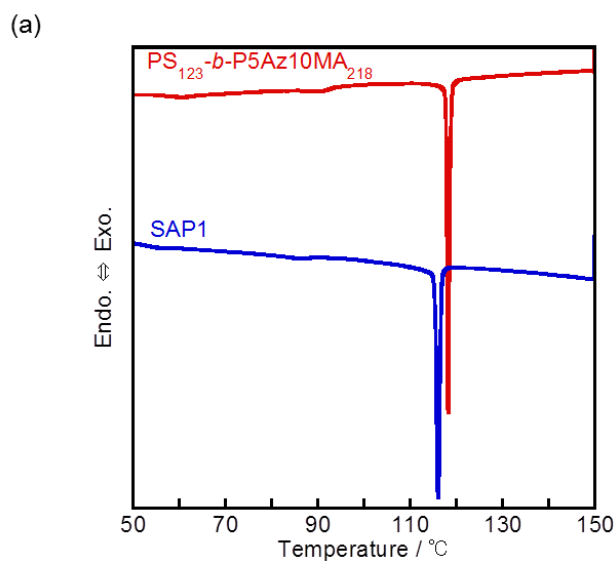
Figure 1. DSC curves of the block copolymers on the second heating of range from 50 to 150 °C (a) and 50 to 100 °C (b) process with a heating rate of ± 2.0 °C/min. Curves are for PS_{123}-*b*-P5Az10MA$_{218}$ and SAP1 are indicated.

A spincast film of PS$_{123}$-*b*-P5Az10MA$_{218}$ prepared from 1 and 2 weight % chloroform solution exhibits cylindrical MPS domains of polystyrene (thickness: 100 − 200 nm. After annealing at 130 °C (above the isotropization temperature of the LC Az block and above T_g of polystyrene) for 10 min followed by gradual cooling via the smectic LC phase to room temperature, this film spontaneously formed a homeotropic orientation of 5Az10MA side mesogens. The surface morphology evaluated by AFM revealed that the vertically oriented cylindrical domains of PS are exposed to the surface in the PS$_{123}$-*b*-P5Az10MA$_{218}$ film (Figure 2a). The AFM image in the phase mode showed a dot array structure (average dot-to-dot distance; 46 ± 0.7 nm). The structure of the MPS cylinders of the PS$_{123}$-*b*-P5Az10MA$_{218}$ film was evaluated by GI-SAXS measurements (Figure 2b). The scattering spots in the GI-SAXS were observed at (q = 0.21 nm^{-1} (d = 42 nm, white arrows), which corresponds to the MPS cylindrical domains.

The annealed PS$_{123}$-*b*-P5Az10MA$_{218}$ film was shown by a significant reduction of the π−π* absorption band of Az unit around 320 nm (Figure 3, 0%). By adding 5, 10 and 20 weight % of SAP1 to PS$_{123}$-*b*-P5Az10MA$_{218}$, the same procedure led to marked spectral changes compare to PS$_{123}$-*b*-P5Az10MA$_{218}$ thin film, showing systematic and considerable increases in the π−π* absorption band. These results indicate that the Az mesogenic groups of the PS$_{123}$-*b*-P5Az10MA$_{218}$ thin film tends to be oriented in more planar directions to the substrate with increasing the amount of blended SAP1.

Addition of the same amount of PBMA homopolymer up to 20 weight % blend did not lead to this effect. This fact strongly suggests the important role of P5Az10MA block in the SAP to cause the orientation change of PS$_{123}$-*b*-P5Az10MA$_{218}$. The PBMA homopolymer did not cover the surface homogeneously but exhibited heterogeneous dewetting on the base PS$_{123}$-*b*-P5Az10MA$_{218}$ film.

Based on these UV-Visible absorption spectra, the in-plane photoalignment control by irradiation with linearly polarized light (LPL) at 436 nm was examined for

(a)

(b)
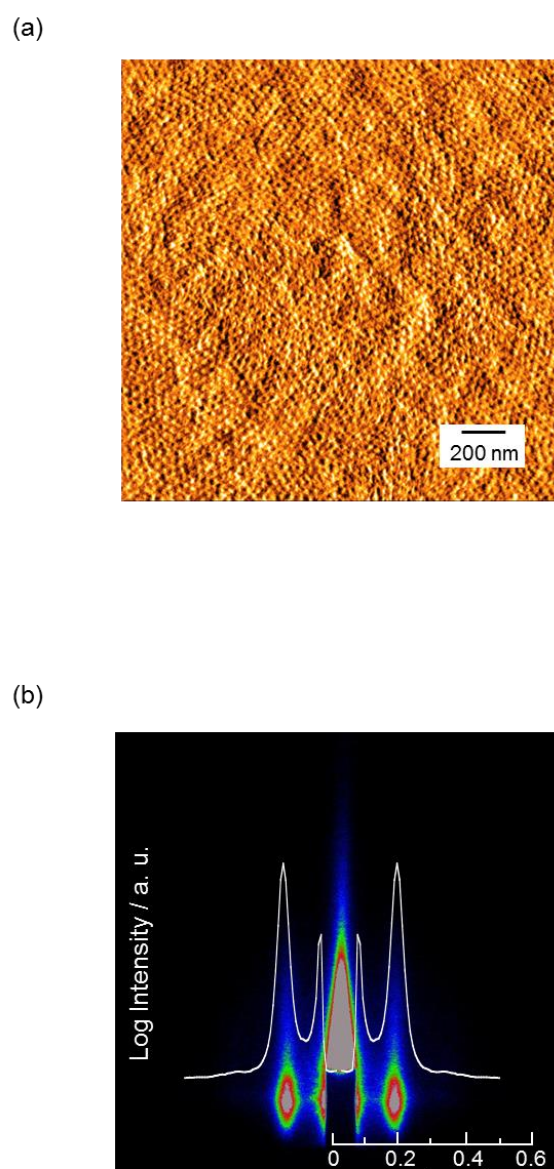
Figure 2. (a) indicate 2.0 x 2.0 µm AFM images (phase mode) of annealed PS_{123}-*b*-$P5Az10MA_{218}$ film after annealing at 130 °C. (taken from reference 12) (b) GI-SAXS patterns for the MPS cylindrical domain detection. In the GI-SAXS patterns, 1D intensity profiles are indicated as white lines.
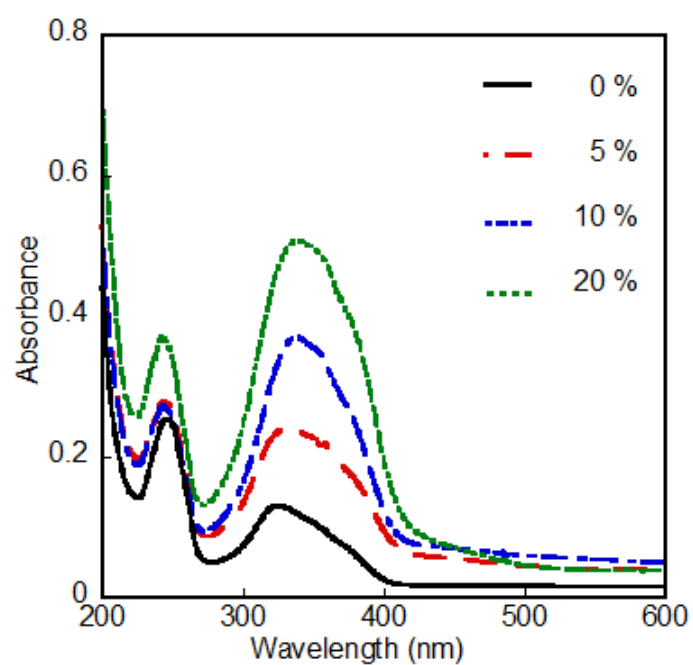
Figure 3. UV-Vis absorption spectra of the PS_{123}-*b*-P5Az10MA$_{218}$ adding 5, 10 and 20 % SAP1 blend thin films after annealing at 130 °C.

the surface-segregated films. The extent of planar orientation of Az mesogenic groups should influence the effectiveness for the photoalignment in the in-plane directions. The resultant polarized UV-Visible absorption spectra are shown in Figure 4 for films containing 5 weight % (a), 10 weight % (b), and 20 weight % (c) of SAP1 in the PS_{123}-b-P5Az10MA$_{218}$ thin film. The degree of in-plane anisotropy was estimated by the order parameter S [$= (A_\perp - A_{//})/(A_\perp + 2A_{//})$], where $A_\perp$ and $A_{//}$ denote absorbance at the λ_{max} of the $\pi - \pi^*$ absorption band of the Az unit (ca. 320 and 350 nm for 10 % and 20 % samples, respectively) obtained by measurements using LPL with E perpendicular and parallel to that of actinic polarized light. When the blend amount was 5 weight %, the photoinduced in-plane anisotropy was of minor (a). Blending 10 and 20 weight % of SAP1 led to clear in-plane anisotropic nature. The pronounced anisotropy was observed for the film containing 20 weight % of SAP1 (c). S values were 0.02, 0.18, and 0.76, for 5, 10 and 20 % blend films, respectively. Thus, in case of SAP1, sufficient in-plane orientation is performed in the 20 % blend film.

The induction of planar orientation of Az mesogenic group by the SAP was found to be strongly dependent on its molecular weight. Figure 5 indicates polarized UV-visible absorption spectra obtained for SAP2 and SAP3 after LPL irradiation and annealing under the same conditions for SAP1 as mentioned above. With these SAP with larger molecular weight, the blend amount of SAP required to attain the sufficient in-plane orientation became significantly smaller. As shown in Figure 5, the blending ratios of 5 and 3 weight % were sufficient for SAP2 and SAP3, respectively, to provide large in-plane anisotropy, in contrast with the fact that 20 weight % is needed for SAP1. S values calculated for SAP2 and SAP3 form the data in Figure 5 were 0.48, and 0.56. The chemical composition of these surface active polymers is essentially the same, however interestigly, SAP2 and SAP3 having molecular weight 2.6 times and 3.8 times larger, respectively, than SAP1 bring about the clear orientation alternation of Az mesogens from the homeotropic to planar mode with substantially smaller amounts of
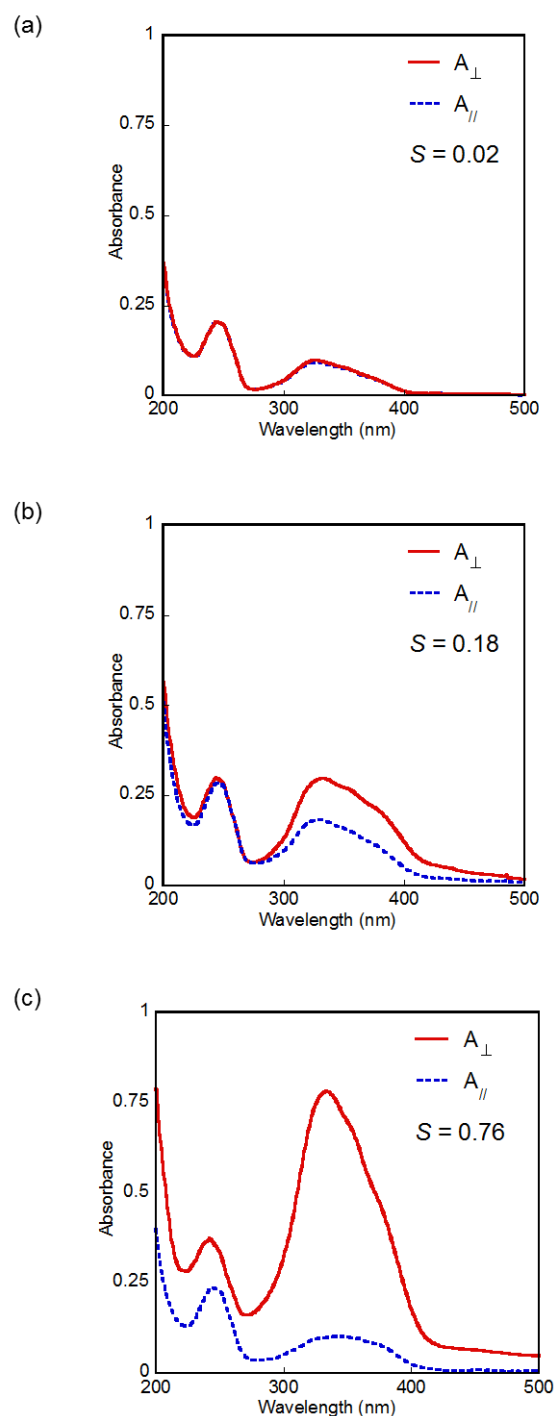
Figure 4. Polarized UV-visible absorption spectra of PS_{123}-*b*-P5Az10MA$_{218}$ films adding 5 (a), 10 (b), and 20 (c) weight % of SAP1 after annealing at 130 °C and irradiation with 436 nm LPL at 1000 mJ cm^{-2}. For procedures see SCHEME 1. The spectra are taken with the probing beam parallel (dotted line) and orthogonal (solid line) to the actuating light.
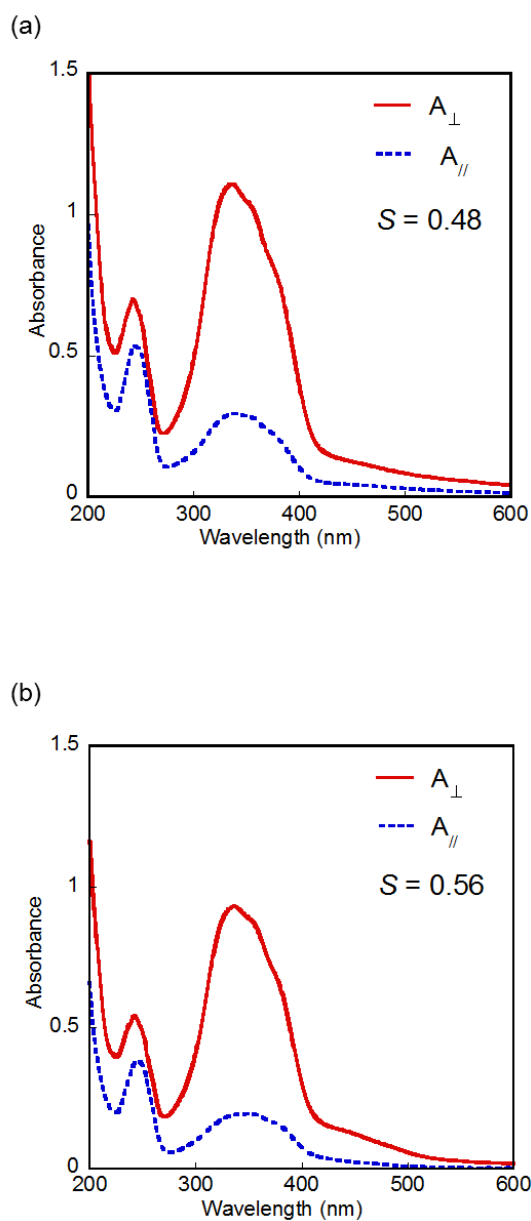
Figure 5. Polarized UV-visible absorption spectra of SAP2 (5 %)/PS_{123}-*b*-$P5Az10MA_{218}$ (a) and SAP3 (3 %)/PS_{123}-*b*-$P5Az10MA_{218}$ (b) blend thin films after irradiation with 436 nm LPL at 1000 mJ cm^{-2}. The spectra were taken with the probing beam parallel (dotted line) and orthogonal (solid line) to the actuating light.

SAP. Such molecular weight effect is interesting but the reasons for this behavior is still unclear. At the moment, we assume that the surface skin layer of SAP with smaller melecular weight is mechanically unstable supposedly showing surface dewetting, therefore, more amount of SAP is required to form homogeneous and stable surface layer.

In this paper, discussions are based only on the characterizations of the molecular orientation of Az units obtained by polarized UV-visible absorption spectroscopic data. However, it is already confirmed that the information at the molecular level obtained by spectroscopic evaluation can be directly related to the orientation of cylinder MPS cylinder domains at the mesoscopic level. It is well established by X-ray measurements and atomic force microscopy that the mesogenic orientation and the MPS domain orientations are parallel with each other to minimize the elastic energy of the system.[5-9,12] Therefore, the total hierarchical structures including Az mesogens and polystyrene cylinder domains should be controlled in the film as displayed in Scheme 1.

3-4. Conclusion

LC block copolymers possessing polystyrene (PS-*b*-P5Az10MA) and poly(butyl methacrylate) PBMA-*b*-P5Az10MA with three different molecular weight are synthesized in the range of narrow dispersions from 1.17-1.29 by the ATRP method. Blending a small amount of PBMA-*b*-P5Az10MA (surface active polymer, SAP) possessing lower surface tension with PS-*b*-P5Az10MA film and successive annealing give rise to the segregation of SAP to the free surface. The segregation causes the homeotropic to planar orientation of the Az mesogen of PS-*b*-P5Az10MA and MPS cylinder of polystyrene. In terms of polymer design and conditions of SAP, the factors influencing the free surface-induced orientational alternation found in this work are summarized as follows. (i) Block copolymers containing the mesogens should be used.

The homopolymer of PBMA is not favorable due to the low compatibility with the base block copolymer, exhibiting dewetting on the surface. (ii) The blend ratio of SAP should be large enough to cover the base polymer surface. (iii) The molecular weight significantly influences the surface coverage, and the smaller amount will be sufficient for the larger molecular weight SAP. The procedure of blending of surface active block copolymer is very simple to place a polymer skin layer on the free surface, but leads to marked effects on the molecular and domain orientations in the base films. Such approach should have potential significances in the inductrial applications in terms of versatility and low-cost processing.

References

1. C. Park, J. Yoon, E.L. Thomas, *Polymer* **2003**, 44, 6725-6760.

2. I. W. Hamley, *Developments in Block Copolymer Science and Technology* **2004**, Wiley: Weinheim, DE.

3. K. Ichimura, *Chem. Rev.* **2000**, 100, 1847-1873.

4. O. Yaroshchuk, Y. Reznikov, *J. Mater. Chem.* **2012**, 22, 286-300.

5. Y. Morikawa, T. Kondo, S. Nagano, T. Seki, *Chem. Mater.* **2007***, 19, 1540-1542.

6. H. Yu, T. Iyoda, T. Ikeda, *J. Am. Chem. Soc.* **2006**, 128, 11010-11011.

7. T. Seki, S. Nagano, M. Hara, *Polymer* **2013**, 54, 6053-6072.

8. H. Yu, T. Ikeda, *Adv. Mater.* **2011**, 23, 2149-2180.

9. S. Nagano, Y. Koizuka, Y. Murase, M. Sano, Y. Shinohara, Y. Amemiya, T. Seki, *Angew. Chem. Int. Ed.* **2012**, 124, 5986-5990.

10. P. Mansky, Y. Liu, E. Huang, T. P. Russell, C. J. Hawker, *Science* **1997**, 275, 1458-1460.

11. T. Xu, C. J. Hawker, T. P. Russell, *Macromolecules* **2005**, 38, 2802-2805.

12. K. Fukuhara, Y. Fujii, Y. Nagashima, M. Hara, S. Nagano, T. Seki, *Angew. Chem. Int. Ed.* **2013**, 52, 5988-5991.

13. Q. S. Bhatia, D. H. Pan, J. T. Koberstein, *Macromolecules* **1988**, 21, 2166-2175.

14. K. Tanaka, A. Takahara, T. Kajiyama, *Macromolecules* **1998**, 31, 863-869.

15. E. Huang, T. P. Russell, C. Harrison, P. M. Chaikin, R. A. Register, C. J. Hawker, J. Mays, *Macromolecules* **1998**, 31, 7641-7650.

16. W. Li, S. Nagano, T. Seki, *New J. Chem.* **2009**, 33, 1343-1348.

Chapter IV

Ubiquitous Photoalignment of Liquid Crystalline Polymers by a Segregated Free Surface Layer

4-1. Introduction

The orientation of liquid crystals (LCs) on solid substrate surfaces have been known since the work by Mauguin[1] at the dawn of LC research. Later, Chatelin[2] clearly revealed the rubbing effect on a substrate regarding LC orientation. Now, rubbing processes on polymer film surfaces are standard procedures used for aligning the surfaces of LCs during LC display panel and optical modulation device fabrication.

An alternative procedure to control LC orientation is to use photoreactions occurring at the substrate surface. The first demonstration of surface photoalignment control was reported by Ichimura et al. in 1988.[3] The photoisomerisation of an azobenzene monolayer on the surface could switch the nematic LCs that are micrometres thick between the homeotropic and planar modes (Scheme 1a). This system is called a "command surface" or a "command layer".[4,5,6,7,8] Shortly after, Gibbons et al.,[9] Dyadyusha et al,[10] and Schadt et al.[11] demonstrated that angular selective excitation with linearly polarised light (LPL) on a photoreactive polymer film enables in-plane alignment control. More than 20 years after these findings, surface photoalignment technology [12, 13] has recently been introduced in the industrial production of LC displays.[14] Surface photoalignment is most often applied to thermotropic nematic LCs, but many types of other LC materials, including LC polymers, can be photoaligned.[6,15,16] The mechanisms of photoalignment have been recently overviewed by Yaroshchuk and Reznikov.[13] To date, all the surface alignments have been mostly achieved through an aligning effect from the solid substrate surface.

Although the importance of the free surface (air-contacting surface) in the anchoring of mesogen orientations has long been recognised theoretically[17,18] and experimentally,[19,20] no attempt had been made to utilise the free surface to exert active orientation control over the LC. In this chapter, it is report the first examples of polymer LC systems commanded by a skin layer at the free surface (Scheme 1b). This method is particularly versatile and should offer various new applications without laborious surface modifications to the substrate, and ubiquitous LC alignment controls can be performed by annealing followed by LPL irradiation or general printing methods.

This approach was inspired by our recent results showing that the surface coverage on the free surface of photoresponsive azobenzene side chain LC polymer films leads to a homeotropic to planar orientational change in the mesogenic groups across the entire film.[21,22] This pre-oriented state leads to an effective in-plane photoalignment using LPL irradiation. The free surface was covered by mixing a small amount of surface segregating polymer and successive annealing. In our previous investigations, the entire film was composed of photoresponsive (self-alignable) LC polymers. The present approach was undertaken to demonstrate photoalignment control over *non-photoresponsive* LC polymer films commanded only by a photoresponsive skin layer at the free surface.

4-2. Experimental

4-2-1. Synthesis of polymers and diblock copolymer

4-2-1-1. Polymerization of PBMA-*b*-PAz *via* ATRP

Synthesis of 4-(10-methacryloyloxydecyloxy)-4'-pentylazobenzene (Az) was described previously. PBMA-Cl macroinitiator was polymerized by ATRP. PBMA-Cl, CuBr, HMTETA, and Az were add into a 15 ml pressure glass tube. The mixture was dissolved in Toluene in glove box. The sealed mixture solution was removed from the
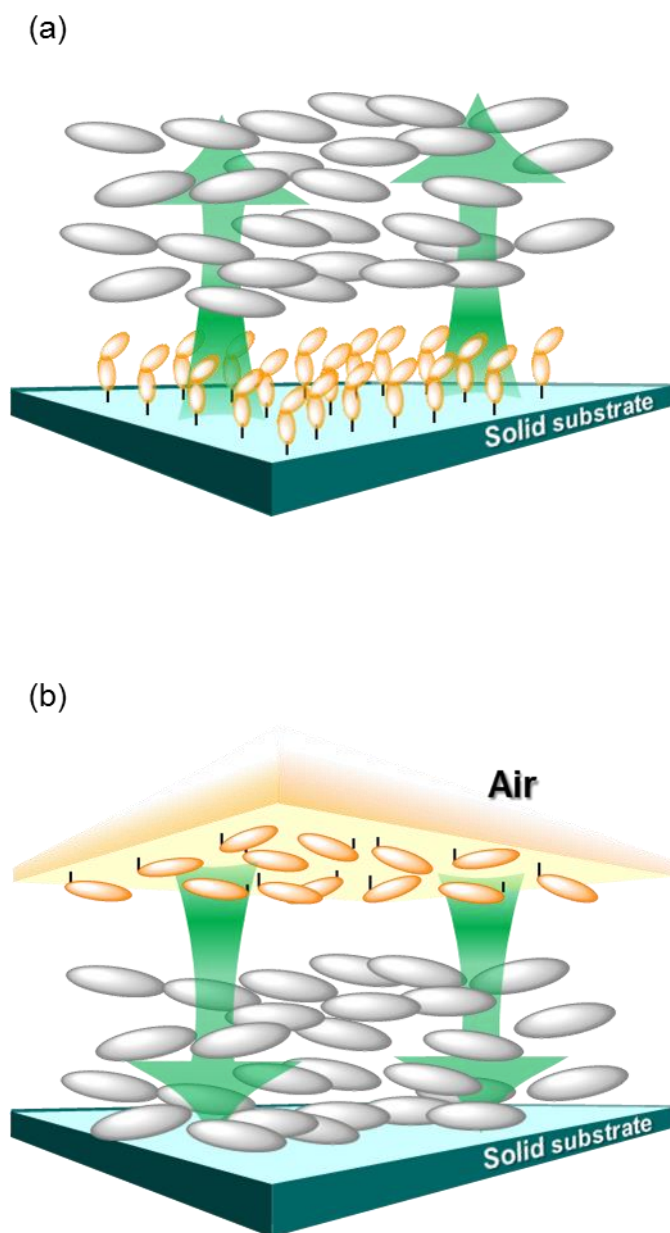
Scheme1. Schematic illustrations of photoalignment control using surface photoreactions.   (a) Alignment control of LC molecules using surface photoreactions from the solid substrate side (command surface effect). (b) New proposal to exert a command effect with a photoresponsive skin layer on the free (air) surface.

glove box and placed for 24 h in a ChemStation at 80 °C. The polymerization was stopped by exposing the catalyst to air. The reaction solution was dissolved in chloroform and passed through an activated neutral alumina column to remove the Cu catalyst. After being concentrated, the solution was poured to methanol to remove PBMA-Cl macroinitiator and Az monomer. The averaged numbers of repeating unit of BMA and Az were 510 and 144, respectively (PBMA$_{510}$-b-PAz$_{144}$). M_n (^{1}H-NMR) = 1.4 x 10^5, M_w/M_n (GPC) = 1.17. In this paper, this polymer will be denoted as PBMA-b-PAz. Thermophysical properties by DSC: glass-56 °C-SmC-90 °C-SmA-114 °C-iso, T_g of PBMA = ca. 20 °C.

4-2-1-2. Synthesis of 4-(6-hydroxyhexyloxy)benzoic acid (BA6OH)

4-Hydroxybenzoic acid was dissolved in ethanol. Potassium hydroxide and catalytic amount of potassium iodide were added dropwise to the above solution. 6-Bromo-1-hexanol was then added dropwise under stirring. The solution was stirred for 3 h at 80 °C. After this solution was dissolved in methanol, acidified with hydrochloric acid and removed Solvent by filtration. The precipitate was recrystallized from hexane twice to give white platelet crystals. Yield: 7.8 g (24.0 %)

4-2-1-3. Synthesis of 4-(6-methacryloyloxyhexyloxy) benzoic acid (BA6MA)

Methacrylic acid, 4-toluene sulfonic acid, hydroquinone and ethyl acetate were added to BA6OH in dry THF solution, and then mixture was stiired for 18 h at 80 °C. The reaction mixture was washed with water and hydroquinone was added. The solution was dried over anhydrous magnesium sulfate and then, was purified with columun chromatography. This product was recrystallized from ethyl acetate to give white solid. Yield: 5.3 g (69.0 %).

4-2-1-4. Synthesis of 4-(6-methacryloyloxyhexyloxy)-4'-pentylphenyl benzoate (5PB6MA)

Hydroquinone and thionyl chloride were added to BA6MA, and then mixture was stiired for 2 h at room temperature under Ar gas. Diethylether was added dropwise

under stirring until distilled thionyl chloride by azeotropy. After the solution was stirred at 110 °C, this product was 4-(6-methacryloyloxyhexyloxy) benzoic chloride (BC6MA). Then, triethylamine was added to 4-pentyl phenol in dry THF solution. The mixture solution was added dropwise to BC6MA in dry THF solution and stirred for 2 h at room temperature. The reaction mixture was washed with water to neutralize and hydroquinone was added. The solution was dried over anhydrous magnesium sulfate and then, was purified with columun chromatography. This product was recrystallized from ethyl acetate to give white solid. Yield: 2.4 g (56.0 %).

4-2-1-5. Polymerization of poly 4-(6-methacryloyloxyhexyloxy)-4'-pentylphenyl benzoate (PPBz)

The phenyl benzoate-containing polymer PPBz was synthesized by free radical polymerization in dry THF solution under nitrogen, using AIBN as an initiator via free radical polymerization of the 5PB6MA monomer. The reaction medium was heated at 60 °C for 24 h, cooled to room temperature, and then poured in to a vigorously stirred hexane for reprecipitation. The resulting polymer was collected by centrifugation. The whitesolid product was dried in vacuum. The reaction conversion was 95% (Yield: 172 mg). M_n (^{1}H-NMR) = 6.6 x 10^4, M_w/M_n (GPC) = 2.04. In this paper, this polymer will be denoted as PPBz. Thermophysical properties by DSC: glass-23 °C-SmA-82 °C-iso.

4-2-1-6. Synthesis of 6-cyanobiphenoyl-1-hexanol (CB6OH)

Potassium carbonate was added to 4-cyano-4'-hydroxybiphenyl in dry DMF solution under N_2 gas. 6-Bromo-1-hexanol in dry DMF was then added dropwise under stirring. The solution was stirred for 2 h at room temperature. After this solution was dissolved in water, extracted with chloroform and water. The precipitate was recrystallized from methanol twice to give white platelet crystals. Yield: 8.35 g (95.0 %)

4-2-1-7. Synthesis of 6-cyanobiphenyloxy-1-hexyl methacrylate (CB6MA)

Trietylamine was added to CB6OH in dry THF solution. A dry THF solution of methacryloyl chloride was added dropwise to the solution at 0 °C. The mixture was

stirred for 30 min at 50 °C and 12 h at room temperature. The reaction mixture was washed with water. The solution was extracted with chloroform and water and then, dried over anhydrous magnesium sulfate. The solvent was evaporated and the residue was recrystallized from methanol. Yield: 5.4 g (60.0 %).

4-2-1-8. Polymerization of poly 6-cyanobiphenyloxy-1-hexyl methacrylate (PCB)

CuCl, Bpy9 and CB6MA monomer were added into a 15 ml pressure glass tube. The mixture was dissolved in THF in glove box. The resulting mixture was stirred for 10 min, and then EBB was added. The sealed mixture solution was removed from glove box and placed for 10 h in ChemStation at 70 °C. The polymerization was terminated by exposing the catalyst to air. The reaction solution was dissolved in chloroform and passed through an activated neutral alumina column to remove the Cu catalyst. After being concentrated, the solution was poured to hexane to remove CB6MA monomer. The reaction conversion was 55%. M_n (^{1}H-NMR) = 3.2 x 10^4, M_w/M_n (GPC) = 1.11. In this paper, this polymer will be denoted as PCB. Thermophysical properties by DSC: glass-50 °C-SmA-113 °C-iso.

4-2-2. Preparation of blend thin films

The thin films of a homopolymer and a blended polymer with 3 weight % PBMA-b-PAz were prepared by spincoating with a 2 weight % PCB and PPBz solution in chloroform, respectively. The blended PBMA-b-PAz (3%)/PPBz cast film was prepared by casting from a 1 weight % chloroform solution. These films were annealed at 125 °C for 10 min.

4-2-3. Light irradiation

LPL irradiation was performed with a REX-250 (ASAHI SPECTRA Co.) equipped with a polariser. The films were irradiated with LPL at 436 nm (visible) and 600 mJ cm^{-2} through an optical polariser. The PPBz and the blended PBMA-b-PAz

(3%)/PPBz thin films were irradiated with 436 nm LPL at 80 °C, while the PCB and the blended PBMA-b-PAz (3%)/PCB thin films were irradiated at 100 °C, respectively. These temperatures were chosen because they are slightly below the isotropidisation temperatures of PPBz or PCB. The blended PBMA-b-PAz/PPBz cast film in the vertical direction relative to the LPL irradiation was rotated by 90 ° and irradiated again with a photomask on the blended substrate. The in-plane anisotropy of the Az chromophore and smectic phase in the were observed with a polariser.

4-2-4. Measurements

4-2-4-1. ^{1}H NMR

^{1}H NMR spectra (JNM-GSX270, JEOL) was recorded 16 th steps using tetramethylsilane as the internal reference for deuterated chloroform solution (Across). A small amount of polymerized solution was measured and conversion of polymerization was calculated by value of integral of a monomer and a polymer. Thus, redeposit samples was checked whether to remain a monomer and a macroinitiator.

4-2-4-2. Gel-permeation chromatography

Gel-permeation chromatography (GPC) has been used a measuring of size-exclusion chromatography (SEC) (Shodex DS-4/UV-41/RI-101) and GPC two columns (Shodex KF-403 and KF-405). THF was used as an eluent at a flow rate of 1.0 mL/min. The calibration of molecular weight was calculated by using polystyrene standards (TSK standard polystyrene, TOSOH). The polymerization products of polymers were used by GPC to calculate distribution of molecular weight.

4-2-4-3. Differential scanning calorimetry

Differential scanning calorimetry (DSC) (TA DSC Q200) has been used a measuring tool of calorimeter. DSC scans were performed within the temperature range 0~140 °C at a heating rate of 5.0 °C min^{-1} under nitrogen. About 5.0 mg mass was used for DSC measurements for all samples. An empty aluminum pan was used as a

reference. The glass transition (T_g) and between the liquid crystal (LC) phase and the isotropic phase transition temperature was determined by DSC scans.

4-2-4-4. UV-Vis absorption spectroscopy

Polarized UV-visible absorption spectra were taken on an Agilent 8453 spectrometer (Agilent Technologies) with a polarizer in front of the samples. A source of illumination used a D_2-W lamp. Quartz was used as a substrate in measuring thin films. Whether to orient a homeotropic or a planar orientation was judged from absorption wavelength of around 260 nm at phenyl benzoate (PBz) molecules, 300 nm at cyanobiphenyl (CB) molecules and 350 nm at azobenzene (Az) molecules, respectively.

4-2-4-5. X-ray measurements (GI-XRD)

GI-XRD measurement was performed on voltage 40 kV, current 40 mA, irradiation time 30 min to create copper Cu Kα radiation (λ = 1.542 Å) and camera length was 300 mm (FR-E X-ray diffractometer and R-AXIS IV two-dimensional (2D) detector) (Rigaku Co.). It was read and measured an X-ray diffraction pattern exposed by an imaging plate (FUJIFILM Co.). The diffraction patterns of the in-plane and out-of-plane direction that obtained from thin film samples were informed about LC structures and surface separation of PBz, CB and Az. Thus, FR-E was carried on by using a ceramic heater attached on the sample holder of FR-E under controlling temperature.

4-2-4-6. Polarized optical microscope

The optical-anisotropy of phenyl benzoate and azobenzene molecules was evaluated by optical microscope observation with polarized incident light using a BX51 (Olympus Co.). The thin film irradiating with the photomask was observed by diffrence contrasts at rotating 0 and 45 °.

4-2-4-7. Atomic force microscopy

Atomic force microscopic measurements for film thickness evaluation were

achieved using Seiko Nanopics 2100 (Seiko Instruments).The film was partly scratched and the height difference in the z-direction profiles was evaluated. The thickness was obtained as an average of several measurements.

4-2-4-8. Inkjet printing

A PBMA-b-PAz solution in o-dichlorobenzene (1 weight %) was poured onto a PPBz thin film using a sub-femtolitre inkjet printing apparatus (SIJ Technology). Printed images of the letters "NU" and a mountain were patterned with a computer control system using DXF-SIJ software. After printing, the film was annealed at 125 °C for 10 min and successively irradiated with LPL (600 mJ cm^{-2}). Line patterning was drawn under the following conditions: the voltage of 600 V, the frequency of 60 Hz and the distance between a substrate and a nozzle of 30 μm, respectively.

4-3. Results

4-3-1. Synthesis of polymers.

The synthetic procedures used to produce the monomers and polymers are described in the supplementary information. Scheme 2 presents the chemical structures and abbreviations of the polymers employed. Poly(butyl methacrylate) (PBMA), poly(butylmethacrylate)-*block*-poly[4-(10-methacryloxydecyloxy)-4′-pentylazobenzene] (PBMA-*b*-PAz), and poly (6-cyanobiphenyloxy-1-hexyl methacrylate) (PCB) were synthesised via atom transfer radical polymerisation, as previously reported,[19] and poly(4-(6-methacryloxyhexyloxy)-4'-pentylphenyl benzoate (PPBz) was synthesized by free radical polymerisation. The number-averaged molecular masses (M_n) and the polydispersity indices (M_w/M_n) were evaluated by gel permeation chromatography: PBMA ($M_n = 7.2$ x 10^4, $M_w/M_n = 1.09$) PBMA-*b*-PAz ($M_n = 1.4$ x 10^5, $M_w/M_n = 1.17$), PPBz ($M_n = 6.6$ x 10^4, $M_w/M_n = 2.04$), and PCB ($M_n = 3.2$ x 10^4, $M_w/M_n = 1.11$).

4-3-2. Thermal Properties

PBMA   **PBMA-*b*-PAz**   **PPBz**   **PCB**
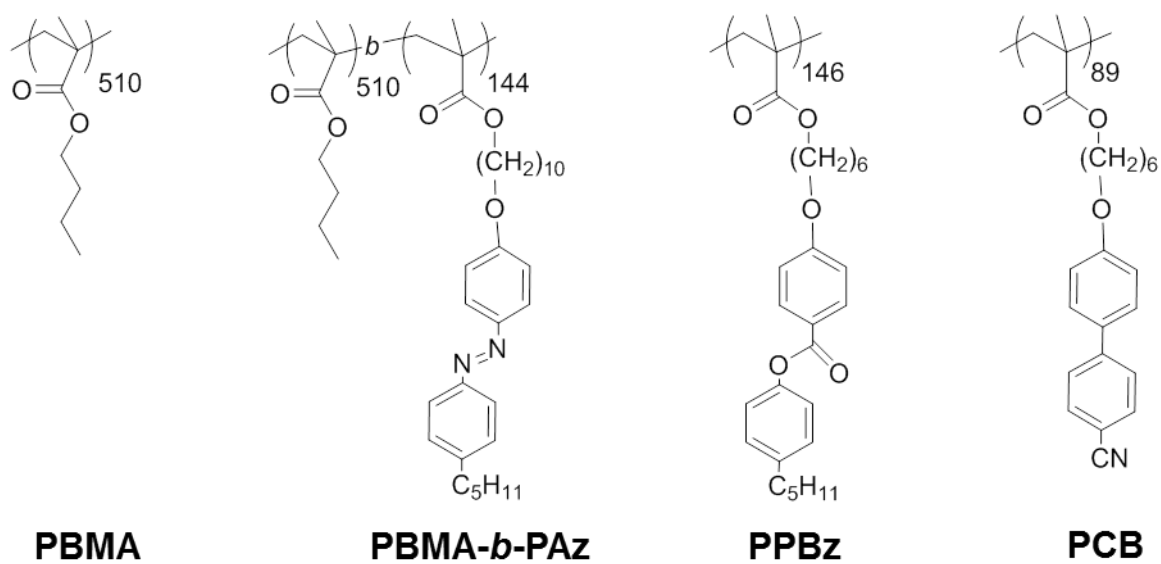
Scheme 2. Chemical structures of polymers. PBMA is the flexible homopolymer used for the reference experiments; PBMA-*b*-PAz is the photoresponsive surface segregating the block copolymer; PPBz and PCB are the non-photoresponsive side chain homopolymers.

Thermal properties of the block copolymers were investigated by DSC. Figure 1 shows the DSC curves of the PBMA-*b*-PAz, PPBz and PCB on their second heating processes. The glass transition temperature (T_g) of the PBMA homopolymer and the block copolymer was approximately 20°C. PBMA-*b*-PAz was used as the photoresponsive minor blending component, and PPBz and PCB are non-photoresponsive side chain LC polymers that constitute the majority of the film. Unless stated otherwise, the LC polymer films were prepared on clean quartz plates. In the case of the PBMA-*b*-PAz, well-defined sharp endothermic transitions was observed at 114 °C, and minor transition were observed at 56 and 90 °C. These transitions were reversible observed on the cooling process at a few degrees lower temperatures due to supercooling. These transitions can be assigned as glass-56 °C-SmC-90 °C-SmA- 114 °C-iso, T_g of PBMA = ca. 20 °C. PPBz gave endothermic peak at 82 °C under the influence of low peak of 5PB6MA monomer (33 °C) and PPBz transition was determined as glass-23 °C-SmA-82 °C-iso. By contrast, PCB gave endothermic peak at 113 °C similar to PBMA-*b*-PAz and PCB transition was determined as glass-50 °C-SmA-113 °C-iso.

4-3-3. Effect of PBMA-*b*-PAz addition on the orientation of LC polymer films.
4-3-3-1. Optical patterning by the skin layer for PPBz film

Figure 2, 3 and 4 shows the UV-visible absorption spectra and the grazing incidence small angle X-ray scattering (GI-SAXS) data used to evaluate the orientations of the mesogen and SmA lamella structure.

The UV-visible absorption spectra of a pure PPBz film after annealing at 125 °C for 10 min exhibited a significant decrease in the π−π* band for phenyl benzoate at 270 nm (Figure 2a). In the GI-SAXS data, a diffraction spot was observed in the out-of-plane direction with a *d* spacing of 3.2 nm (Figure 2b). These data revealed that the SmA lamella and the phenyl benzoate mesogens are oriented parallel and perpendicular to the substrate, respectively. The mesogen and lamella orientations are
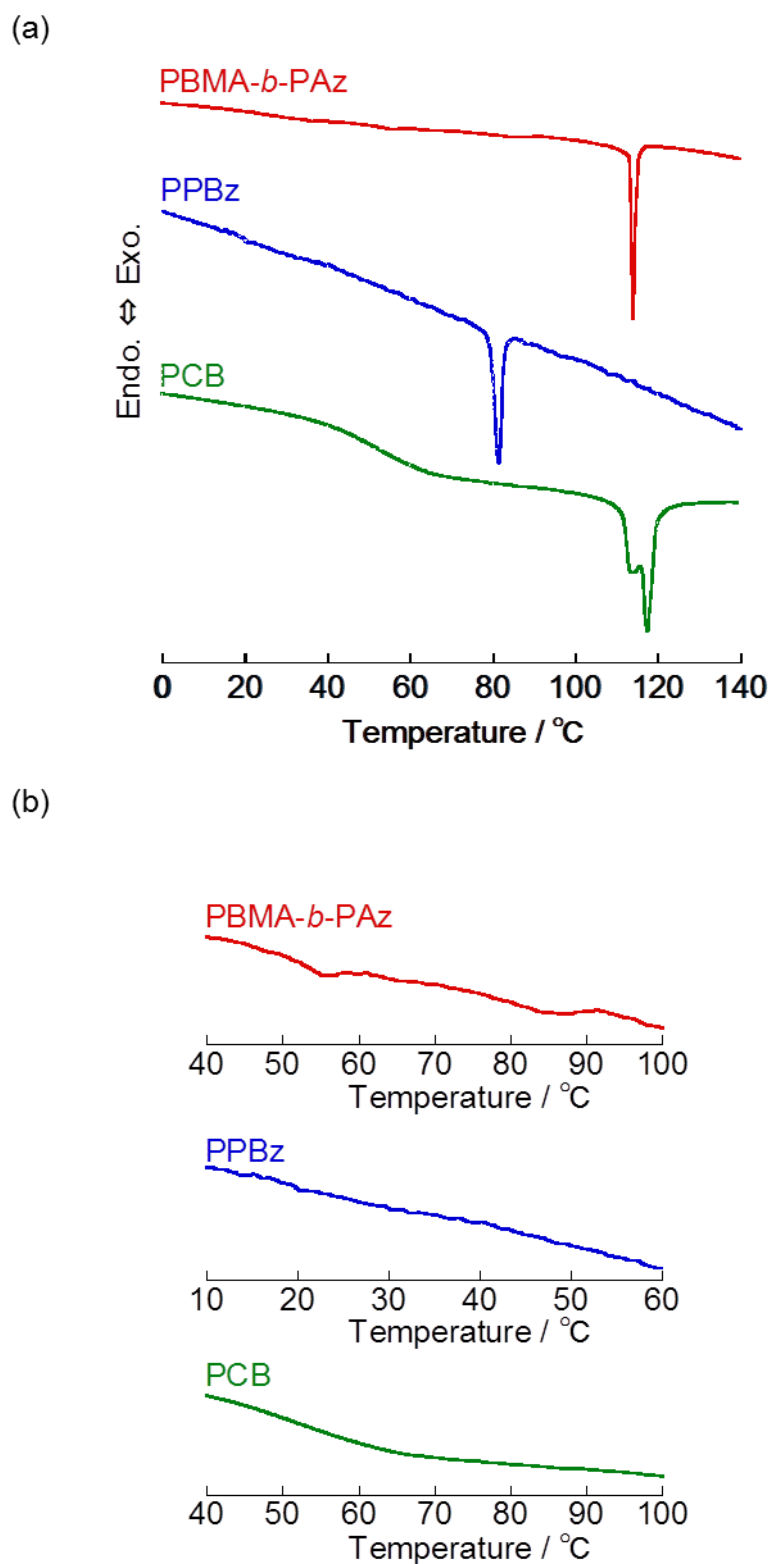
(a)

(b)

Figure 1. DSC curves of the block copolymer and homopolymer on the second heating process from 0 to 140 °C. The heating rate was 5.0 °C/min. Curves for PBMA-*b*-PAz, PPBz and PCB are shown.
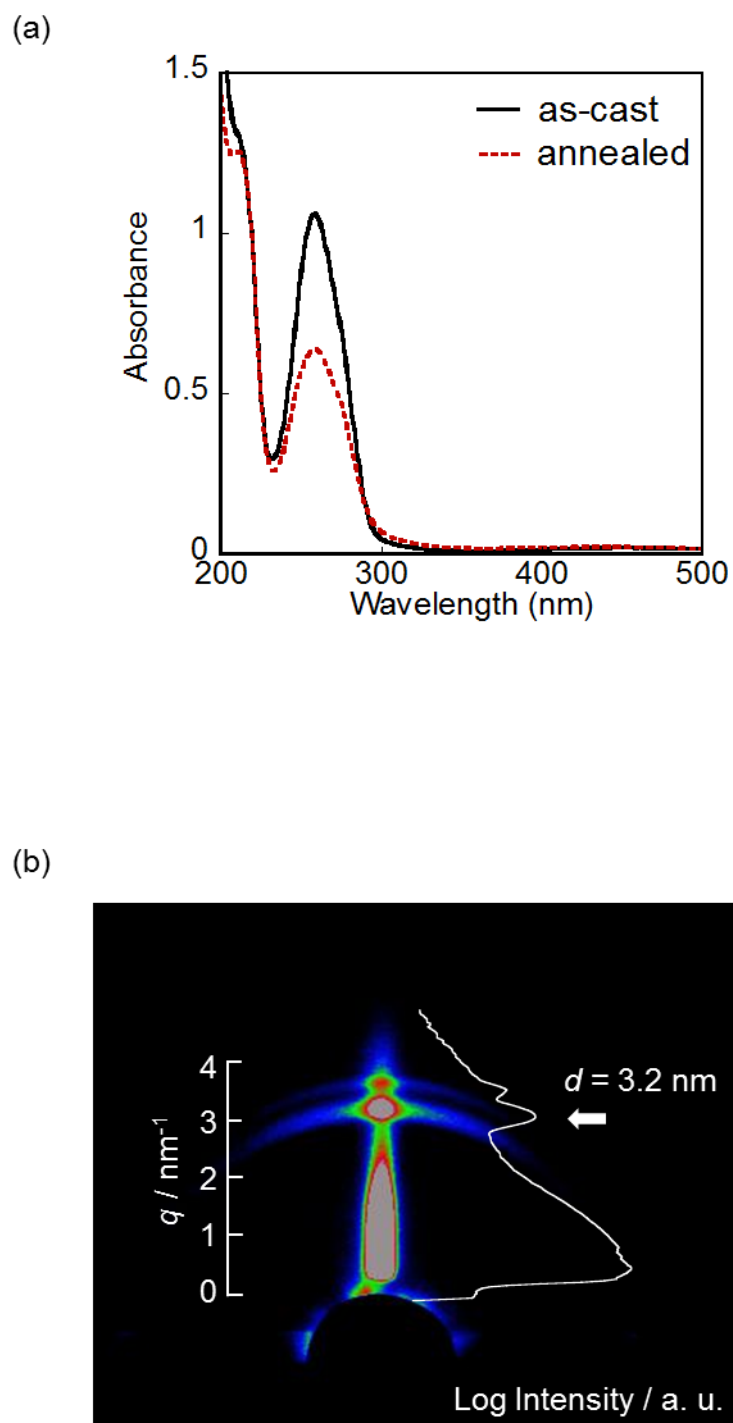
(a)

(b)

Figure 2. LC molecular orientations in the LC films. UV-visible absorption spectra of a pure PPBz film (a). The solid and dotted lines indicate the spectra before and after annealing at 125°C for 10 min. (b): the 2D GI-SAXS images and 1D profiles are shown for the above corresponding films from (a).
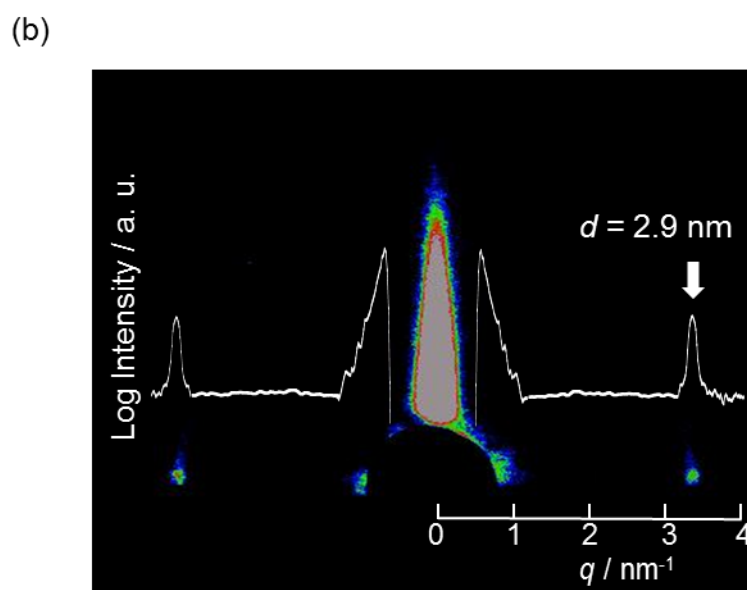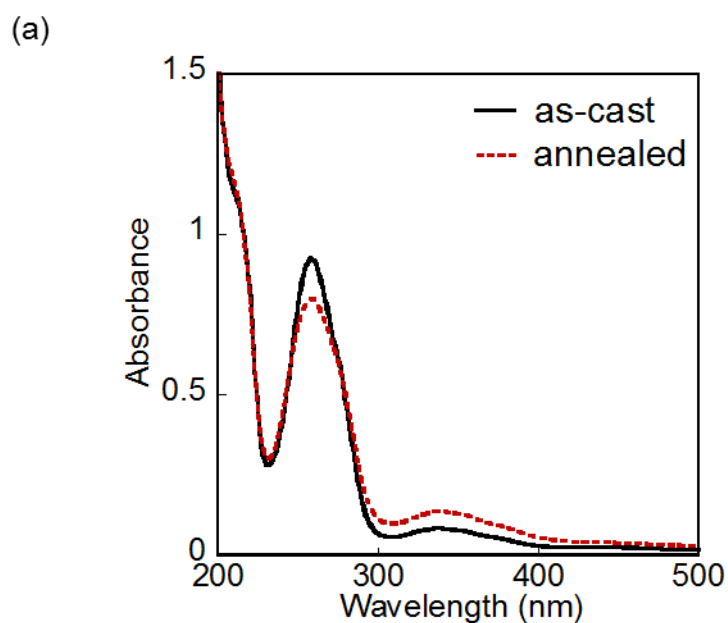
(a)

(b)

Figure 3. LC molecular orientations in the LC films. UV-visible absorption spectra of a PBMA-*b*-PAz (3 weight %)/PPBz film (a). The solid and dotted lines indicate the spectra before and after annealing at 125°C for 10 min. (b): the 2D GI-SAXS images and 1D profiles are shown for the above corresponding films from (a).
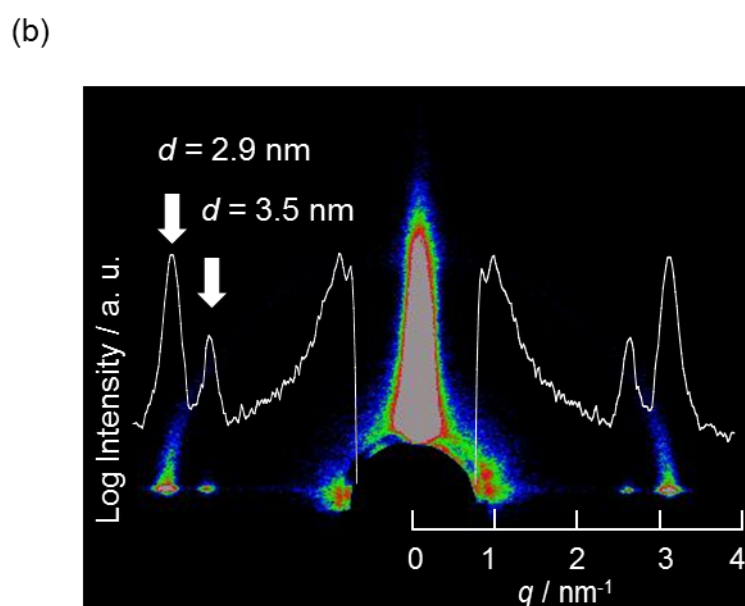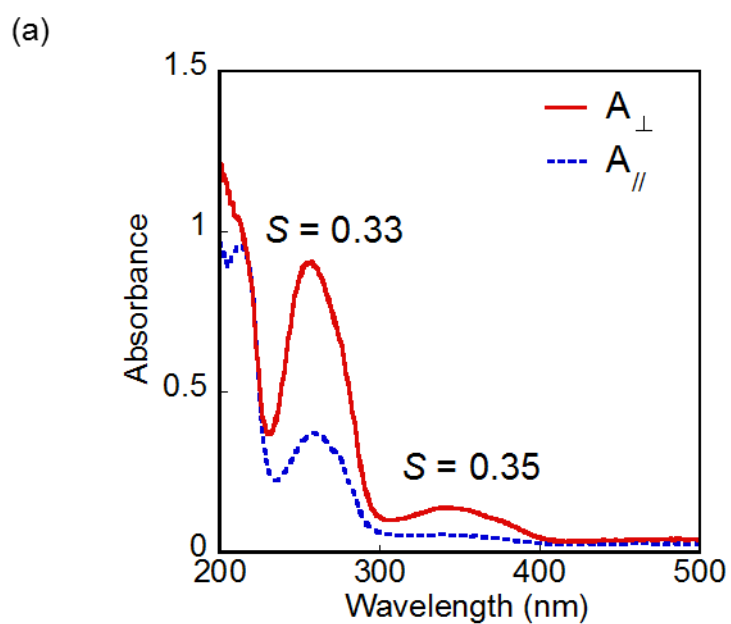
(a)

(b)

Figure 4. Polarised UV-visible absorption spectra of the annealed PBMA-*b*-PAz (3%)/PPBz film after LPL irradiation (600 mJ cm^{-2}) at 80°C taken with probing polarised light set perpendicular (A$_\perp$) and parallel (A$_{//}$) to the actinic LPL light (a). (b): the 2D GI-SAXS images and 1D profiles are shown for the above corresponding films from (a).

schematically drawn in Scheme 3a. These results agree with the general understanding that rod-like mesogenic groups tend to be anchored vertically at the free surface.[15-18]

In contrast, when 3 weight % of PBMA-*b*-PAz was blended with the PPBz, the film exhibited only minor changes in the absorption spectrum upon annealing (Figure 3a), and the orientation of the lamella structure changed to the in-plane directions with *d* = 2.9 nm (Figure 3b). This orientational change should be attributed to the segregation of PBMA-*b*-PAz at the free surface during the annealing treatment, blocking the vertical anchorage of phenyl benzoate mesogens to the free surface. Before this annealing, the scattering spots in the in-plane directions with arcs were observed, indicative of disordered orientation of smectic layers (Figure 5). Direct evidence for the surface segregation of PBMA-*b*-PAz will be demonstrated in the next section. The molecular orientation model is displayed in Scheme 3b. It is assumed that this in-plane orientation can also be achieved by the molecular level orientation of PBMA-*b*-PAz thin film. When a flexible PBMA block is positioned at the top surface, the backbone of the azobenzene polymer block is preferentially oriented vertically relative to the surface. Therefore, the azobenzene mesogens should be oriented in the parallel direction, aligning the phenyl benzoate mesogens in the same direction. The absorption intensity of the $\pi-\pi^*$ (approximately 350 nm) for azobenzene was approximately 1/10 of that for phenyl benzoate (approximately 270 nm). Because the molar extinction coefficient of the $\pi-\pi^*$ band for phenyl benzoate (approximately 1×10^4 dm^3 mol^{-1} cm^{-1}) was approximately one third that of azobenzene,[8] the observed absorption intensity in Figure 3a is appropriate for the sample containing 3 weight % of PBMA-*b*-PAz.

When the annealed blend polymer was irradiated using 436 nm LPL at 600 mJ cm^{-2}, a strong optical in-plane anisotropy appeared (Figure 4a). The in-plane orientational order parameter (*S*) was estimated: $S = (A_\perp - A_\parallel)/(A_\perp + 2A_\parallel)$, where $A_\perp$ and $A_\parallel$ denote the absorbance at the peak maximum obtained through measurements using polarised light with *E* perpendicular and parallel to that of the actinic polarised light,

(a)

Homeotropic

(b)

Air

planar

(c)

Air

photoalignment
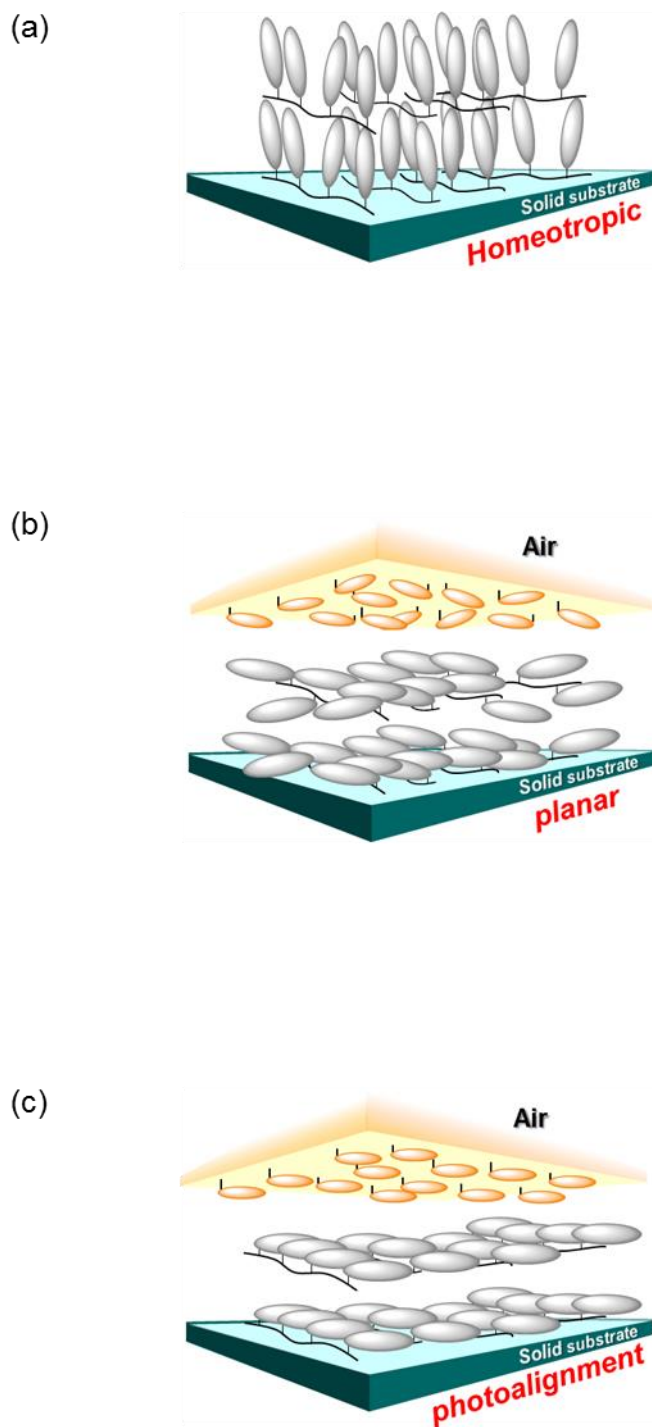
Scheme 3. Schematic drawings for each state are displayed from of a pure PPBz film (a), a PBMA-*b*-PAz (3 weight %)/PPBz film (b) and after irradiated with LPL (c).
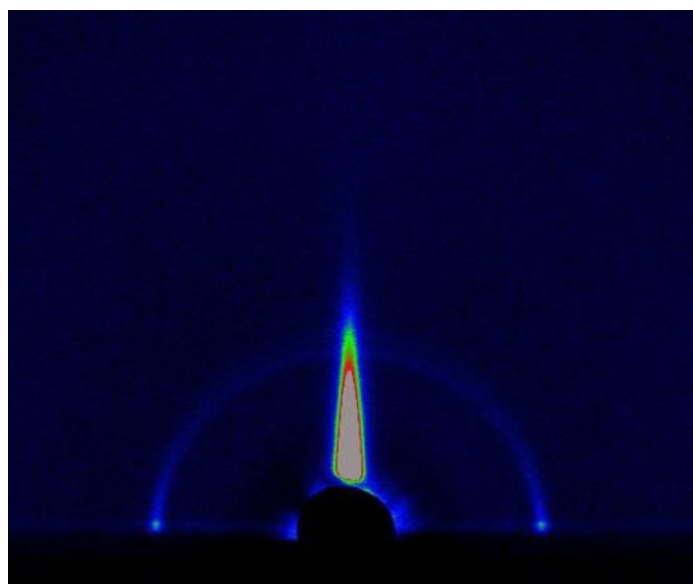
Figure 5. The 2D GI-XRD patterns shows the PBMA-*b*-PAz (3 %)/PPBz blend thin film before annealing.

respectively. The *S* values obtained for the azobenzene and phenyl benzoate bands were 0.35 and 0.33, respectively. Both order parameters agreed with one another. GI-SAXS also revealed a uniformly photoaligned lamella structure in the film. The diffraction peaks became more pronounced (Figure 4b), and additional diffraction peaks from the PBMA-*b*-PAz layer (*d* = 3.5 nm) were also observed, reflecting the more ordered layer structure for both mesogens. Schematic illustrations of the mesogenic orientations in the blended films before and after LPL irradiation are shown in Scheme 3a and 3c. These non-photoresponsive LC mesogens are photoaligned (commanded) by the free-surface photoresponsice layer.

4-3-3-2. Optical patterning by the skin layer for PCB film

Essentially the same results were obtained with another non-photoresponsive LC polymer: PCB (supplementary information). In this report, data obtained with PPBz are mainly discussed because the π−π* band for phenyl benzoate is separate from that of azobenzene. This situation enables observation of the orientations held by the two mesogenic groups independently; however, the π−π* absorption band for cyanobiphenyl partially overlapped in the PCB system (Figure 6).

A spincast film of PCB exhibits transparency LC material (around 150 nm thickness) like PPBz. After annealing at 125 °C (above the isotropization temperature of the LC CB block), this film spontaneously formed a planar orientation of CB6MA side mesogens. However, PCB thin film of planar orientation did not orient by irradiating with LPL. By adding 3 wt% of PBMA-*b*-PAz, blend thin film separated CB peak (300 nm) and Az peak (360 nm), respectively. After being annealed, the peaks that separated between CB and Az shifted at wavelength of 315 nm by interaction and changed the peak of one spot (Figure 6a). The resultant polarised UV-Vis absorption spectra are shown in Figure 6b. PBMA-*b*-PAz/PCB blend thin film aligned CB and Az mesogens in the in-plane direction were obtained by influence of this interaction, although PCB thin film did not align. The order parameter reached 0.27. In the GI-XRD measurement
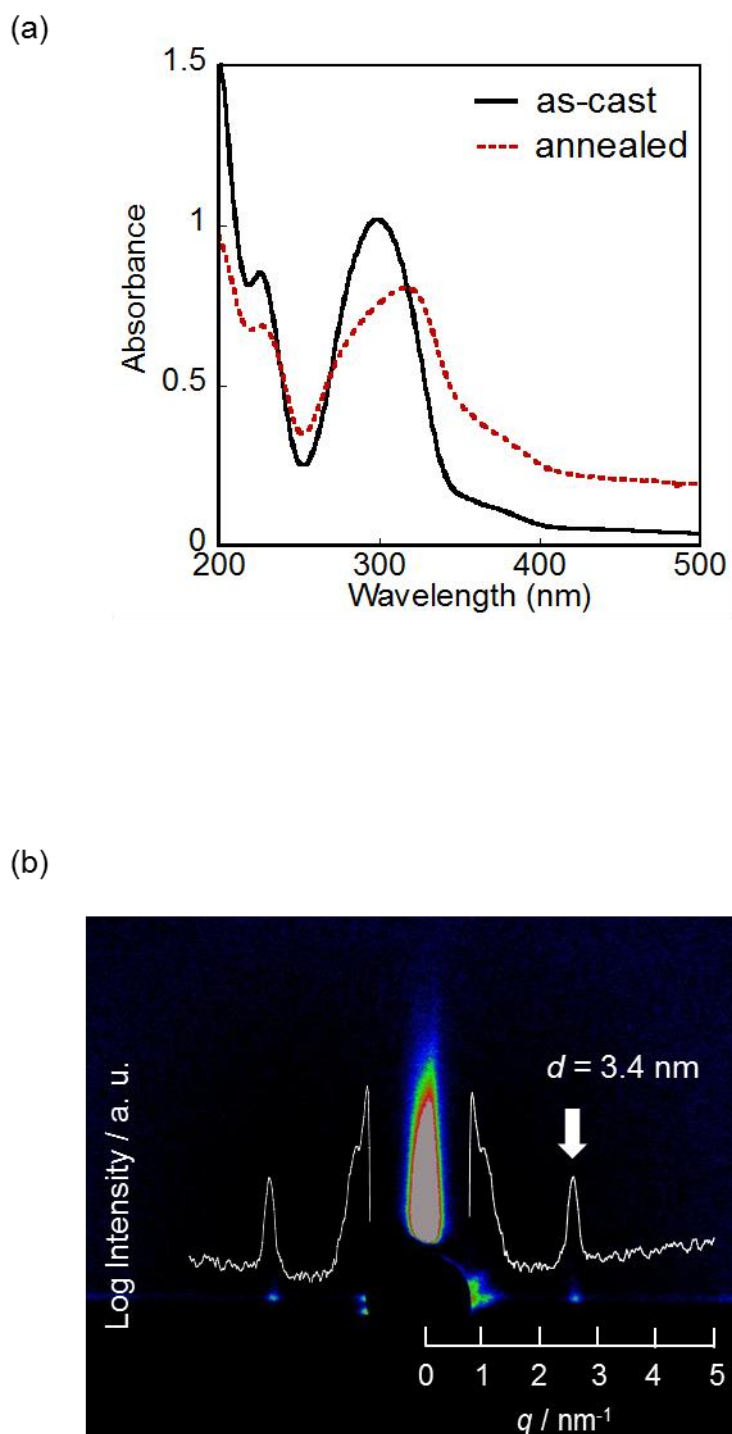
(a)

(b)

Fuigure 6. UV-visible absorption spectra of a PBMA-*b*-PAz (3 weight %)/PCB film (a). The solid and dotted lines indicate the spectra before and after annealing at 125°C for 10 min. (b): the 2D GI-SAXS images and 1D profiles are shown for the above corresponding films from (a).

(Figure 7a), the diffraction spots ascribed to the smectic layer structure of PBMA-*b*-PAz/PCB blend thin film of the CB (d = 3.6 nm) and Az (d = 3.5 nm) mesogens were observed in-plane (horizontal, d = 3.4 nm) directions. Thus, marked orientational alternations in the molecular and layer orientations were observed by the adding PBMA-*b*-PAz. Moreover, the GI-XRD results indicate the existence of more ordered vertically aligned smectic layers in the film when the direction of the X-ray beam incidence was set orthogonal to the actinic LPL direction (Figure 7b).

4-3-4. Evidence for the formation of the surface skin layer.

The contact angles of a water droplet (θ_w) on various annealed polymer film surfaces are summarised in Figure 8a. The θ_w values for the PPBz and PCB surfaces were 110 ° (blue bar) and 95 ° (green bar), respectively. The polymer films (PBMA, PBMA-*b*-PAz, and PBMA-*b*-PAz(3%)/PPBz blend) usually exhibited values of approximately 100° (red bars). These data suggest two significant issues. First, when 3% PBMA-*b*-PAz is blended into PPBz and annealed, the surface free energy matches that of PBMA and PBMA-*b*-PAz. Therefore, the PBMA segments of PBMA-*b*-PAz should be located at the topmost surface in the two blended films. This situation should be an entropic requirement that flexible moieties with larger mobility are segregated at the free surface.[23,24] Second, the surface free energy of the pure PPBz and PCB are lower and higher than PBMA-*b*-PAz, respectively. Therefore, the surface free energy of the LC polymer relative to PBMA-*b*-PAz was less significant. Therefore, the present method is widely applicable to many side chain LC polymers.

The existence of PBMA-*b*-PAz skin layer in the blend film was directly confirmed by transmission electron microscopy (TEM). A surface skin layer with a thickness of 20 nm was successfully observed by TEM in our previous work with a block copolymer that forms microphase separated (MPS) polystyrene cylinders.[19] In that case, staining with a heavy metal compound led to a clear contrast in the MPS
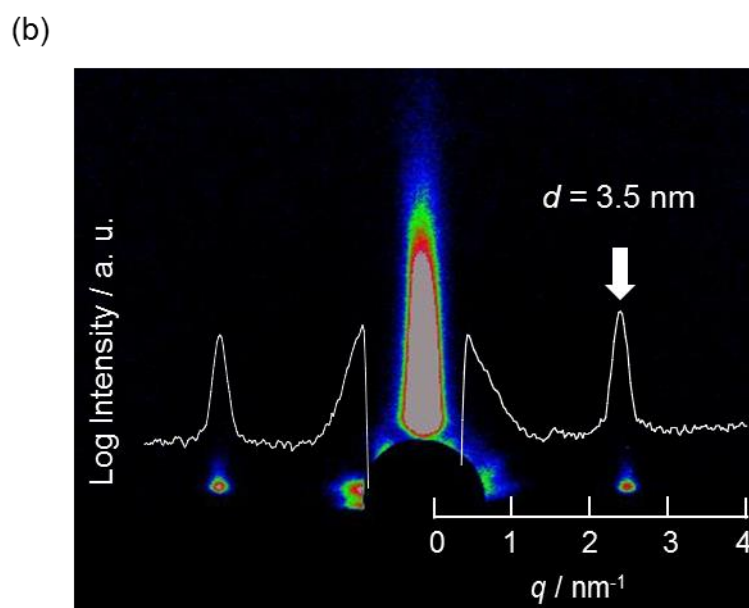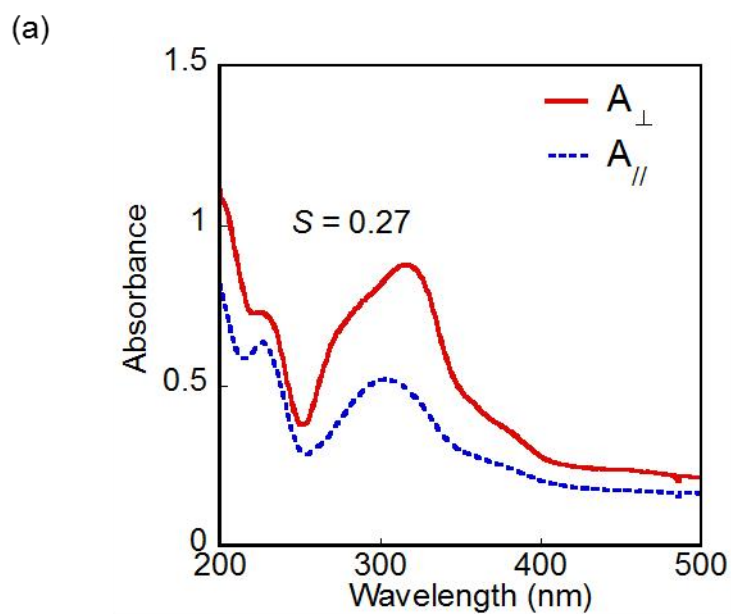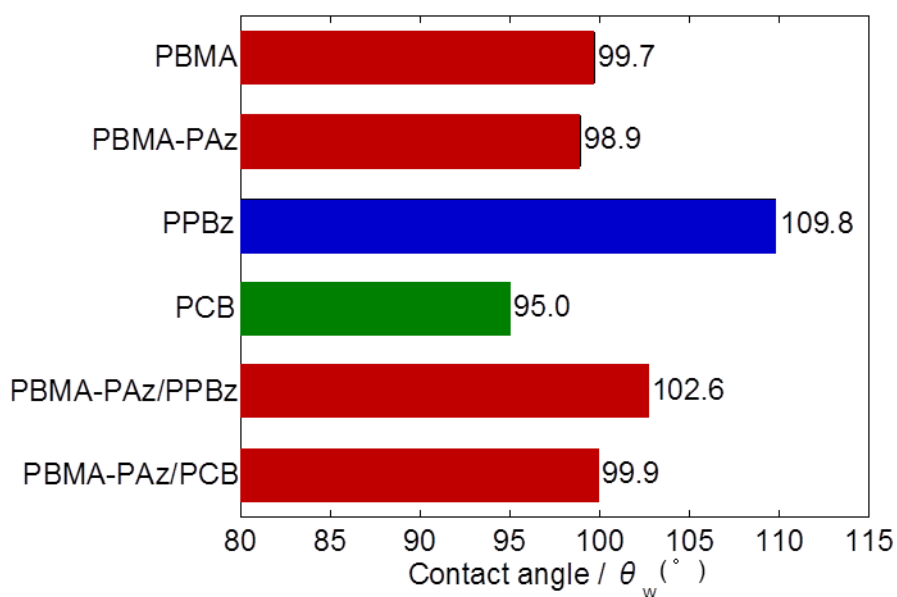
(a)

(b)

Figure 7. Polarised UV-visible absorption spectra of the annealed PBMA-*b*-PAz (3%)/PCB film after LPL irradiation (1000 mJ cm^{-2}) at 110°C taken with probing polarised light set perpendicular (A$_\perp$) and parallel (A$_{//}$) to the actinic LPL light (a). (b): the 2D GI-SAXS images and 1D profiles are shown for the above corresponding films from (a).
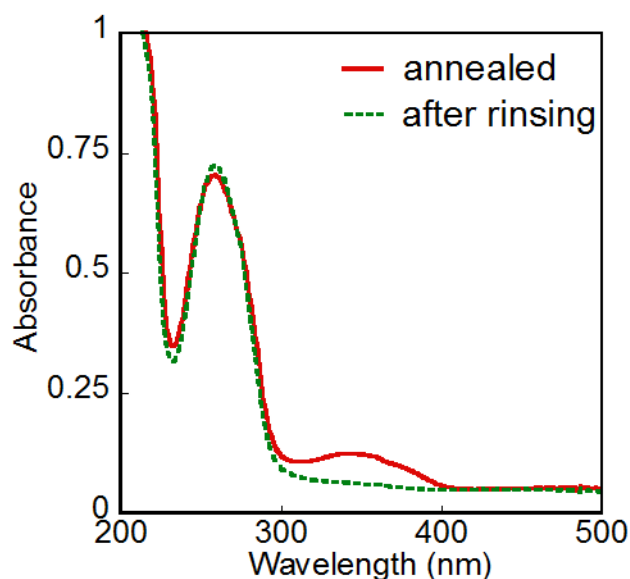
(a)

(b)

Figure 8. (a) Contact angle of a water droplet (q_w) on various polymer surfaces after annealing at 125 °C for 10 min. (b) UV-visible absorption spectra of an annealed PBMA-*b*-PAz (3%)/PPBz film (red solid line) and the identical film after rinsing with cyclohexane at 45 °C for 5 min (green dotted line). Note that the $\pi-\pi^*$ band for the azobenzene (approximately 350 nm) completely disappeared, while that of the phenyl benzoate (approximately 270 nm) remained unchanged.

structure, confirming the existence of the skin layer. However, in the present system, no contrast would be available between the chemically similar side chain polymers (PPBz and PBMA-*b*-PAz). To validate the surface segregation of PBMA-*b*-PAz in the present system, we adopted a simple procedure using UV-visible spectroscopic measurements. The annealed blended film was immersed into an organic solvent that dissolves only PBMA-*b*-PAz. After screening various solvents, cyclohexane was used at 45°C for 5 min. Figure 8b denotes the UV-visible absorption spectra of the annealed PBMA-*b*-PAz(3%)/PPBz film before and after rinsing with cyclohexane. After this treatment, only the $\pi-\pi^*$ absorption band at approximately 350 nm for azobenzene disappeared, while that of phenyl benzoate at approximately 270 nm remained unchanged, unequivocally indicating that PBMA-*b*-PAz is located at the outermost surface and only this block copolymer is dissolved. This result also indicates that the PBMA-*b*-PAz component almost fully migrated to the free surface.

Atomic force microscopic measurements revealed that the average film thicknesses before and after rinsing were approximately 150 and 130 nm, respectively, indicating that the thickness of the surface segregated PBMA-*b*-PAz layer was approximately 20 nm. This thickness is comparable to that observed by TEM in our previous system.[19]

4-3-5. Planar-planar mode photopatterning from the surface skin layer.

Next, we attempted to develop patterns with the in-plane LC orientations triggered via the surface skin layer. Scheme 4 shows a scheme with the procedures and resulting patterns. A cast PBMA-*b*-PAz (3%)/PPBz blend film (about 5 μm thick) was prepared (Scheme 4a) and annealed at 125°C for 10 min to form a PBMA-*b*-PAz skin layer. Afterward, 436 nm LPL was irradiated across the entire area at 600 mJ cm^{-2} and 80 °C (Scheme 4b). Subsequently, 436 nm LPL orthogonal to that of the initial step was irradiated through a photomask under the same conditions (Scheme 4c).

(a)

(b)

(c)

(d)
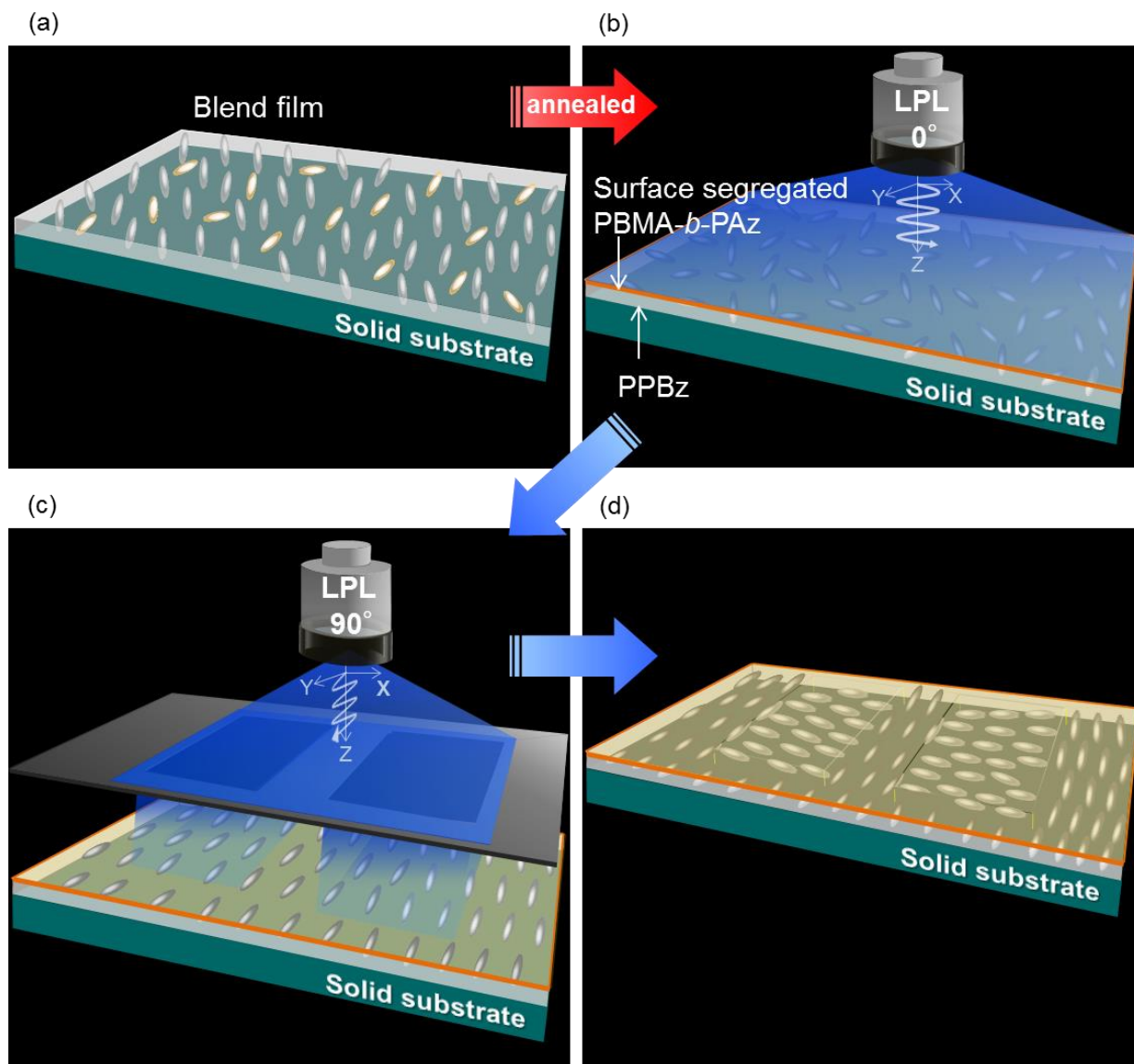
Scheme 4. Scheme showing the procedures for the in-plane photopatterning of the side chain polymer films ((a) to (c)). (a) An as-cast film of the side chain polymer (PPBz or PCB) blended with a small amount of PBMA-*b*-PAz (3 weight %) prepared by simple solvent casting or spincasting. (b) After annealing at 125 °C for 10 min, a skin layer of photoresponsive PBMA-*b*-PAz is formed at the free surface. At this stage, the side chain mesogens adopt a random planar orientation. This film is irradiated with LPL at 80 °C for 10 min (600 mJ cm^{-1}) across the entire area of the film, providing a uniform, in-plane aligned film. (c) Successive patterning irradiation with LPL rotated 90° through a photomask, patterning in a planar-planar orientation mode for the PPBz film (scheme in d).

Figures 9a and 9b display POM images of the resulting film under crossed polarisers rotated 45 ° from one another. As shown, the patterns containing the positive and negative contrast tones of the photomask were fully switched. This result clearly indicates successful planar-planar mode patterning of the mesogens in the PPBz film (Scheme 4d). This two-step photopatterning process demonstrates that the in-plane photoalignment can be readily overwritten by successive LPL irradiation. The overwriting could be repeated many times. A resolution of a few micrometres was obtained according to the discrimination of the patterns.

4-3-6. Orientation memory after removing the surface top layer

After the PBMA-*b*-PAz/PPBz blend thin film irradiating with LPL and rotating at 45 °, the photomask on blend thin film was irradiated with LPL again. The thin film irradiating with the photomask was observed by diffrence contrasts at rotating 0 and 45 ° (Figure 9) as well as cast film (Figure 11a). The command skin layer could be removed selectively with cyclohexane, as mentioned above (see Figure 8b). The thin film after rinsing in cyclohexane for 5 min are shown in Figure S4b. Interestingly, the LC orientation patterning remained unchanged, even after the removal of the photoresponsive surface skin layer. Consequently, a pure photopatterned PPBz film was obtained. The blend thin film indicated different contrasts by POM as rising in solvent and disappearing Az molecules absorption spectrum around 350 nm.

Successively, the rinsed film was irradiated with LPL again at 10 mJ cm^{-2} and 80 °C. The high contrast birefringent and photopatterning images immediately disappeared in the POM observation (Figure 11a). The UV-visible absorption spectra exhibited a significant decrease in the $\pi-\pi^*$ band for phenyl benzoate at 270 nm due to an induction of homeotropic orientation. The resultunt film showed no trace of in-plane alignment was admitted ($S = 0.00$) (Figure 11b).
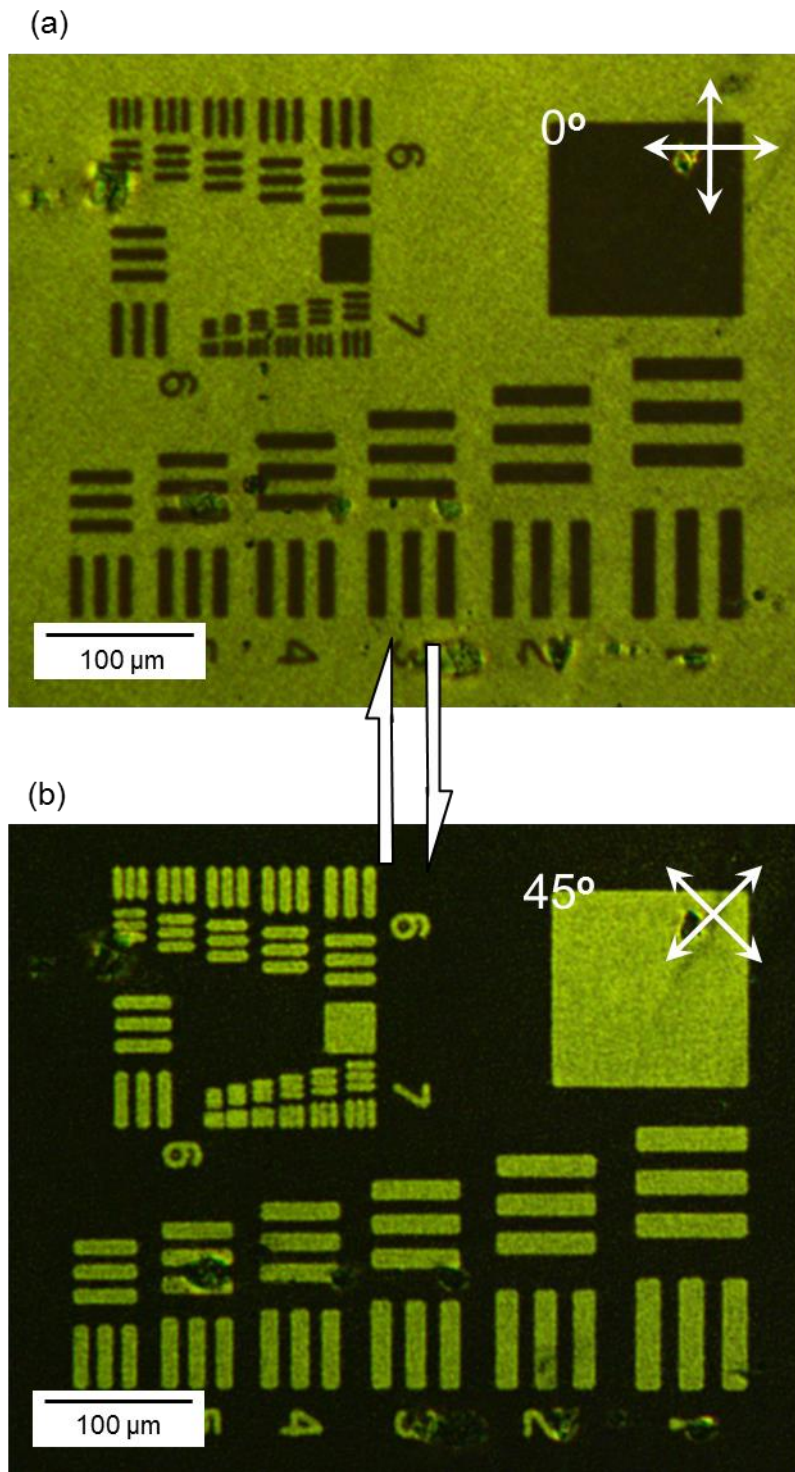
Figure 9. (a) and (b) show the POM images under crossed polarisers that were rotated 45° from each other. Note that the positive and negative tone patterns are reversed.
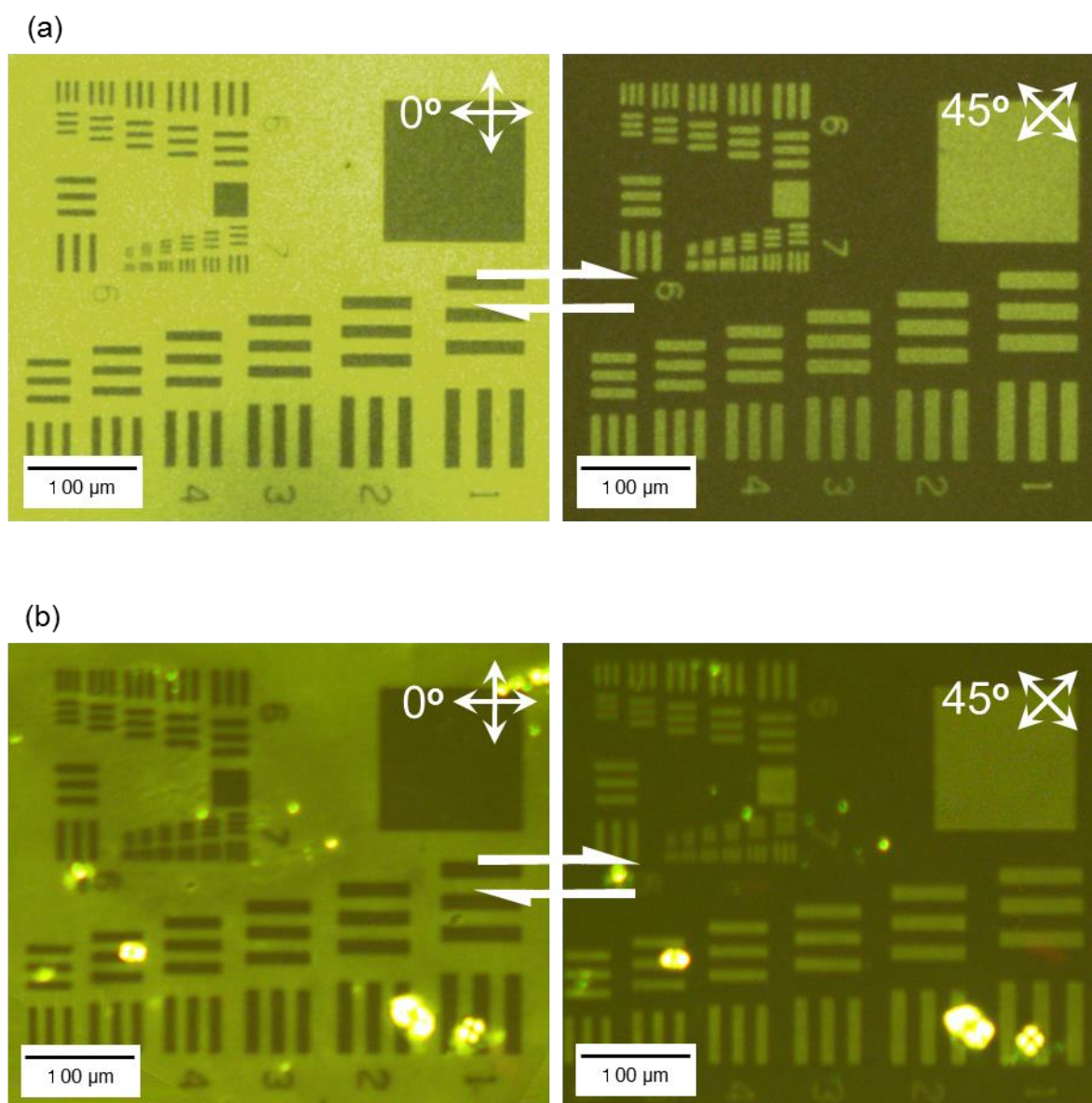
(a)

(b)

Figure 10. The POM images of the PBMA-*b*-PAz (3 %)/PPBz blend thin film after irradiating with LPL used by the photomask (a), after rinsing in cyclohexane for 5 min (b) and after irradiating with LPL. These were observed by difference contrasts at rotating 0 and 45 °.
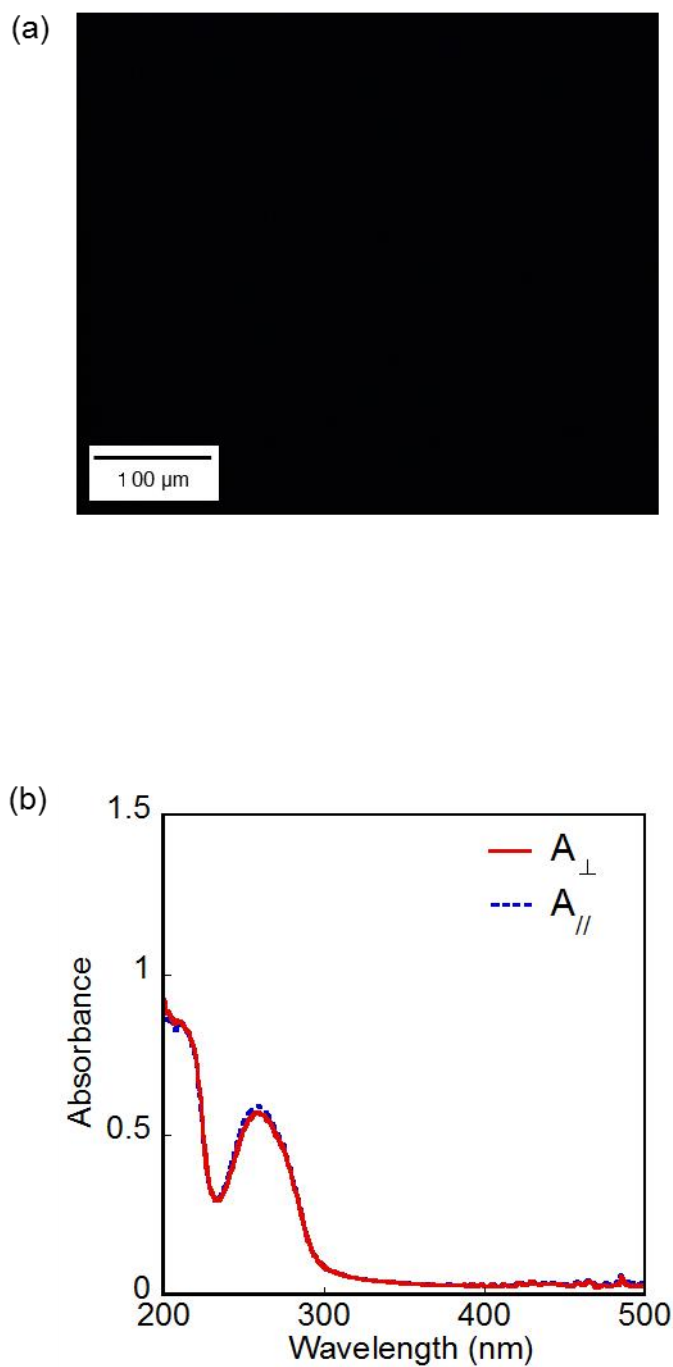
Fifure 11. POM image (a) and UV-Vis absorption spectra of the rinsed film after successive irradiation with 436 nm LPL at 10 mJ cm^{-2} are also displayed. In b, the spectra were taken with the probing beam parallel (dotted line) and orthogonal (solid line) to the actinic light.

4-3-7. Homeotropic-planar mode patterning by inkjet printing.

During the above patterning methods, the entire PPBz film area was covered with a photoresponsive top layer. Next, printing methods were utilised to place the layer at specific locations. Consequently, we chose an inkjet printing method, precluding any effects on the LC orientation caused by pressing during the printing process. PBMA-*b*-PAz was dissolved in *o*-dichlorobenzene (1% by weight) and applied using a sub-femtolitre inkjet printer (Scheme 5). With this apparatus, a resolution approaching 1 µm was available.

In the unprinted areas, the PPBz mesogens are oriented homeotropically after annealing (see Scheme 3a), while in the printed regions, they adopt a planar orientation. Therefore, the patterning could occur between the homeotropic and planar orientation modes (see Scheme 5). Only an annealing process without photoirradiation could make patterns in this mode (between Scheme 3a and Scheme 3b). In this case, the contrast of the POM images under crossed polarisers was not sufficient. The rotation of the crossed polarisers did not alter the bright/dark contrast, indicating that the bright regions were composed of randomly oriented planar domains.

When the photoalignment by LPL irradiation was also performed, refined clear patterns with dark/bright contrast were obtained during POM observation. In Figure 12 and 13, two representative POM images of PPBz films obtained after inkjet printing PBMA-*b*-Paz, annealing and irradiation with LPL are displayed. Here, the letters "NU" (Figure 12a and Figure 12b) and a drawing of a mountain (Figure 13a and Figure 13b) are shown. The printed images appeared and disappeared when rotating the crossed polarisers 45°. Therefore, the homogeneous planar alignment (Scheme 3c) and the homeotropic orientation (Scheme 3a) regions are patterned in the printed and unprinted parts, respectively.

The resolution of this printing process was estimated using line patterns. Line patterning of dissolved PBMA-*b*-PAz solution was drawn in around 1 and 5 µm width
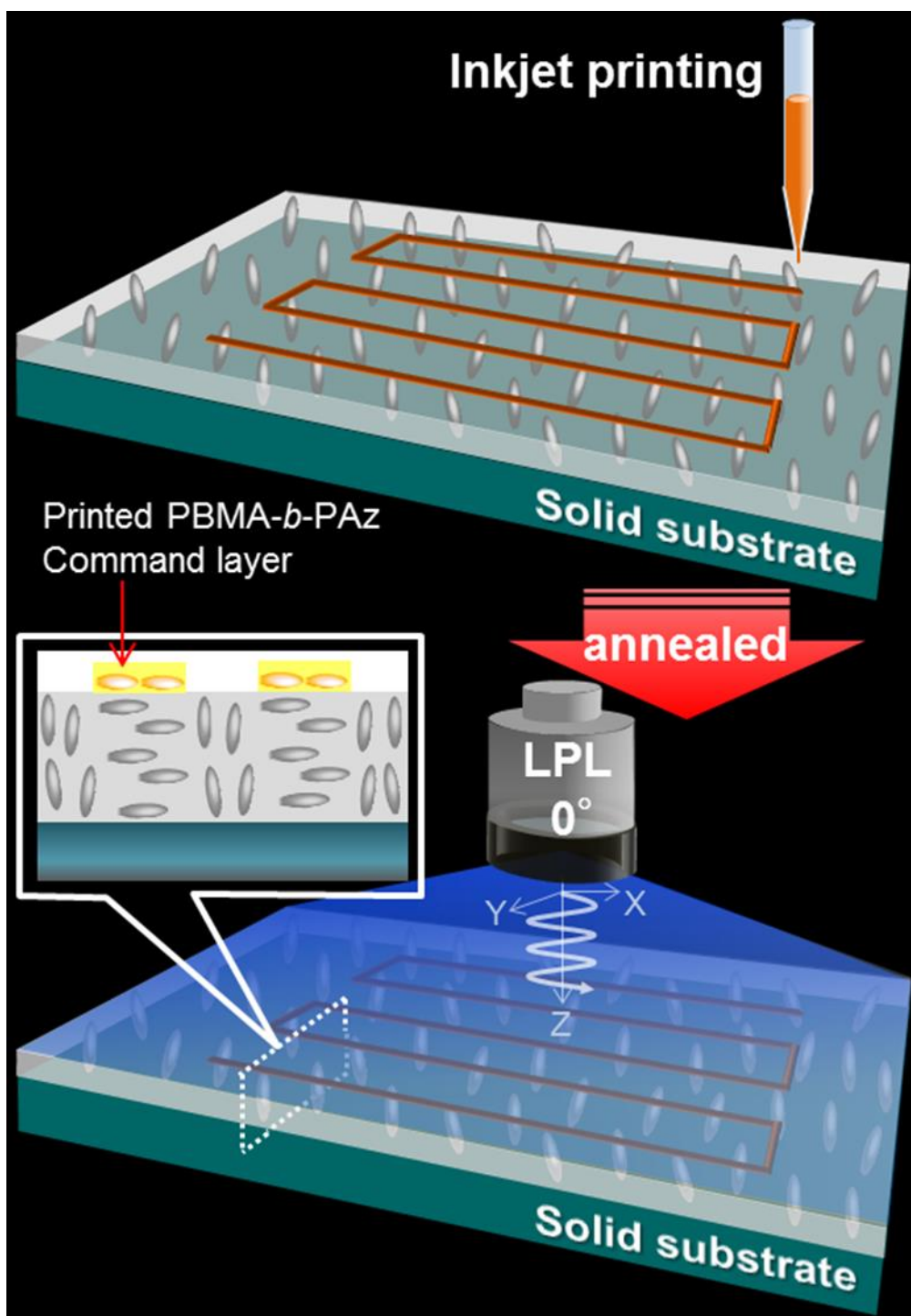
Scheme 5. Scheme of the inkjet printing on a PPBz thin film. After the inkjet printings were performed, the film was annealed at 125 °C for 10 min and successively irradiated with LPL at 80 °C.
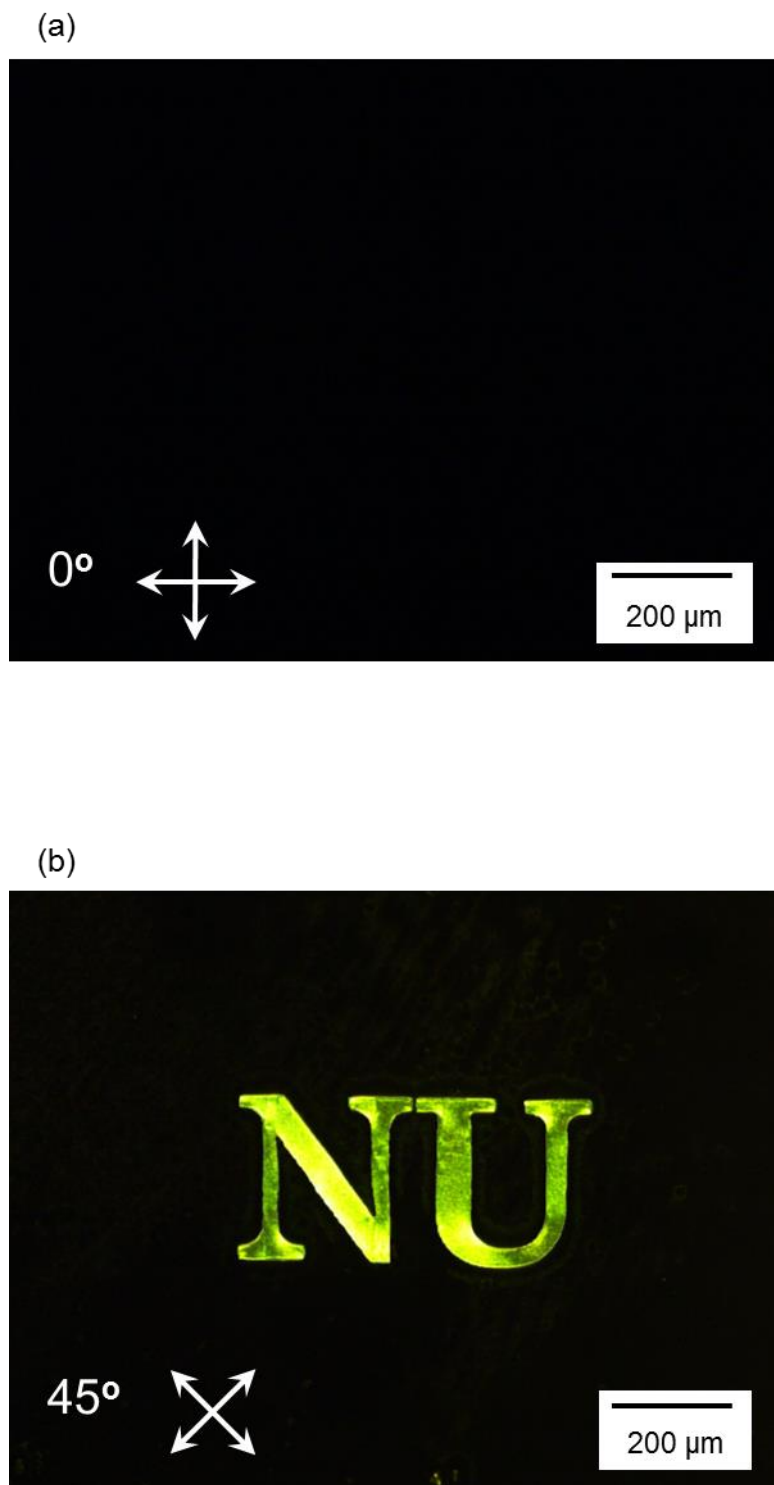
Figure 12. (a) and (b) indicate the appearance and disappearance of a birefringence patterning of "NU" characters in the POM observations under crossed polarisers 45 ° from one another.
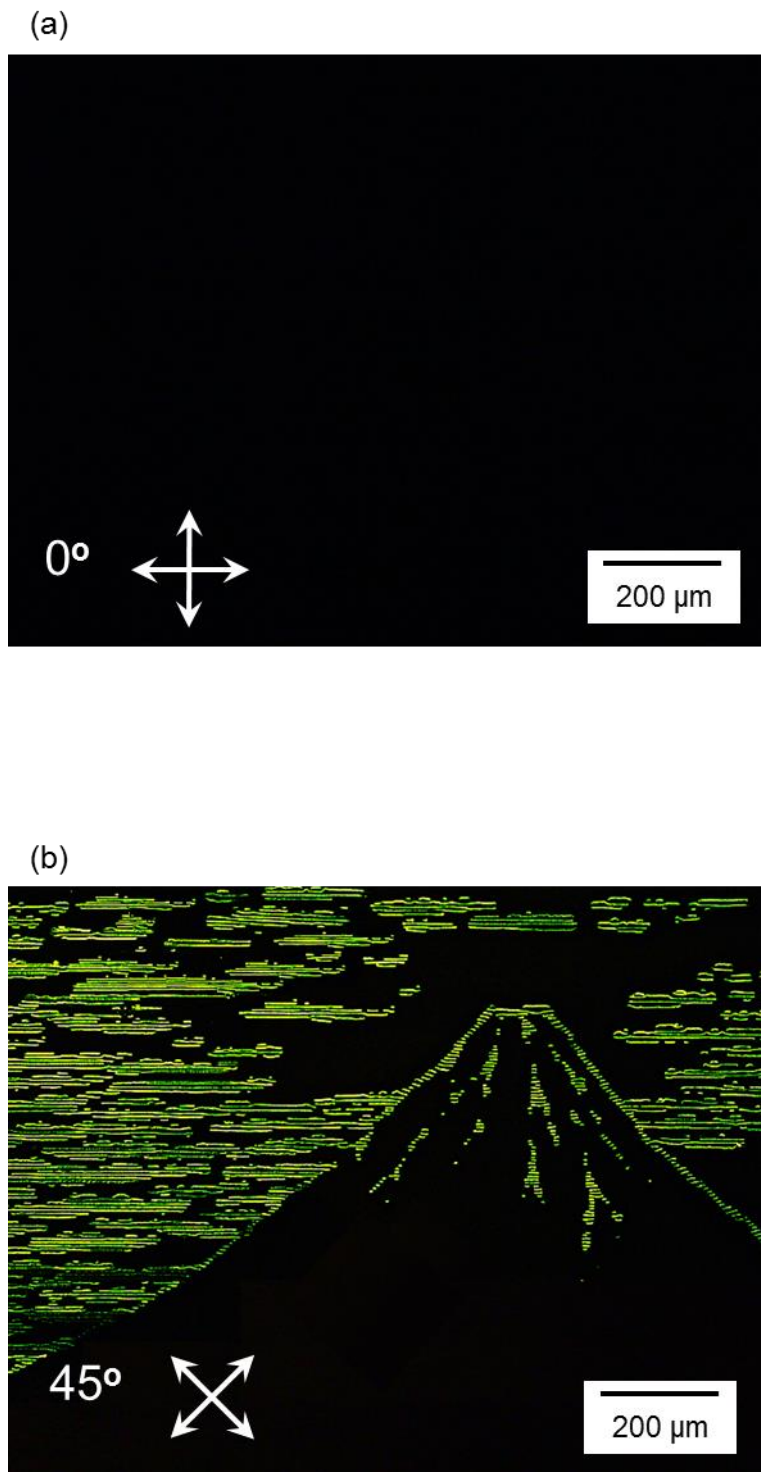
(a)

(b)

Figure 13. (a) and (b) show another example of a drawn picture of a mountain. Note that the emergence of the images was fully switched during this procedure.

on PPBz thin film by inkjet printing. Figure 14 displays examples POM images of the PPBz film after inkjet printing drawings of PBMA-*b*-PAz and successive annealing (125 °C for 10 min) and irradiation with LPL (600 mJ cm^{-2}). The drawing image appeared and disappeared alternatively by rotating the crossed polarizers by 45 °, indicating that the homogeneous alignment patterns were obtained in the printed regions. A 1-µm line width was successfully obtained with some distortions. At a 5-µm width, a linear outline was clearly observed (Figure 14b). It is assumed that a resolution of a few micrometres is appropriate for this process. Nearly identical resolutions are obtained for both patterning modes: planar-planar and homeotropic-planar orientations.

These drawings may be performed by photopatterning with the corresponding photomask; however, the preparation of complex photomasks can be laborious and expensive. With the printing method, on-demand drawings containing any characters or figures are readily accessible, benefitting various applications.

4-3-8. Variations in the substrate.

The experiments were continued using various substrates. In addition to the clean quartz plate ($\theta_w = 10° - 20°$), the same procedures were performed over a hydrophobilised quartz surface ($\theta_w = 85°$) treated with 1,1,1,3,3,3,-hexamethyldisilazane vapour. In addition, commercially available plastic sheets, such as polyimide and poly(ethylene terephthalate) films, were used as flexible, soft substrates. In all cases, the effective induction of birefringence and patterning on PPBz films could be performed in the same way, strongly suggesting that the nature of the substrate surface not significant; the state of the free surface primarily controls the mesogen orientation in the film. With flexible polymer sheets, the substrates do not need to be flat, making any curved or fabricated substrates applicable.
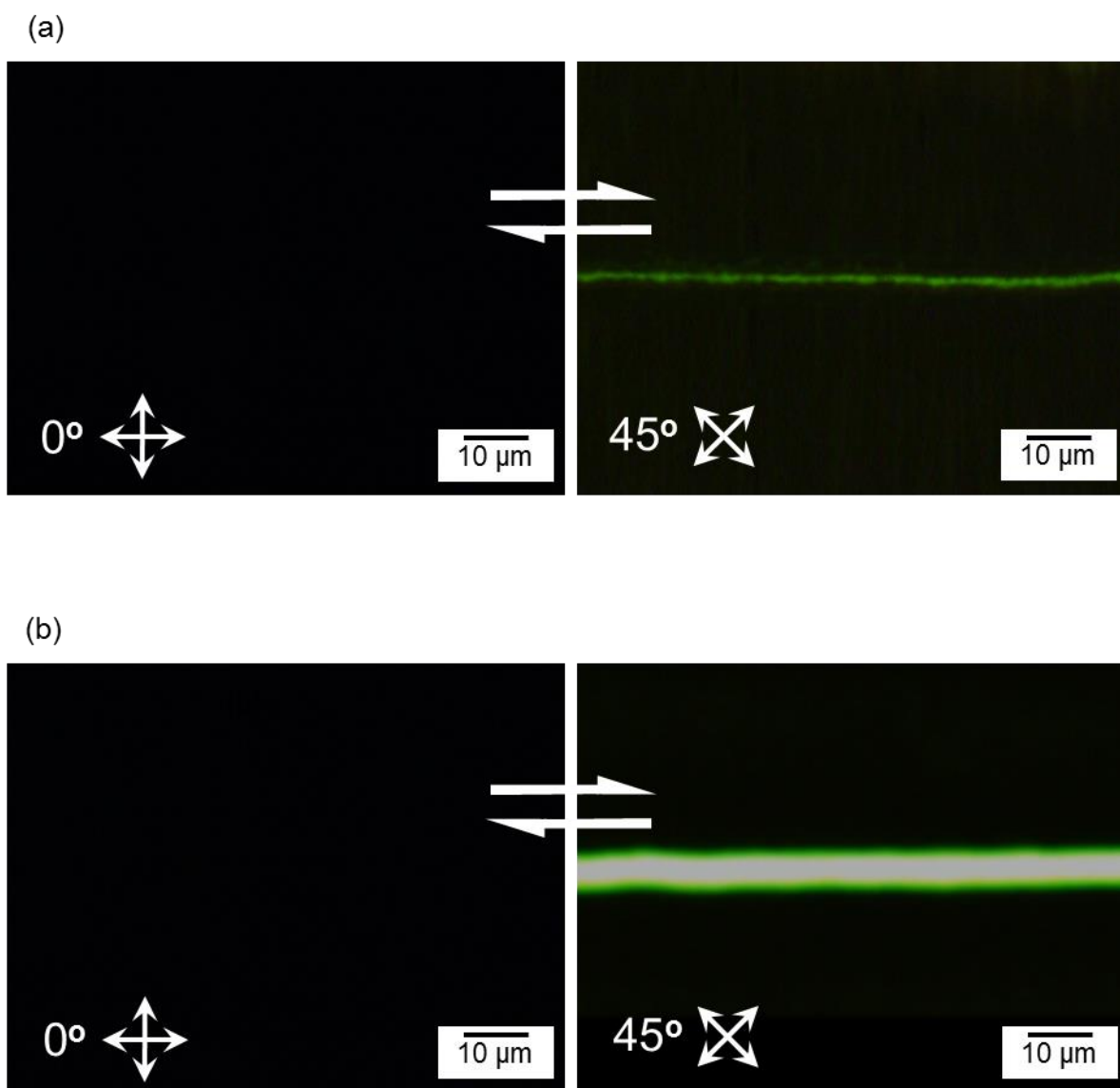
(a)

(b)

Figure 14. The POM image of the PPBz film after inkjet printing drawings of PBMA-b-PAz and successive annealing (125 °C for 10 min) and irradiation with LPL (600 mJ cm^{-2}). These was observed by diffrence contrasts at rotating 0 and 45°.

4-4. Discussion

The low-molecular-mass nematic LCs which used in LC display panels are highly fluid and sandwiched between two solid substrate walls; therefore, the LC orientations are influenced only by the solid surfaces. In contrast, highly viscous or solidified LC materials, such as polymer LCs, are often exposed to air. Until now, the role of the free surface regarding the LC orientation has hardly been taken into account, except for the discotic LC film systems that form a hybrid orientation between an alignment film on a solid surface and the air.[25,26,27] In these cases, modifications on the solid substrate side are still required. In our approach, the solid surface side does not require any modification; manipulations on the free surface can control both in- and out-of-plane modes.

The optical alignment and patterning of side chain LC polymer films have been studied extensively for optical memory and photonic applications.[28,29,30,31,32] In these cases, the photoresponsive units are integrated with the LC polymer films. Therefore, the light must penetrate the films. However, by utilising a free surface command layer, the applicability of our method can be extended to various LC functional systems, including non-transparent LCs. For example, deeply coloured, light-emitting molecules or semiconducting materials exhibiting anisotropic functionalities may be embedded. Patterned polarised light emission devices and semiconducting circuits for transistors and solar cells are likely to be fabricated. Importantly, the surface command layer can be selectively removed while retaining the molecular orientation from the patterned LC film, allowing subsequent piling fabrications using another material.

In both patterning procedures (photomask irradiation and inkjet printing), the molecular orientations of the film remain unchanged when room temperature is maintained. During inkjet printing, the high contrast birefringent images appear only after annealing and LPL irradiation. Specifically, the free surface skin layer possesses latent images that are not recognised by optical detection or the naked eye during the

initial stage. Plausible applications utilising this property might include identification of and protection against forgery.

4-5. Conclusions

The photoalignment processes proposed here are highly versatile and ubiquitous in many aspects: (1) no pretreatment of the substrate is required; (2) various side chains on the LC polymer materials may be used (furthermore, the LC materials need not be transparent); (3) simple annealing and LPL irradiation procedures are sufficient for developing clear images; (4) on-demand patterns are readily available through a commercially available printing method; and (5) various substrates, including inorganic and flexible polymer substrates, can be used. These simple but powerful methods should broaden the applicability of LC photoalignment to access various systems, providing new opportunities for optical[25,26] and mechanical[27, 33] device fabrication.

References

1. C. V. Mauguin, *Bull. Soc. Fr. Mineral.* **1911**, *34*, 71-117.

2. P. Chatelain, *Bull. Soc. Fr. Mineral.* **1944**, *88*, 105-130.

3. K. Ichimura, Y. Suzuki, T. Seki, A. Hosoki, K. Aoki, *Langmuir* **1988**, *4*, 1214-1216.

4. K. Ichimura, *Chem. Rev.* **2000**, *100*, 1847-1874.

5. J. Hoogboom, T. Rasing, A. E. Rowan, R. J. M. Nolte, *J. Mater. Chem.* **2006**, *16*, 1305-1314.

6. J. Hoogboom, P. M. L. Garcia, M. B. J. Otten, J. A. A. W. Elemans, J. Sly, S. V. Lazarenko, T. Rasing, A. E. Rowan, R. J. M. Nolte, *J. Am. Chem. Soc.* **2005**, *127*, 11047-11052.

7. T. Seki, S. Nagano, M. Hara, *Polymer* **2013**, *54*, 6053-6072.

8. T. Seki, M. Sakuragi, Y. Kawanishi, T. Tamaki, R. Fukuda, K. Ichimura, Y. Suzuki, *Langmuir* **1993**, *9*, 211-218.

9. W. M. Gibbons, P. J. Shannon, S.-T. Sun, B. J. Swetlin, *Nature* **1991**, *351*, 49-50.

10. A. Dyadyusha, Ukr. Fiz. Zh. **1991**, *36*, 1059-1062.

11. M. Schadt, K. Schmitt, V. Kozinkov, V. Chigrinov, *Jpn. J. Appl. Phys.* **1992**, *31*, 2155.

12. V. G. Chigrinov, V. M. Kozenkov, H. S. Kwok, Photoalignment of liquid crystalline Materials. Wiley-SID Series in Display Technology, **2008**, West Sussex.

13. O. Yaroshchuk, Y. Reznikov, *J. Mater. Chem.* **2012**, *22*, 286-300.

14. K. Miyachi, K. Kobayashi, Y. Yamada, S. Mizushima, *SID Sym. Dig. Tech. Papers* **2010**, *41*, 579-582.

15. M. Kidowaki, T. Fujiwara, K. Ichimura, *Chem. Lett.* **1999**, *28*, 643-644.

16. K. Fukuda, T. Seki, K. Ichimura, *Macromolecules* **2002**, *35*, 1951-1957.

17. H. Kimura, H. Nakano, *J. Phys. Soc. Jpn* **1985**, *54*, 1730.

18. N. Scaramuzza, C. Berlic, E. S. Barna, G. Strangi, V. Barna, A. T. Ionescu, *J. Phys. Chem. B* **2004**, *108*, 3207-3210.

19. S. Faetti, L. Fronzoni, *Solid State Commun.* **1978**, *25*, 1087-1090.

20. B. M. Ocko, A. Braslau, P. S. Pershan, J. Als-Nielsen, M. Deutsch, *Phys. Rev. Lett.* **1986**, *57*, 94-97.

21. K. Fukuhara, Y. Fujii, Y. Nagashima, M. Hara, S. Nagano, T. Seki, *Angew. Chem. Int. Ed.* **2013**, *125*, 6104-6107.

22. S. Nagano, Y. Koizuka, T. Murase, M. Sano, Y. Shinohara, Y. Amemiya, T. Seki, *Angew. Chem. Int. Ed.* **2012**, *51*, 5884-5888.

23. K. Tanaka, A. Takahara, T. Kajiyama, *Macromolecules* **1998**, *31*, 863-869.

24. M. A. Carignano, I. Szleifer, *Europhys. Lett.* **1995**, *30*, 525-530.

25. K. Ichimura, S. Furumi, S. Morino, M. Kidowaki, M. Nakagawa, M. Ogawa, Y. Nishiura, *Adv. Mater.* **2000**, *12*, 950-953.

26. M. Okazaki, K. Kawata, H. Nishikawa, M. Negoro, *Polym. Adv. Technol.* **2000**, *11*, 398-403.

27. K. Kawata, *Chem. Rec.* **2002**, *2*, 59-80.

28. T. Ikeda, *J. Mater. Chem.* **2003**, *13*, 2037-2057.

29. V. Shibaev, A. Bobrovsky, N. Boiko, *Prog. Polym. Sci.* **2003**, *28*, 729-836.

30. H. Yu, T. Ikeda, *Adv. Mater.* **2011**, *23*, 2149-2180.

31. N. Kawatsuki, *Chem. Lett.* **2011**, *40*, 548-554.

32. J. Stumpe, O. Kulikovska, L. M. Goldenberg, Y. Zakrevskyy, in *Smart Light-Respon.*

Mater., John Wiley & Sons, Inc., **2009**, pp. 47-94.

33. T. Ikeda, J.-i. Mamiya, Y. Yu, *Angew. Chem. Int. Ed.* **2007**, *46*, 506-528.

Chapter V

Summary and Outlook

The main activities in the studies on the orientation of liquid crystal (LC) molecules have been targeted to solid substrate surfaces heretofore. In contrast, the work in this thesis proposes a new concept focusing to the importance of the free surface control. The procedures involved in this work are simple: a small amount of surface active polymer (SAP) is blended before spin-coating and annealing is performed successively. It is demonstrated that the alignment control of LC and microphase cylinder structure in thin films can be readily achieved by the *free surface* modification. Adding a small amount of the low surface energy and flexible SAP brings about a homeotropic to planar orientation transition of the LC polymer underneath due to the surface segregation and coverage of PBMA at the *free surface*.

The surface segregation of polymer blends has been studied as an important method to control a top surface property of polymer films. Almost all applications, for examples, a biocompatible surface, have been focused on functions toward outsides contacting with the polymer surface. On the other hand, the approach taken in this thesis proposes a new performance which controls "inside" of the film structure by the segregation to the free surface.

The proposed method is of technological significance. In general, syntheses of block copolymers are tedious and they are high-cost materials. The use of small amount of the block copolymer is sufficient to make drastic effect as indicated in this work. This will be a good example for the practical use of block copolymers, which may be applicable to industries. Summary and outlook of each chapter are described as follows.

In Chapter 2, the first demonstration for the clear orientational alternations of LC mesogens and the MPS domains is made by modifying the free surface. Formation of a skin layer at the free surface is achieved by simply blending a surface-active polymer and performing the appropriate annealing step. This strategy is very simple and versatile, and is therefore expected to open up new possibilities for orientation controls of various types of LC materials. In addition to functions accessing the 'exterior' phase as so far considered, this approach indicates that the free surface segregation is also valuable for the control of the 'interior' structure of the polymer film.

In Chapter 3, the exploration is focused onto the design of the surface active block copolymer. In terms of polymer design and conditions of SAP, the factors influencing the free surface-induced orientational alternation are summarized as follows. (i) Block copolymers containing the mesogens should be used. The homopolymer of PBMA is not favorable due to the low compatibility with the base block copolymer, exhibiting dewetting on the surface. (ii) The blend ratio of SAP should be large enough to cover the base polymer surface. (iii) The molecular weight significantly influences the surface coverage, and the smaller amount will be sufficient for the larger molecular weight SAP.

In Chapter 4, the system from the free surface is found to applicable to non-photoresponsive LC films. Suchphotoalignment processes are highly versatile and ubiquitous in many aspects: (1) no pre-treatment of the substrate is required; (2) various side chains LC polymer materials may be used (furthermore, the LC materials need not be transparent); (3) simple annealing and LPL irradiation procedures are sufficient for developing clear images; (4) on-demand patterns are readily available through a commercially available printing method; and (5) various substrates, including inorganic and flexible polymer substrates, can be used.

The processes proposed in this thesis are simple but powerful, which are expected to broaden the applicability of LC photoalignment to access various systems,

providing new opportunities for optical and mechanical device fabrication.

Publications

1. <u>Kei Fukuhara</u>, Takemune Yamada, Akihiro Suzuki, "Characterization of Fluoropolymer Nanofiber Sheets Fabricated by CO_2 Laser Drawing without Solvents", ***Industrial & Engineering Chemistry Research***, 51(30), 10117-10123 (2012).

2. <u>Kei Fukuhara</u>, Yasuyoshi Fujii, Yuki Nagashima, Mitsuo Hara, Shusaku Nagano, Takahiro Seki, "Liquid Crystalline Polymer and Block Copolymer Domain Alignment Controlled via Free-Surface Segregation", ***Angewandte Chemie International Edition***, 52(23), 5988-5991 (2013).

3. <u>Kei Fukuhara</u>, Mitsuo Hara, Shusaku Nagano, Takahiro Seki, "Free Surface-Induced Planar Orientation in Liquid Crystalline Block Copolymer Films: On the Design of Additive Surface Active Polymer", ***Molecular Crystals and Liquid Crystals***, *in press.* (2013).

4. <u>Kei Fukuhara</u>, Mitsuo Hara, Shusaku Nagano, Takahiro Seki, "Free-surface molecular command systems: Ubiquitous photoalignment of liquid crystalline materials", *submitted.* (2014).

Books

1. <u>福原　慶</u>・永野　修作・関　隆広, *高分子液晶薄膜の光配向における空気界面の役割*, ㈱広信社「表面」, 51(2), pp. 78-88 (2013).

Presentations at International Conferences

1. <u>Kei Fukuhara</u>, Takemune Yamada and Akihiro Suzuki, "Tetrafluoroethylene-perfluoroalkyl Vinylether Copolymer Nanofiber Sheets prepared by CO_2 Laser Supersonic Multi-drawing", 4th Annual Symposium, Nagoya, Japan (2011).

2. <u>Kei Fukuhara</u>, Soutarou Kakehi, Shusaku Nagano and Takahiro Seki, "Photoalignment and structural study on polynorbornene brush having azobezene liquid crystalline via surface initiated ROMP", KJF-ICOMEP2011, Gyeongju, Korea (2011).

3. <u>Kei Fukuhara</u>, Soutarou Kakehi, Shusaku Nagano and Takahiro Seki, "Photoalignment and structural study on polynorbornene brush having azobezene liquid crystalline by surface initiated ROMP", International Symposium on Elucidation and Design of Materials and Molecular Functions & 7th and 8th Yoshimasa Hirata Memorial Lectures, Nagoya, Japan (2011).

4. <u>Kei Fukuhara</u>, Soutarou Kakehi, Shusaku Nagano and Takahiro Seki, "Photoalignment and structural study on polynorbornene brush having azobezene liquid crystalline via surface initiated ROMP", NTTH Joint Symposium, Chengdu, China (2011).

5. <u>Kei Fukuhara</u>, Koichiro Beppu, Shusaku Nagano and Takahiro Seki, "Introduction of the Photo-Acid-Generating Unit in a Photoalignable Block Copolymer", 14th International Conference on Organized Molecular Films, Paris, France (2012).

6. <u>Kei Fukuhara</u>, Yuma Serizawa, Shusaku Nagano and Takahiro Seki, "Preparation of Surface Deployed Polymer Particles used by Subfemt Ink Jet Processing Equipment", KJF-ICOMEP2012, Sendai, Japan (2012).

7. <u>Kei Fukuhara</u>, Yasuyoshi Fujii and Shusaku Nagano, "Induced Planer Alignment and Photo-reorientation of Liquid Crystalline Azobenzene Block Copolymer Consisting of Polystyrene", IUMRS-International Conference on Electronic

Materials, Yokohama, Japan (2012).

8. <u>Kei Fukuhara</u>, Shusaku Nagano and Takahiro Seki, "Air Side-directed Planar Alignment and Photo-reorientation of Liquid Crystalline Azobenzene Block Copolymers Consisting of Polystyrene and Polyalkylmethacrylate", MRS Fall Meeting, Boston, US (2012).

9. <u>Kei Fukuhara</u>, Shusaku Nagano and Takahiro Seki, "Air Side-directed Planar Alignment and Photo-orientation of LC Block Copolymers", IGER Annual meeting 2012, Nagoya, Japan (2013).

10. <u>Kei Fukuhara</u>, Yuki Nagashima, Shusaku Nagano and Takahiro Seki, "Alignment Control of Liquid Crystal and Block Copolymer Domains via a Segregated Free Surface Layer", M&BE7, Fukuoka, Japan (2013).

11. <u>Kei Fukuhara</u>, Yuki Nagashima, Mitsuo Hara, Shusaku Nagano and Takahiro Seki, "Alignment Control of Liquid Crystalline Polymer and Block Copolymer Domains by a Segregated Free Surface Layer", ADMD2013, Shanghai, China (2013).

12. <u>Kei Fukuhara</u>, Yuki Nagashima, Mitsuo Hara, Shusaku Nagano and Takahiro Seki, "Liquid Crystalline Polymer and Block Copolymer Domain Alignment Controlled via Free Surface Segregation", KJF-ICOMEP2013, Busan, Korea (2013).

13. <u>Kei Fukuhara</u>, Yuki Nagashima, Mitsuo Hara, Shusaku Nagano and Takahiro Seki, "Alignment Control of Liquid Crystalline Polymer and Block Copolymer Domains via a Segregated Free Surface Layer", MRS Joint Symposium, Kyoto, Japan (2013).

14. <u>Kei Fukuhara</u>, Yuki Nagashima, Mitsuo Hara, Shusaku Nagano and Takahiro Seki, "Liquid Crystalline Polymer and Block Copolymer Domain Alignment Controlled by Free Surface Segregation", ISOP2013, Berlin, Germany (2013).

Acknowledgements

January, 2014

Kei Fukuhara